University of Washington Department of Orthopaedics and Sports Medicine
2006 Research Report

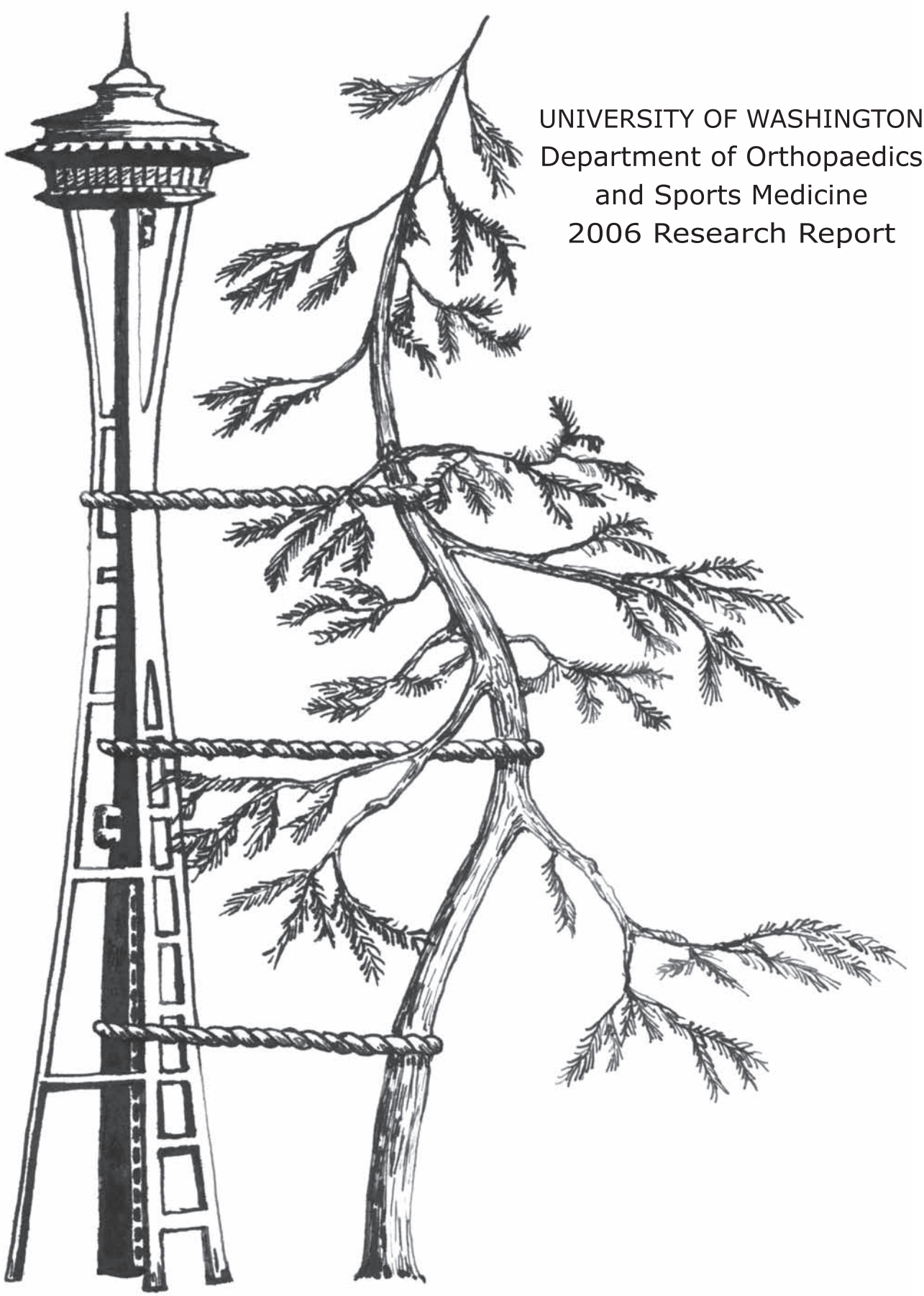

UNIVERSITY OF WASHINGTON
Department of Orthopaedics
and Sports Medicine
2006 Research Report

UW Medicine
SCHOOL OF MEDICINE

Department of Orthopaedics and Sports Medicine
University of Washington
Seattle, WA 98195

Editor:
Frederick A. Matsen III, M.D.
Fred Westerberg

Design & Layout:
Fred Westerberg

Cover Illustration: "Woman with Umbrella Turned Towards the Left"
by Claude Monet, 1886.
Photograph: Erich Lessing
Musee d'Orsay, Paris, France.
Photo Credit: Erich Lessing / Art Resource, NY

Contents

Foreword

Dear Friend,
Welcome to the 2006 Orthopaedics and Sports Medicine Research Report.

I am sure you will have no difficulty determining the identity of our cover artist and perhaps identifying with him. Claude Monet was born in Paris in 1840. He left the tradition of studio painting and took his brushes and canvas out of doors embracing the open air tradition of the Barbizon school, "I only had the merit to paint directly in front of nature." Monet's friend, Manet, painter of the controversial 1863 Le Dejeuner sur l'herbe, was another strong influence (although Monet's 1865 painting of the same title had everyone clothed). Camille Doncieux, Monet's model and subsequently his wife, was the central figure of some of his most beloved paintings Camille ou La Robe Verte (Lady in Green) is a fine example. In Femmes au jardin (Women in the Garden) all four women are Camille. My all-time favorite is Coquelicots (Poppies, near Argenteuil). He commemorated Camille's 1879 death in the haunting Camille sur son lit de mort (Camille on her deathbed). It is fascinating that he painted her in 1875 as 'The Walk, Lady with a Parasol: facing left' and again in 1886, more abstractly, after her death, in the painting shown on our cover as 'Woman with Parasol; facing left'. In 1926, to celebrate the signing of the Armistice, Monet donated 12 large paintings of the Water Lilies to France where they were housed in a special room at the Orangerie. He died later that year of lung cancer. To learn more about Monet, check out http://www.abcgallery.com/M/monet/monetbio.html, and http://www.impressionniste.net/monet_claude.htm.

Monet emblemized the essence of academic orthopaedics. I would have loved to have him as a faculty member. First, he was a specialist: he used the illusionistic style of impressionism to allow the optical mixture of brushstrokes in pure color to represent the essence and evanescence of nature. Second, he was not afraid to separate himself from the established art schools of the day. Monet attended the famed Ecole des Beaux-Arts but rejected its official classical training and left to study at the Academie Swisse, where classes were less structured and students drew from live models as opposed to traditional casts. Even though his refusal to conform cost him rejection and financial hardship, he persevered until he successfully established himself as one of the artistic leaders of all time. Thirdly, he researched the application of his method, investigating its generalizabiilty – to haystacks, harbors, streets, train stations, fields and water lillies. Fourthly, he refined his art through practice – he painted the façade of the Cathedral of Rouen (where Joan of Arc was interrogated) well over twenty times all from the same second-floor window above a shop opposite the façade, exploring the effect of the hours of the day and the degree of cloud cover on the resultant image.

In this Research Report you will see these same attributes demonstrated by our faculty, residents and staff: specialization, courage to persist in challenging the traditional paradigm, active research to achieve a better understanding, and refinement of technique in the pursuit of excellence. As you read these articles, recognize that you are getting a glimpse of great artists at work. In selecting these articles from the many great works published by our Department each year, I tried to represent the variety of techniques used by the investigators. The observant reader will note cadaver modeling, three dimensional motion in living subjects, collagen synthesis by cultured chondrocytes, murine model of the effect of weakened muscles, muscle action in classical ballerinas, clinical outcomes, the effects of funding source on the published literature, confidence of doctors in managing common problems, the effect of loading on cultured bone-forming cells, molecular biology, human finger development, surgical simulation, surgical failure analysis and more. Like other artists, these investigators need a special environment in which they can develop their ideas, their techniques and their clinical applications. We are proud that

Frederick A. Matsen III, M.D.
Professor and Chairman

the Department of Orthopaedics and Sports Medicine at the University of Washington provides such a nurturing environment. The fact that we continue to attract and retain outstanding faculty and residents is in large part due to the generous philanthropic support we receive from friends, grateful patients, industry, former trainees, and concerned citizens. To all who support our efforts, we send our heartfelt thanks. To those who would like to learn more about what is going on here, I invite you to drop me an email at matsen@u.washington.edu or to check out our website http://www.orthop.washington.edu where you can find all our past research reports under the "our research" tab.

Best wishes,

F. A. Matsen III

Frederick A. Matsen III, M.D.
University of Washington
Department of Orthopaedics and Sports Medicine
1959 NE Pacific Street, Box 356500
Seattle, WA 98195
Office Phone (206) 543-3690
matsen@u.washington.edu
www.orthop.washington.edu

Department of Orthopaedics and Sports Medicine Faculty

Frederick A. Matsen III, M.D.
Professor and Chair

Christopher H. Allan, M.D.
Associate Professor

Dheera Ananthakrishnan, M.D.
Assistant Professor

David P. Barei, M.D.
Assistant Professor

Carlo Bellabarba, M.D.
Associate Professor

Daphne M. Beingessner, M.D.
Assistant Professor

Stephen K. Benirschke, M.D.
Professor

Stanley J. Bigos, M.D.
Professor Emeritus

Richard J. Bransford, M.D.
Assistant Professor

Howard A. Chansky, M.D.
Professor

Jens R. Chapman, M.D.
Professor

Ernest U. Conrad III, M.D.
Professor

Robert P. Dunbar, M.D.
Assistant Professor

David R. Eyre, Ph.D.
Professor

Russell J. Fernandes, Ph.D.
Research Assistant Professor

John R. Green III, M.D.
Associate Professor

Theodore K. Greenlee, Jr., M.D.
Associate Professor Emeritus

Ted S. Gross, Ph.D.
Associate Professor

Douglas P. Hanel, M.D.
Professor

Sigvard T. Hansen, Jr., M.D.
Professor

M. Bradford Henley, M.D.
Professor

Nancy J. Kadel, M.D.
Associate Professor

Leonid I. Katolik, M.D.
Assistant Professor

Roger V. Larson, M.D.
Associate Professor

Seth S. Leopold, M.D.
Associate Professor

Paul Manner, M.D.
Assistant Professor

Sohail K. Mirza, M.D.
Professor

Vincent S. Mosca, M.D.
Associate Professor

Sean E. Nork, M.D.
Associate Professor

John W. O'Kane, M.D.
Associate Professor

Milton L. Routt, Jr., M.D.
Professor

Bruce J. Sangeorzan, M.D.
Professor

Gregory A. Schmale, M.D.
Assistant Professor

John A. Sidles, Ph.D.
Professor

Douglas G. Smith, M.D.
Professor

Kit M. Song, M.D.
Associate Professor

Sundar Srinivasan, Ph.D.
Research Assistant Professor

Lynn T. Staheli, M.D.
Professor Emeritus

Lisa A. Taitsman, M.D., M.P.H.
Assistant Professor

Carol C. Teitz, M.D.
Professor

Allan F. Tencer, Ph.D.
Professor

Thomas E. Trumble, M.D.
Professor

Theodore Wagner, M.D.
Clinical Professor

Christopher J. Wahl, M.D.
Assistant Professor

Jason S. Weisstein, M.D., M.P.H.
Assistant Professor

Klane White, M.D.
Assistant Professor

Jiann-Jiu Wu, Ph.D.
Research Associate Professor

Adjunct Faculty

Basia R. Belza, R.N., Ph.D.
Associate Professor, Physiological Nursing

Jack W. Berryman, Ph.D.
Professor, Medical History & Ethics

Charles H. Chesnut, M.D.
Professor, Nuclear Medicine

Randal P. Ching, Ph.D.
Associate Professor, Mechanical Engineering

Richard A. Deyo, M.D.
Professor, Medicine

Gregory C. Gardner, M.D.
Professor, Rheumatology

Thurman Gillespy III, M.D.
Associate Professor, Radiology

Daniel O. Graney, Ph.D.
Professor, Biological Structure

Frederick A. Mann, M.D.
Professor, Radiology

Susan M. Ott, M.D.
Associate Professor, Division of Metabolism

Wendy Raskind, M.D., Ph.D.
Professor, General Internal Medicine

Michael L. Richardson, M.D.
Professor, Radiology

Peter A. Simkin, M.D.
Professor, Medicine

Tony J. Wilson, M.D.
Professor, Radiology

Miqin Zhang, Ph.D.
Associate Professor, Materials Science and Engineering

Joint Faculty

Michael M. Avellino, M.D.
Associate Professor, Neurological Surgery

Randy M. Chestnut, M.D.
Associate Professor, Neurological Surgery

Janet F. Eary, M.D.
Professor, Radiology

Mark A. Harrast, M.D.
Clinical Assistant Professor, Rehabilitation Medicine

John E. Olerud, M.D.
Professor, Division of Dermatology

Nathan J. Smith, M.D.
Professor Emeritus, Pediatrics

Michael D. Strong, Ph.D.
Research Professor, Surgery

Nicholas B. Vedder, M.D.
Professor, Plastic Surgery

Clinical Faculty

Sarah E. Jackins, R.P.T.
Assistant Professor, Rehabilitation Medicine

University of Washington

UW Medicine
SCHOOL OF MEDICINE

University of Washington School of Medicine

Department of Orthopaedics and Sports Medicine

1959 N.E. Pacific Street
Box 356500
Seattle, Washington 98195-6500
Phone: (206) 543-3690
Fax: (206) 685-3139

Affiliated Institutions

Children's Hospital and
Regional Medical Center
4800 Sand Point Way NE
Seattle, WA 98105
(206) 987-1776

Harborview Medical Center
325 Ninth Avenue
Seattle, WA 98104
(206) 731-3466

University of Washington
Medical Center
Bone and Joint Center
4245 Roosevelt Way NE
Seattle, WA 98105
(206) 598-4288

VA Puget Sound Health Care System
1660 South Columbian Way
Seattle, WA 98108
(206) 764-2215

Visiting Lecturers

Alexander R. Vaccaro III, M.D.
2006 LeCocq Lecturer

This year at our annual LeCocq Lecture on January 19th and 20th, we were honored to have Dr. Alexander Vaccaro as our 2006 LeCocq Lecturer. Dr. Vaccaro is currently a Professor of Orthopaedic Surgery and Neurosurgery at Thomas Jefferson University and the Rothman Institute in Philadelphia, PA. Dr. Vaccaro is Co-Director of the Regional Spinal Cord Injury Center of the Delaware Valley, one of the largest tertiary referral centers for spinal cord injuries in the nation. He is also the Co-Director of the Spine Fellowship program at Thomas Jefferson University and is responsible for teaching residents and fellows the principles of spinal care.

He is a board certified orthopaedic surgeon and licensed to practice in Pennsylvania, New Jersey, Delaware and California. He specializes in the management and treatment of disorders of the spine. Dr. Vaccaro holds numerous society memberships including the American Academy of Orthopaedic Surgeons, the Philadelphia Orthopaedic Society, the Philadelphia College of Surgeons, the Cervical Spine Research society, the North American Spine Society, the Scoliosis Research Society, the American Orthopaedic Association and the International Society for the Study of the Lumbar Spine. In 2000, he was selected to be an AOA-Japanese Orthopaedic Traveling Fellow where he toured various academic universities in Japan. In the summer of 2003 he toured Europe as a Scoliosis Research Society traveling fellow.

Dr. Vaccaro has done extensive research on numerous topics related to spinal disorders. He has published well over 400 peer-review and non-peer review articles. He has authored over 180 book chapters and edited 10 textbooks. His current research projects include the timing of surgery after traumatic spinal cord injury, the use of alternative bone grafts substitutes including recombinant tissue engineering and the study of the concentration of osteoprogenitor stem cells in various locations of the skeletal system. The faculty, residents, and community physicians were treated to 3 innovating lectures from Dr. Vaccaro during the 2 days: "Disk Degenerative and Repair," "Contemporary Concepts Cervical Spine Trauma," and "A New T-L Facture Classification System."

Scott D. Boden, M.D.
2006 OREF Hark Lecturer, Residents' Research Days

This year at our annual Residents' Research Days on May 4 – 5th, 2006, we were honored to have Dr. Scott D. Boden as our OREF Hark Lecturer. Dr. Boden is currently a tenured Professor of Orthopaedic Surgery at the Emory University School of Medicine and serves as the Director of the Emory Orthopaedics & Spine Center. He is also the Clinical Director of the Whitesides Orthopaedic Research Laboratory and has received many awards including the Volvo Award for Low Back Pain Research (4 times), the Marshal Urist Young Investigator Award, the North American Spine Society Outstanding Paper Award (7 times), and the AAOS/ORS Kappa Delta Research Award. He has received the Leon Wiltse Award for Outstanding Contributions to the field of spine surgery from the North American Spine Society. Dr. Boden has authored over 130 peer-reviewed articles on spine and basic science topics as well as 30 chapters and 6 textbooks.

Dr. Boden is also the Co-Editor of Seminars in Spine Surgery, a Deputy Editor of SPINE, and an Associate Editor for Basic Science for the Journal of Bone and Joint Surgery. He has served as Program Chair of the American Orthopaedic Association in 2005 after serving on the Executive, Finance, Membership, and Critical Issues Committees for two years as a Member-at-Large. He has recently served as Secretary on the Board of Directors of the Orthopaedic Research Society, the International Society for Study of the Lumbar Spine, and the Eastern Orthopaedic Association of which he will serve as President in 2007.

Dr. Boden's basic research focus has centered on gaining an understanding of the biology of spine fusion healing and bone graft substitutes as well as the molecular control of bone formation and gene therapy applications for bone and intervertebral disc cartilage regeneration. Dr. Boden's interests also include innovative health care delivery strategies in a managed care environment and he is Founder and Chairmen of the National Spine Network, a collaboration of 25 Spine Centers of Excellence around the U.S. focusing on outcomes research and quality improvement. During the 2 days of lectures, the faculty, residents, and community physicians were treated to 2 lectures from Dr. Boden: "Osteoblast Regulation: It's a Smad, Smad World' and "Bone Graft Substitutes: Update 2006." In addition to Dr. Boden's lectures, the R3's and the R4's presented the progress of their research, while the R5's presented the completion of their research projects.

Msx1 Expression Pattern in Developing Human Digits

Abby L. Navratil, B.S., Kathleen K.S. Berfield, B.S., Philip Fleckman, M.D., Marcia L. Usui, and Christopher Allan, M.D.

Regeneration, as an alternative to the use of prosthetic devices, is an ultimate goal to improve the quality of life for limb amputees. Msx1, a gene encoding for a transcription repressor, has been shown to play a key role in development, tissue remodeling and regeneration. This transcription repressor is thought to prevent differentiation and is involved in a signaling pathway in regenerative organisms such as newts and salamanders. This pathway includes the proteins BMP4, a signaling ligand, and Notch1, a signaling cell surface receptor. In digit tip regeneration studies in mice, the regenerative region has been shown to express Msx1. When amputated within the Msx1 expressing region of the developing nail bed, mouse digits were able to regenerate, but when amputation occurred proximal to this region, regeneration did not occur. Msx1 has also been found within the region of the nail bed in human fetal digits. Clinically, it has been observed that children 11 years or younger are capable of regenerating digit tips if the amputation occurs in the nail bed.

Our study focuses on the expression pattern of the transcription repressor Msx1 across a developmental series of human fetal digits. As Msx1 has been found to be associated with regeneration, our goal is to describe the pattern of Msx1 expression during initial development of human fetal digits. This may help determine in which structures Msx1 expression is associated with in the developing digit and whether this correlates with the pattern of expression in the digit tip observed in mice and regenerative capabilities in humans. Understanding the pattern of Msx1 expression during development will also help us interpret ongoing studies of its expression in the human fetal digit after tip amputation.

Materials and Methods

Tissue

Fetal digits of an estimated gestational age (EGA) between 45 and 80 days were obtained from the University of Washington Center for Human Embryology with University of Washington Institutional Review Board approval. A total of 13 digits, of estimated gestational ages 43, 45, 46, 54, 57, 59, 67, 70, and 76 days, were studied. Digits were frozen in O.C.T. (Finetek, Sakura, Inc., Torrance, CA) and stored at -70°C. Six micron sagittal sections were cut with the use of a Leica cryostat. The structures of the developing nail unit and calcifying cartilage were used to confirm orientation and location within the digits. Sections from the mid section of the digit were selected for staining.

Immunohistochemistry

Standard immunoperoxidase immunohistochemistry was performed

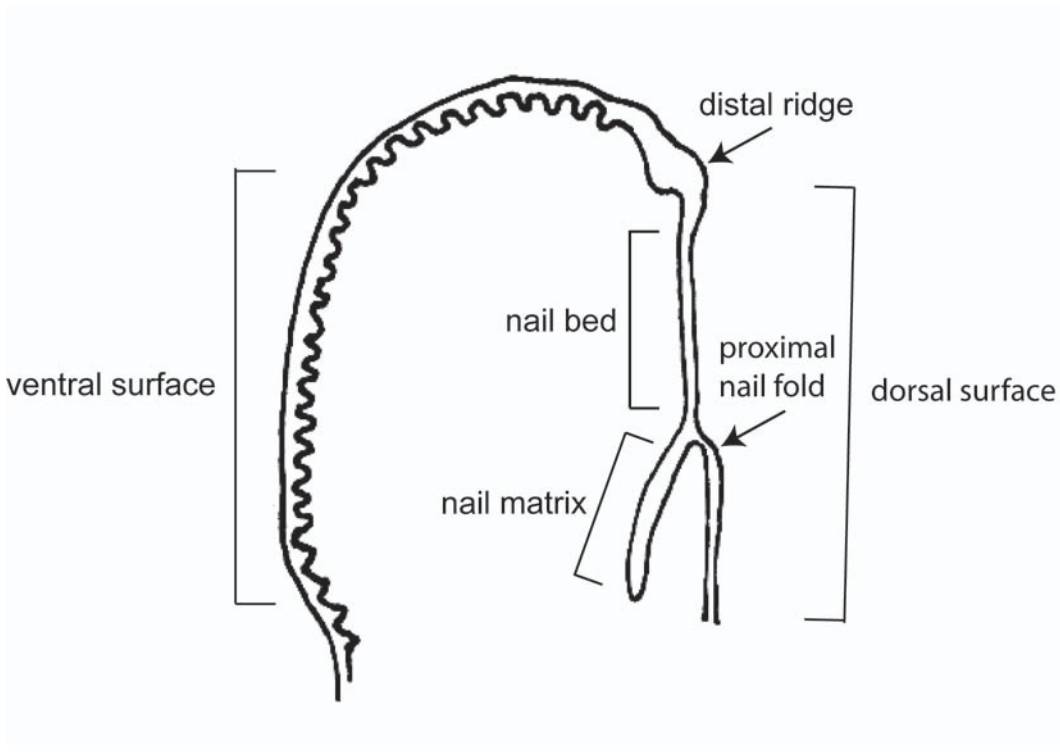

Figure 1: Human digit tip. Diagram shows important structures of the digit tip.

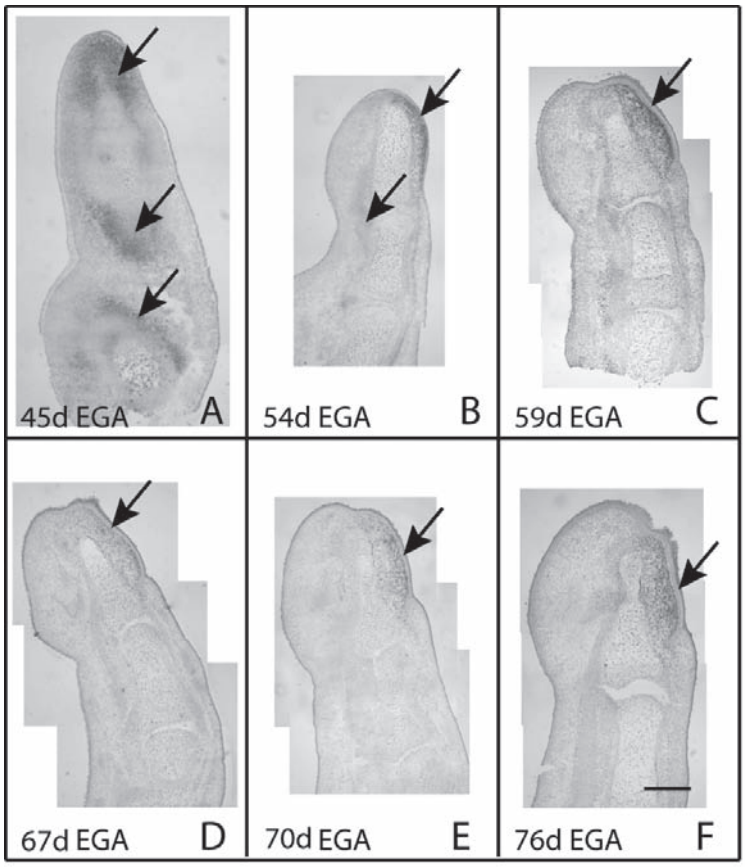

Figure 2A-F: Developmental series of Msx1 expression in human fetal digits. Images of digit sections of various ages immunostained for Msx1. All are sagittal sections taken near the middle of the digits. The magnification bar represents 408μm. Arrows point to areas of Msx1 expression. Msx1 staining is found throughout digit tip in areas surrounding developing bone in Figure 2A, restricted to the distal ridge and nail bed in Figures 2B and 2C and found only in the nail bed in Figures 2D-F.

to localize Msx1 expression. Briefly, tissue sections were fixed in cold acetone for 10 minutes, incubated with goat anti-Msx1 (Santa Cruz Biotechnology, Santa Cruz, CA) as primary antibody, biotinylated rat anti-goat as secondary antibody (Vector Laboratories Inc., Burlingame, CA), Vector Elite kit for streptavidin (Vector Laboratories Inc., Burlingame, CA) and 3-3′ diaminobenzidine as chromogen. Tris buffered saline was used for all washes and all incubations were conducted at room temperature.

Photomicrography

The stained tissue was photographed using a Nikon Microphot-SA microscope equipped with a Photometrics Sensys digital camera. Images were saved as Photoshop Pict files and the color was adjusted using Adobe Photoshop®.

Results

Up to three different digits from separate donors were used for each division of age, starting at 45 days and increasing by 5 days up to 80. Figure 1 shows a diagram of a digit with the relevant structures used to describe the location of Msx1 expression in this study.

The images in figure 2 are a representation of the expression pattern of MSX1 through a developmental series of digits with orientation in the same direction as in the diagram.

At an EGA of 45 days, the nail fold and distal ridge are not yet identifiable, as seen in Figure 2A. At this age, expression is present throughout the digit tip surrounding the developing bone. In addition, some expression is present in the proximal regions of the digit. In the 54 day digit (Figure 2B) the phalangeal precursors (cartilage) and interphalangeal joints have formed as the digit has matured. Expression is only present on the dorsal side of the digit in the region of the distal ridge and in the nail bed. The amount of proximal staining is considerably decreased when compared to the 45 day digit (Figure 2A). At 59 days of development (Figure 2C), the structures of the distal ridge, nail fold, and nail matrix have begun to form. Expression of Msx1 is restricted to the nail matrix, nail bed, and the developing distal ridge. In the 67 (2D), 70 (2E), and 76 (2F) day digits, the nail fold, nail matrix, nail bed, and distal ridge become increasingly more clearly defined and the staining continues to be closely associated with these structures.

The changes in expression of Msx1 correlate with previous mouse studies. The potential significance of this expression pattern is a possible association of Msx1 expression with retention of capacity for regeneration. The expression of Msx1 in the proximal regions of the 45 and 54 day human digits was not seen as an expression pattern in the developing mouse or rabbit studies. The more ubiquitous Msx1 staining in the early ages may be associated with undifferentiated connective tissue, as suggested by the association of Msx1 with loose connective tissue lying between the nail bed and distal phalangeal bone in mice.

Conclusions

Msx1 expression is present in the developing nail bed of human fetal digits. If Msx1 maintains cells in an undifferentiated state, it is likely that the zone of expression decreases as differentiation in the fetus progresses with maturity. Presence of Msx1 may play a key role in the regenerative capacity of amputated young human digits. We are presently using an organ culture system to study the possible regeneration after tip amputation of human fetal digits. This work may further elucidate the role of Msx1, if any, in human digit tip regeneration. These studies may also help to determine whether Msx1 is up-regulated during digit tip regeneration or if Msx1-expressing cells are recruited to the site of injury.

Recommended Reading

Han M, Yang X, Farrington JE, Muneoka K. Digit regeneration is regulated by Msx1 and BMP4 in fetal mice. Development 2003;130(21):5123-32.

Hu G, Lee H, Price SM, Shen MM, Abate-Shen C. Msx homeobox genes inhibit differentiation through upregulation of cyclin D1. Development 128:2373–2384.

Illingworth CM. Trapped fingers and amputated finger tips in children. J Pediatr Surg 1974;9(6):853-58.

Odelberg, S. Unraveling the Molecular Basis for Regenerative Cellular Plasticity. PLoS Biology 2004; 2(8):E232.

Reginelli AD, Wang YQ, Sassoon D, Muneoka K. Digit tip regeneration correlates with regions of Msx1 (Hox 7) expression in fetal and newborn mice. Development 1995; 121(4):1065-76.

Rinaldi A. The newt in us. EMBO Rep 2005; 6(2):113-5.

Acknowledgements

The authors gratefully acknowledge financial support from the Roberts Helping Hand Fund, the University of Washington Engineered Biomaterials project (NSF Cooperative Agreement EEC-9529161), the Council for Nail Disorders, and the George F. Odland Endowed Research Fund. We also thank the Dermatology Research Center at the University of Washington for assistance with immunohistochemistry and imaging.

Kinematic, Kinetic and Electromyographic (EMG) Analysis of Muscle Activity During Rise to the "Pointe" Position

Nancy Kadel, M.D., E.A. Donaldson-Fletcher, B.A., Ava Segal, B.A.S., and Michael Orendurff, M.S.

Overuse injuries and errors in the technical execution of dance movements leading to injury have been reported among female ballet dancers (Teitz, 1996; Macintyre, 2000). Knowledge of muscle activity and forces in the lower extremities during ballet movements, especially on pointe, may contribute to better understanding of these injuries and preventative strategies.

Electromyography (EMG) has been used to describe muscle activity during pliés, grand pliés, and many movements specific to ballet (Chatfield 1993-1994; Ryman and Ranney 1978-1979; Trepman 1994; Trepman 1998). However, to date EMG has not been combined with sophisticated motion analysis systems using force plates. Such a combination allows for the correlation of muscle activity with calculated moments, forces, and angles at the joints.

The purpose of this study is to describe kinematic, kinetic, and electromyographic analyses of ballet dancers performing four common dance movements on pointe, with the hypothesis that muscle activity and joint moments vary among different maneuvers used to achieve the en pointe position.

Materials and Methods

Subjects were four female ballet dancers from regional ballet companies, aged 22 to 24. All subjects were healthy and free of active injury at the time of study. Written informed consent for participation in the study was obtained from each subject, as was IRB approval.

Thirty-eight reflective markers were placed on each subject's head, trunk, pelvis, arms, hands, and feet in accordance with the Vicon's plug-in gait model. EMG surface electrodes were placed in pairs on the medial gastrocnemius, lateral soleus, peroneal, and tibialis anterior muscles as described by Delagi (Delagi ,1975). Subjects wore their own pointe shoes (SoDanca, Freed, and Bloch Alpha).

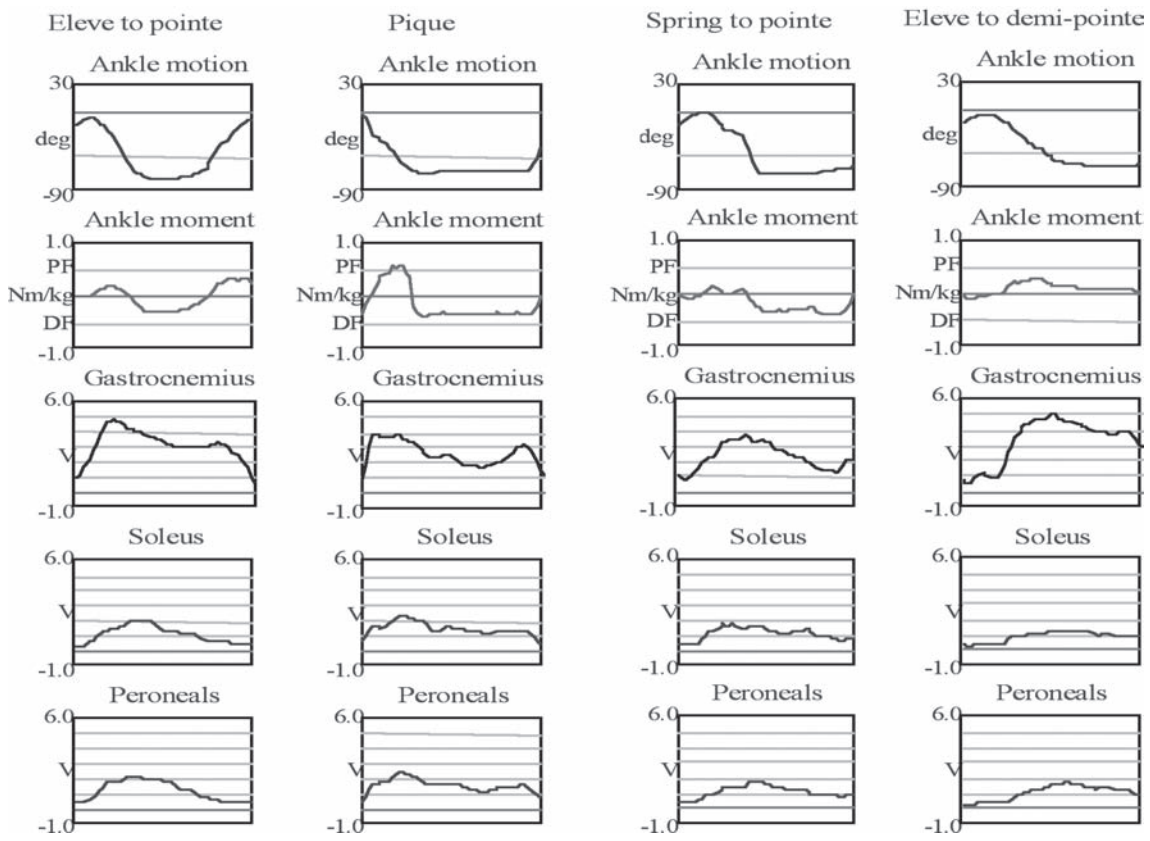

Figure 1: Graphs of ankle motion, moments and EMG activity of dancers for 4 different movements.

		Eleve-demi	Eleve-pointe	Spring up	Pique
Ankle Motion (degrees DF)	max	-6.924	-5.481	0.109	-1.248
	min	-63.708	-74.792	-71.651	-68.745
Ankle Moment (Nm/kg)	max	0.269	0.362	0.150	0.600
	min	-0.069	-0.293	-0.358	-0.350
Gastrocnemius (V)	max	5.091	4.922	3.706	3.930
	min	0.523	1.050	0.935	1.250
Soleus (V)	max	1.308	2.158	1.825	2.394
	min	0.334	0.353	0.424	0.651
Peroneals (V)	max	1.708	2.205	1.915	2.533
	min	0.301	0.447	0.374	0.571
Tibialis Anterior (V)	max	1.015	1.154	1.279	1.549
	min	0.466	0.599	0.566	0.573

Table 1: Maxima and minima of averaged data.

After sufficient warm-up the subjects stood with one foot on each of two force plates. Data were then collected using a ten-camera Vicon 612 system; marker displacements were recorded by infrared camera at 120 Hz, and EMG and force plate data were recorded at 600 Hz. Data were smoothed with a Woltring quintic spline with an MSE of twenty.

Each dancer performed three trials of each of four conditions. These included (with maximum voluntary isometric contraction of all muscles with the foot in plantarflexion): rise to demi-pointe position, rise to the pointe position (elevé), piqué passé (onto one foot), and a two-foot spring up to pointe.

Data analysis

Data were analyzed in Polygon. For each movement all trials were averaged, and maxima and minima were recorded for ankle motion (in degrees) and ankle moment (Nm/kg). For the EMG data the trials were averaged and maxima and minima were recorded for the

Figure 2A: Dancers performing arabesque on pointe unsupported.

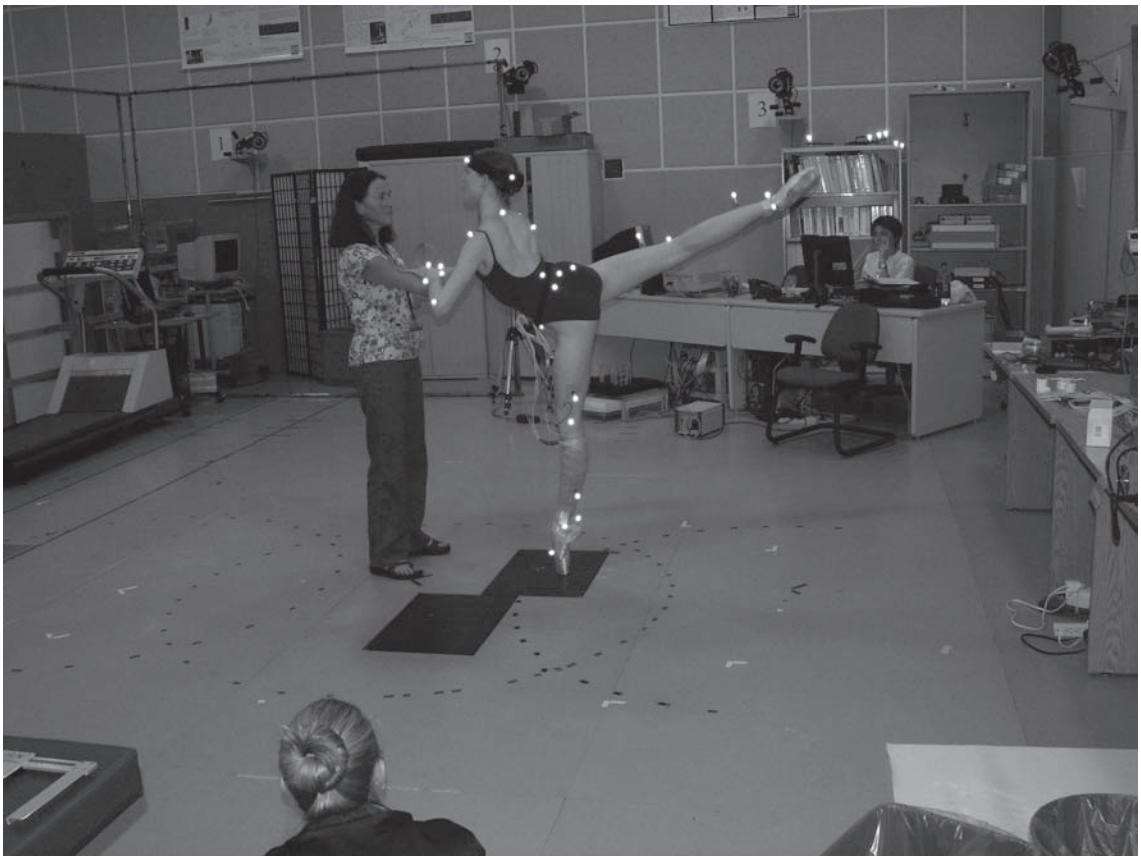

Figure 2B: Dancers performing arabesque on pointe supported.

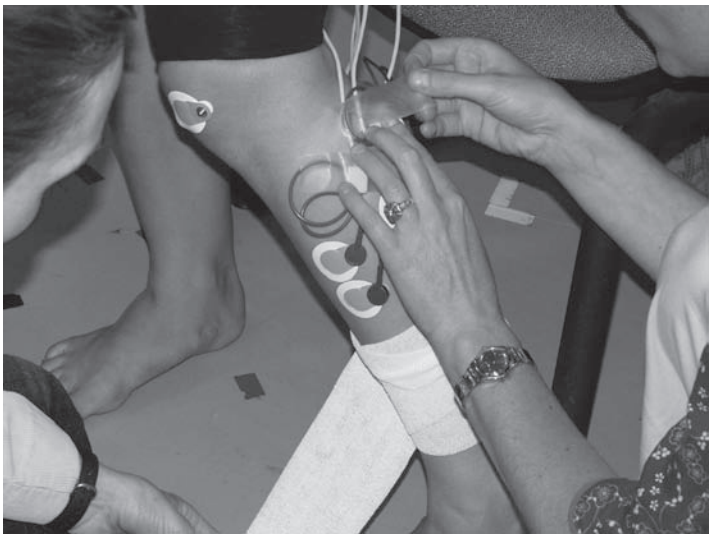

Figure 2C: Placement of EMG leads.

gastrocnemius, soleus, peroneals, and tibialis anterior.

Results

Graphs of the averaged twelve trials (four dancers with three trials each) for each ballet movement are shown in Figure 1. The maxima and minima of the averaged data for ankle motion (in degrees dorsiflexion, DF), ankle moment, EMG gastrocnemius, EMG soleus, EMG peroneals, and EMG tibialis anterior are presented in Table 1.

Discussion

Kinematically, the results indicate that dancers experience the greatest degree of plantarflexion on pointe following an elevé, rather than a spring onto pointe or a step onto pointe (a piqué). This may be due to the fact that the elevé takes the most time, allowing the dancer to bend the shoe as much as possible. It is also interesting to look at the ankle motion in Figure 1 at the initiation of the rise to pointe; for the three moves on two feet (elevé to pointe and demi-pointe, and the spring to pointe), the ankle dorsiflexes slightly at first, providing momentum for the rise to pointe. Once on pointe, the ankle moment graphs show dorsiflexion moments. This suggests that the dancers have plantar-flexed beyond vertical, resulting in the ankle ligaments creating a dorsiflexion moment.

Muscle activity (as shown by the EMG results) for all four muscles was

Figure 2D: Dancer on pointe on the force plate.

highest during the rise to pointe, and then decreased once the en pointe position was achieved. There were differences between the ballet moves in terms of muscle activity during rise to pointe. Gastrocnemius activity was markedly higher for the elevé to pointe and the elevé to demi-pointe. This finding could be due to a lower angular velocity during the elevé movements compared to the spring up or step to pointe. Soleus activity was lowest during the rise from foot-flat to demi-pointe. Upon further rise to full pointe the soleus activity was similar to the spring up to pointe and the piqué, suggesting that soleus activity contributes to achieving the en pointe position. Biomechanical understanding of common athletic and ballet movements is necessary for developing effective training strategies, and for the prevention and treatment of injuries among dancers and athletes.

Recommended Reading

Barringer, J., and Schlesinger, S.: The Pointe Book: Shoes, Training & Technique. Edited, Hightstown, NJ, Princeton Book Co., 1998.

Chatfield, S.J.: Electromyographic response of dancers to isokinetic work and select dance movements. Kinesiology and Medicine for Dance 16(1): 60-82, 1993-1994.

Delagi, E.F., Perotto A., Iazzetti J., Morrison D. Anatomic Guide for the Electromyographer, Springfield IL, CC Thomas, pp. 144-157, 1975.

Dozzi, P. A., and Winter, D. A.: Biomechanical analysis of the foot during rises to full pointe: implications for injuries to the metatarsal-phalangeal joints and shoe redesign. Kinesiology and Medicine for Dance, 16(1): 1-11, 1993-4.

Galea, V., and Norman, R. W.: Bone-on-bone forces at the ankle joint during a rapid dynamic movement. International Series on Biomechanics IX-A, 5A: 71-76, 1985.

Musculoskeletal Workload vs. Musculoskeletal Clinical Confidence Among Primary Care Physicians in Rural Practice

Joseph R. Lynch, M.D., Gregory C. Gardner, M.D., and Rex R. Parsons, M.D.

Musculoskeletal problems are a major source of pain and disability in our society. The most recent data from the National Health Interview Survey indicates that currently there are 40 million people in the US with musculoskeletal conditions, and by 2020 it is projected that 60 million will be affected. In addition, more than two-thirds of the population has sustained musculoskeletal injuries, and greater than one-third of these injuries result in long-term sequela. The prevalence of locomotor disability secondary to musculoskeletal disorders rises from 3.1% in those less than 60 to almost 50% in those aged more than 75 years. In 1995, more than 38 million new problem visits were made to physicians in an office-based practice for musculoskeletal disease, at a cost exceeding $215 billion.

To achieve high-quality, cost effective musculoskeletal care all physicians must understand the basic principles of diagnosis and management of musculoskeletal disorders. Primary care physicians must be facile with musculoskeletal medicine as they are often the first to evaluate, treat, and determine the need for referral. This is particularly true in rural areas, such as the area under study, where there is no full-time orthopedic surgeon or rheumatologist. The purpose of this study is to evaluate the prevalence of musculoskeletal visits in a rural Oregon primary care office and the self-assessed knowledge and skills for such conditions.

Methods

Setting: An internal medicine clinic in rural Oregon serving approximately 5,000 patients with an average age of 55 years. It is one of three primary care offices serving the local county with a population of approximately 23,800.

Study Population: The study population consisted of all patients seen between 1 April 2002 and 30 April 2002 on an outpatient basis in the clinic. In addition, all nine primary care physicians (four internal medicine physicians and five family physicians) serving the county population were given a self-administered questionnaire (Table 1).

Data Collection: The number of patients presenting with musculoskeletal complaints was recorded. A patient was considered to have a musculoskeletal complaint if the problem was significant enough to receive medical intervention during that visit – pharmacotherapy, physical therapy, or referral to a musculoskeletal specialist (orthopedic surgeon, rheumatologist, or physiatrist). In those patients where multiple medical problems were being managed, distinction was not made between primary and secondary reasons for the office visit. The prevalence of musculoskeletal complaints was then calculated as a percentage of the total number of patients seen during the designated period of study. Referral or need for hospitalization was also recorded.

Self-administered questionnaires were distributed to the nine primary care physicians in the county. Personal

Please indicate your RELATIVE comfort and expertise in performing the following: ***Not confident Extremely confident*** ***1 2 3 4 5 6 7 8 9 10***										
(1) Comprehensive musculoskeletal examination	1	2	3	4	5	6	7	8	9	10
(2) Comprehensive neurological examination	1	2	3	4	5	6	7	8	9	10
(3) Comprehensive cardiovascular examination	1	2	3	4	5	6	7	8	9	10
(4) Comprehensive pulmonary examination	1	2	3	4	5	6	7	8	9	10
(5) Joint aspiration of the knee	1	2	3	4	5	6	7	8	9	10
(6) Joint injection of the knee	1	2	3	4	5	6	7	8	9	10
(7) Joint aspiration of the shoulder	1	2	3	4	5	6	7	8	9	10
(8) Joint injection of the shoulder	1	2	3	4	5	6	7	8	9	10
(9) Performing a paracentesis	1	2	3	4	5	6	7	8	9	10
(10) Performing a lumbar puncture	1	2	3	4	5	6	7	8	9	10
(11) Performing a flexible sigmoidoscopy	1	2	3	4	5	6	7	8	9	10
(12) Performing a bone marrow biopsy	1	2	3	4	5	6	7	8	9	10
(13) Principles of cardiac rehabilitation	1	2	3	4	5	6	7	8	9	10
(14) Principles of fracture casting/bracing/rehabilitation	1	2	3	4	5	6	7	8	9	10

Table 1: Self-administered questionnaire used to assess physicians' level of confidence.

Diagnosis	*Number*	*Referral*	*Hospital Admission*
Osteoarthritis	11	2 (ortho)	
Back Pain	11	2	
Osteoporosis	5	(ortho/rheum)	
Carpal tunnel syndrome	2		
Cervical radiculopathy	2		
Polymyalgia Rheumatica	2		
Shoulder Impingement	2		1 (shoulder pain)*
Wrist Fracture	1	1 (ortho)	
Ankle Sprain	1	1 (ortho)	
Psoriatic arthritis	1		
Trapezius strain	1		
Cellulitis, r/o joint infection	1		
Unknown elbow mass	1		
Synovial cyst	1	1 (ortho)	
ACL injury	1		
MCL strain	1		
Dislocated patella	1		
Patello-femoral syndrome	1		
Gout	1		
Bursitis	1		
Total Musculoskeletal Disorders	48		
Total Patients evaluated (April 1 – 30)	274		
Prevalence of Musculoskeletal Disorders	17.5%		

Table 2: Musculoskeletal disorders evaluated between 1 April 2002 and 30 April 2002. * This patient was admitted for an acute episode of shoulder pain, treated with intra-articular injection of lidocaine + steroids by the consulting orthopaedic surgeon, and discharged on hospital day #2 with a diagnosis of shoulder OA.

reminders with additional copies of the questionnaire were provided to each physician after the initial distribution. Fourteen questions were designed to elicit self-reported confidence in the management of commonly seen musculoskeletal and medical disorders. Confidence was measured on a 10-point Likert scale. Response options varied from 1 (not confident) to 10 (extremely confident) (Table 1). Six of the 14 items dealt with the management of musculoskeletal disorders. For comparison purposes eight questions addressed common medical issues. Four questions addressed confidence with skills for musculoskeletal, neurological, cardiac, and pulmonary examinations. Similarly, eight questions addressed confidence with simple office procedures (four common musculoskeletal procedures and four common medical procedures). Lastly, physician confidence was self-assessed regarding musculoskeletal and cardiac rehabilitation. Confidence scores for each question were summed among all returned questionnaires and 'level of confidence' was reported as an average of the summed scores. Trends in physician confidence were interpreted by comparing average confidence scores between individual questions.

Results

Two hundred seventy four patients were evaluated in an outpatient medical setting between 1 April 2002 and 30 April 2002. The prevalence of musculoskeletal disorders was 17.5% (n=48) among these office visits (Table 2). Sixteen percent (n=8) of patients presenting with musculoskeletal disorders were referred to other physicians – orthopedic surgeons receiving the majority of referrals (75%, n=6). One case of acute shoulder pain (with no other co-morbid illness) resulted in hospital admission representing 2% (n=1) of all musculoskeletal complaints seen as an outpatient in the one-month period of study.

Of the nine self-administered surveys, six were returned. Three physicians did not complete the survey. Among the six physicians who completed the survey, three were internal medicine physicians and three were family physicians. Physician confidence as measured by an average of the summed score for each question is listed in Table 3. The physicians surveyed felt most confident performing comprehensive cardiovascular examinations and least confident performing comprehensive musculoskeletal examinations (avg. confidence score 9.6 and 7.0, respectively). The physicians felt most confident with the performance of flexible sigmoidoscopy and least comfortable with joint injection of the shoulder (avg. confidence score=9.6 and 3.0, respectively). Lastly, the physicians surveyed appeared more confident with the principles of cardiac rehabilitation than with the principles of bracing and casting (average confidence score 8.6 and 3.6, respectively). Overall, the physicians reported higher confidence managing medically related outpatient problems when compared to outpatient musculoskeletal problems (avg. confidence scores 9.0 and 4.2,

Management	*Mean Confidence Score*
Comprehensive musculoskeletal examination	7.0
Comprehensive neurological examination	8.6
Comprehensive cardiovascular examination	9.6
Comprehensive pulmonary examination	9.3
Joint injection of the knee	3.6
Joint aspiration of the knee	5.3
Joint injection of the shoulder	3.0
Joint aspiration of the shoulder	3.0
Performing a Paracentesis	8.6
Performing a lumbar puncture	9.0
Performing a Flexible Sigmoidoscopy	9.6
Performing a Bone Marrow Biopsy	9.0
Principles of cardiac rehabilitation	8.6
Principles of fracture casting/bracing and rehabilitation	3.6
Total Musculoskeletal Management	4.2
Total Medical Management	9.0

Table 3: Mean confidence scores for selected conditions.

respectively).

Discussion

The prevalence of musculoskeletal disorders evaluated in various primary care settings has been examined previously and ranges between 23% and 37%. Based on the frequency of musculoskeletal problems seen in primary care offices in both urban and rural areas of the United States, competence in managing musculoskeletal disorders is a necessity for any primary care physician. In this study physician confidence is used as an indirect measure of competence. Confidence relates to the concept of perceived self-efficacy, which reflects personal judgments of one's capacity to perform a given type of activity. The lower levels of confidence relating to the management of musculoskeletal disorders suggest that there is a disparity between musculoskeletal knowledge and the skill level required by primary care physicians. Required training in musculoskeletal medicine during medical school and the postgraduate years is a means of addressing this disparity. However, emphasis should be placed on common musculoskeletal disorders encountered in a primary care practitioner's office. Clinical rotations where students and residents are afforded the opportunity to practice physical exam skills, correlate clinical findings with musculoskeletal anatomy, and perform outpatient procedures are likely to be more beneficial than required rotations on an orthopaedic service, for example, which may emphasizes the surgical management of disease. These concerns may become more pressing as the prevalence of musculoskeletal disorders continues to rise over the next two decades.

Recommended Reading

Helmick CG, Lawrence RC, Pollard RA Lloyd E, Heyse SP. Arthritis and other rheumatic conditions: who is affected now and who will be affected later. Arthritis Care Res 1995;8:203-211.

Vernec A, Shrier I. A teaching unit in primary care sports medicine for family medicine residents. Acad Med 2001;76:293-296.

Kahl LE. Musculoskeletal problems in the family practice setting: guidelines for curriculum design. J Rheumatol 1987;14:811-814.

Rosenblatt RA, Cherkin DC, Schneeweiss R, Hart LG, Greenwald H, et al. The structure and content of family practice: current status and future trends. J Fam Pract 1982;15:681-722.

Donohoe, MT, Kravitz RL, Wheeler DB, Chandra R, Chen A, Humphries N. Reasons for outpatient referrals from generalists to specialists. J Gen Intern Med 1999;14:281-286.

Positive Outcomes Observed in Commercially-Funded Studies at a National Orthopaedic Meeting are not Associated with Better Study Design or Larger Sample Size

Mary R.A. Cunningham, M.D., Winston J. Warme, M.D., Douglas C. Schaad, Ph.D., Fredric M. Wolf, Ph.D., and Seth S. Leopold, M.D.

The association between commercial research funding and "positive" and/or pro-industry outcomes of published research has been examined in dozens of studies across a spectrum of specialties. But most of these reports do not control for potential scientific factors, including quality of study design or sample size, which may account for observed findings.

The present study evaluates the following hypotheses in an analysis of the research presented at the annual meeting of the 2004 American Academy of Orthopaedic Surgeons (AAOS): (1) Non-scientific factors, such as funding source, orthopaedic subspecialty, and geographic region of origin, are associated with positive study outcome; (2) scientific factors, including study design, sample size, and presence or absence of control groups, are associated with positive outcome; (3) commercially funded studies do not differ from either non-funded or other-source-funded studies in terms of outcome, design, use of control groups, or sample sizes.

Materials and Methods

We evaluated all 747 abstracts of podium and poster presentations published in the meeting. Purely descriptive abstracts, non-clinical papers, registry studies, and meta-analyses were excluded, the latter to avoid duplicate inclusion of data. This left a total of 661 studies for analysis.

Two experienced orthopaedic surgeons independently evaluated blinded copies of each abstract to classify each study as to its outcome (positive or not positive) based on previously published and well-accepted criteria.

A dataset was then compiled that included each abstract's country of origin, orthopaedic subspecialty (e.g. adult reconstruction, spine, etc), and funding source. For purposes of this analysis, three funding subgroups were created, based on disclosures provided by the authors of each abstract: (1) any commercial funding, (2) only non-commercial funding (e.g., exclusively through philanthropic or government-based sources), and (3) no funding conflicts disclosed.

Formal evaluation of study quality and levels of evidence is not possible using only the material provided in the AAOS 250-word abstract format; therefore, we used surrogate endpoints for scientific quality. The elements of study design, including use of a control group and prospective or retrospective evaluation, were taken to be surrogate measures of study quality (Tables 1 and 2); we also recorded sample sizes for treatment and control groups to give insight into the likelihood of type-II statistical error as a potential cause of non-positive study outcomes.

Analysis of Scientific Factors	N (661)	Percentage
Study Design		
Prospective	192	29.0
Retrospective	147	22.2
Not Stated/Indeterminate	135	20.4
Cadaveric	49	7.4
Basic Science/Bench	77	11.6
Descriptive/Observational	61	9.2
Use of Control Group		
Yes	263	39.7
No	257	38.9
Not Stated/Indeterminate	142	21.5

Table 1: Analysis of scientific factors.

Results

Of the 661 studies analyzed, 481 (72.8%) concluded with a positive outcome. Commercially funded studies were significantly more likely to conclude with positive outcomes than were non-funded studies ($p=0.04$; odds ratio=1.61, 95% C.I.=1.02 to 2.55). Receipt of commercial funding was the only non-scientific factor associated with positive outcome. By contrast, non-commercially funded studies were no more likely to be positive than non-funded studies ($p>0.05$), and neither orthopaedic subspecialty nor geographic origin were associated with positive study outcomes ($p=0.07$, and $p=0.24$, respectively). Studies utilizing control groups were significantly more likely to conclude with non-positive outcomes ($p<0.001$); however, prospective studies were not significantly more likely to conclude positively than were retrospective studies ($p=0.065$). Sample sizes for control and treatment groups were

Funding	Commercial	Non-funded	p-value
Scientific Factors			
Study Design			
Prospective	88	44	
Retrospective	66	41	0.57
Control Group			
Yes	101	62	
No	165	80	0.39

Table 2: Comparison of Commercially-funded and Non-funded Trials as to Scientific Factors. Among studies that provided financial disclosures for all authors; excludes 22 studies that received philanthropic but no commercial funding.

not found to be significantly different between positive and non-positive outcomes (p=0.27, and p=0.17, respectively), suggesting that non-positive studies were not more likely to be hampered from beta error.

Between commercially-funded and non-funded studies, there were no statistically significant differences in use of prospective study design (p=0.57), inclusion of a control group (p=0.39), or size of the control groups when controls were used (p=0.85). The increased frequency of positive outcomes observed in commercially-funded studies compared to non-funded studies could not be explained by any observable differences in the quality of the study design (prospective or controlled), or by meaningful differences in sample sizes of the control groups.

Discussion

Numerous studies identify an association between receipt of commercial funding and study outcomes that are supportive of the industry sponsor's product; however, the designs of these studies are generally insufficiently robust to examine the potential causes of the observed association. This is a major limitation to the literature as it now exists as scientific factors have been posited as perhaps explaining what first appears to be a finding related to the presence of financial conflicts of interest. Some scientific factors that have been proposed as potential explanations for this finding include the possibility that:

• Ample levels of funding provided by commercial sources may allow for larger sample sizes which, in turn, diminish the likelihood of type-II error.

• Commercially-funded investigators may be "better" investigators.

• Large commercial firms may conduct extensive in-house experimentation before collaborating with academic scientists, perhaps leading to collaborative areas of inquiry that are more likely to succeed.

It is widely agreed that this third explanation is not as relevant to orthopaedic implant manufacturers as it might be to pharmaceutical firms; thus, the present study investigated the first two potential explanations, but found no evidence in support of them. We observed that although commercially funded research is more likely to conclude with a positive or industry-friendly outcome, those commercially funded projects were no more likely than non-funded research to have used better study design or larger sample sizes.

The strengths of our study include its cross-sectional nature and a large sample size. This supports the conclusion that observed, no-difference findings were not the result of inadequate statistical power. Additional strengths included blinded analysis, use of standardized criteria by experienced reviewers, and evaluation of the most-commonly cited potential scientific factors that previously have been used as explanations for the consistent funding-outcome relationship.

The present report is limited by the inability to perform an in-depth analysis of study quality, either using levels-of-evidence scale or other accepted tools, given only the limited material presented in an abstract. Surrogate measures analyzed may not have been sufficiently robust to identify important differences in quality or relevance that result in acceptance for presentation at the annual meeting; however, the surrogates chosen for study quality are hallmarks of the scientific method and benchmarks of well-designed research. Another concern centers on assessment of funding. While funding was evaluated in this report as a categorical variable, it may behave more like a continuous variable. Investigators who disclosed commercial relationships may get support ranging from low-level laboratory support or sample implants to test up to six-figure (or more) consulting salaries or royalties; AAOS disclosures do not provide sufficient information to render a deeper analysis of this issue. That said, there is evidence that the relationships between physicians and industry are complex, and do not require tremendous dollar amounts to generate commitment, and that psychosocial influences on investigators may play a role in addition to financial ones.

There are two critical questions to this line of research:

• Is the preponderance of positive outcomes in published or presented research indicative of actual bias?

• If bias does exist, is it truly the result of commercial influence or does it derive from other sources such as investigator self-censorship, reviewer-based issues such as framing effects, or editor-level publication bias?

The bias question is important. First, publication bias is insidious and undetectable to even the most careful reader of individual trials. Such bias can only be demonstrated when analyzing a large sample size drawn from a particular universe of research (i.e., research proposed, submitted for review, presented, or published). Second, the science of meta analysis substantially depends upon the absence of publication bias, as meta analyses are largely limited to evaluation of research presented and published. As we grow increasingly reliant upon meta-analyses of published trials to make informed treatment decisions, we should, as a specialty, give greater attention to studies designed to identify, define, and address the possibility of

publication bias.

Our report did not analyze the universe of experiments submitted to the AAOS, and so it cannot conclude that the apparent preponderance of positive studies—in particular, the association between commercial funding and positive outcome—represents true bias. However, the present report did investigate the most commonly proposed potential scientific explanations for the very high frequency of positive findings in commercially funded research, namely better study quality and larger sample size. We found no evidence to support a scientific explanation for the disproportionate frequency with which commercially funded studies reached industry-friendly conclusions.

Recommended Reading

Leopold SS, Warme W, Fritz Braunlich E, Shott S. Association between funding source and study outcome in orthopaedic research. CORR 2003;415:293-301.

Dickersin K. The existence of publication bias and risk factors for its occurrence. JAMA 1990;263:1385-9.

Bhandari M, Busse J, Jackowski D, Montori V, Schunemann H, Sprague S, Mears D, Schemitsch E, Heels-Ansdell D, Devereaux P. Association between industry funding and statistically significant pro-industry findings in medical and surgical randomized trials. CMAJ 2004;170-4:477-80.

Olson C RD, Cook D, Dickersin K, Flanagin A, Hogan J, et al. Publication bias in editorial decision making. JAMA 2002;287:2825-8.

Botox Induced Muscle Paralysis Equally Diminishes Bone Mass in Young and Old Mice

Laura J. Matsen, Sarah E. Warner, Ph.D., Sandra L. Poliachik, M.D., Sundar Srinivasan, Ph.D., Philippe Huber, B.S., and Ted S. Gross, Ph.D.

Enhanced skeletal fragility associated with aging occurs in parallel with diminished muscle function. However, it is unknown whether acutely diminished muscle function in the elderly precipitates an equivalent loss of bone mass as occurs in young skeletons. Given that muscle strength has already substantially declined in the elderly, it is reasonable to speculate that further diminishment of muscle function by acute paralysis would be less influential in contributing to decreased bone mass than paralysis in a young adult skeleton. We have recently demonstrated that acute hindlimb muscle paralysis induced by Botox provokes a precipitous loss of bone in the young adult mouse. As older mice, like humans, demonstrate reduced bone morphology and diminished muscle function compared to young adult mice, we hypothesized that the aged skeleton would be less sensitive to bone loss associated with acute muscle paralysis.

Methods

Female C57B6/J mice of two ages (16 wk vs 2 yr) were contrasted in this study. Mice of both ages were randomly assigned to either saline (16 wk: n=10; 2 yr: n=6) or Botox (16 wk n=10, 2 yr: n=6) groups. At day zero all mice received IM injections of saline (10 µl) or Botox (10 µl of 2.0 unit/100 g) in both the quadriceps and calf of the right leg. Following sacrifice, quadriceps and calf wet weights were determined (the tibia of one 2 yr saline mouse fractured during dissection and was not included in further analyses). The right tibia of each mouse was imaged via micro-CT at a 10.5 µm voxel nominal resolution. Analyses were performed at the proximal tibial metaphysis of each tibia to determine tissue volume (mm^3), bone volume (mm^3), bone volume/tissue volume (BV/TV; %), trabecular number (#/mm), thickness (mm), and spacing (mm). At the tibia mid-diaphysis, a cortical bone site, periosteal volume (mm^3), cortical volume (mm^3), endocortical volume (mm^3), and cortical thickness (mm) were each quantified.

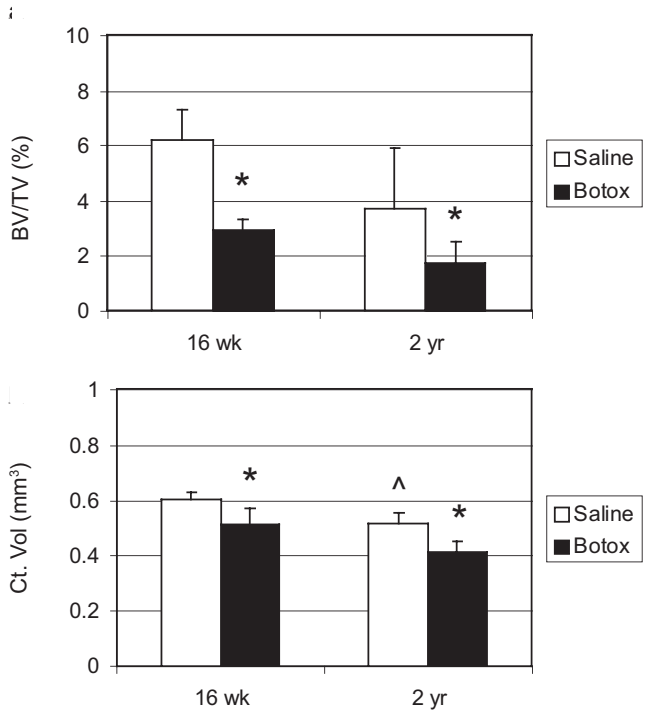

Figure 1: The mean (S.D.) ratio of tibia metaphysis bone volume to tissue volume (BV/TV, %, a) and mid-diaphysis cortical volume (Ct.Vol, mm^3, b) in the right tibia of 16 wk and 2 yr old saline and Botox treated mice. Ct.Vol, but not BV/TV, was significantly diminished in older vs younger saline mice (^, p=0.001). Acute hindlimb muscle paralysis significantly diminished both BV/TV and Ct.Vol in both 16 wk and 2 yr old mice (*, all $p < 0.01$).

Results

At the tibia metaphysis, the mean (± S.D.) BV, TV, BV/TV, trabecular number, thickness and spacing did not differ statistically in the saline treated limbs of 16 wk and 2 yr mice. Trabecular number was increased 25.5% in 2 yr old mice (p=0.13), while trabecular thickness was decreased -17.9% (p=0.001). Mean trabecular spacing was unchanged. At the mid-diaphysis, cortical bone volume was decreased -14.5% in the 2 yr compared to 16 wk mice (p=0.001). The loss was achieved via a 57.7% expansion of the endocortical volume (p=0.001), which overwhelmed the 14.0% increase in periosteal, or outer surface, volume (p=0.002). As a result, cortical thickness was decreased -22% in the older mice (p=0.001).

Compared to their respective saline groups, Botox induced muscle paralysis similarly diminished calf muscle mass in both 16 wk (-59.7%, p<0.001) and 2 yr old mice (-58.7%, p<0.001). At the tibia metaphysis, Botox reduced BV/TV in 16 wk (-53.2%, p<0.001) and 2 yr old mice (-55.7%, p<0.01). Trabecular thickness was significantly decreased by Botox treatment for young adult and old mice, but more substantially in the 2 yr old mice (16 wk: -24.9%, p<0.001; 2 yr: -43.6%, p<0.01). Conversely, trabecular spacing was increased in Botox mice compared to saline mice but the older mice did

not reach statistical significance due to group size (16 wk: 7.2%, p=0.05; 2 yr: 25.8%, p=0.07). At the tibia mid-diaphysis, Botox treatment served to substantially diminish cortical bone volume in both 16 wk (-15.0%, p<0.001) and 2 yr old mice (-18.9%, p<0.01).

When compared between Botox and saline groups, periosteal volume was reduced but did not reach statistical significance either for 16 wk (-2.6%, p=0.12) or 2 yr old mice (-3.8%, p=0.07). Diminished cortical bone volume was therefore achieved primarily via endocortical expansion at both ages (16 wk: 16.4%, p=0.002; 2 yr old: 9.9%, p=0.02). Cortical thickness was similarly diminished by muscle paralysis in 16 wk (-16.3%, p<0.001) and 2 yr old mice (-19.5%, p=0.02).

Discussion

By 16 wk of age, C57 mice have ceased rapid growth and demonstrate a plateau in trabecular and cortical bone properties. By 2 yr of age, the mice are noticeably less active and demonstrate a near 50% mortality rate consistent with classification as an aged population. The tibia of the 2 yr old mice demonstrated significantly reduced cortical bone volume compared to 16 wk mice, but differences at the metaphysis were more subtle. While BV/TV was maintained, increased trabecular number and decreased trabecular thickness in the 2 yr mice were suggestive of accumulated remodeling over time. Contrary to our hypothesis, however, acute hindlimb muscle paralysis induced equivalent losses in both trabecular and cortical bone in 2 yr old vs 16 wk old mice relative to respective saline mice. Startlingly, the mean cortical thickness of the 2 yr old mice following Botox treatment was only 2.7 fold greater than the mean trabecular thickness found in a 16 wk old mouse. In both the 16 wk and 2 yr old mice, micro-CT data suggested that bone alterations were primarily achieved via substantial osteoclastic activation, but this observation remains to be confirmed via histomorphometry. These data do suggest that whatever role muscle function plays in maintaining bone homeostasis, age induced musculo-skeletal alterations do not mitigate this effect. In fact, given that the aged skeleton already demonstrates reduced structural capacity, the superimposition of further degradation may extract an increased structural cost. Given that the aged are more likely to undergo acute bouts of diminished muscle function due to illness or surgery, such events may serve to incrementally elevate fracture risk and emphasize the need to maintain muscle strength in the elderly.

Acknowledgements

This work was supported by NIH (AR45665) and the Sigvard T. Hansen, Jr. Endowed Chair for Orthopaedic Traumatology.

Supported in part by a grant from the Washington Women's Foundation.

Recommended Reading

Parfitt, AM, The attainment of peak bone mass: what is the relationship between muscle growth and bone growth, Bone, 34:767-770, 2004.

Warner SE, Sanford DA, Berker BA, Bain SD, Srinivasan S, Gross TS, Botox induce muscle paralysis rapidly degrades bone, Bone, in press.

Brodt, MD, Ellis, CB, Silva, MJ, Journal of Bone and Mineral Research, 14:2159-66, 1999.

The Posteromedial Fragment in Bicondylar Tibial Plateau Fracture Patterns: Fracture Morphology and Relationship to the Tibial Less Invasive Stabilization System

David P. Barei, M.D., F.R.C.S.C., Timothy J. O'Mara, M.D.,
Alexis Falicov, M.D., Ph.D., Lisa A. Taitsman, M.D., M.P.H., and Sean E. Nork, M.D.

Articular comminution complicates bicondylar tibial plateau fracture management. A notable injury pattern of the medial plateau appears to be a coronal plane fracture resulting in a separate posteromedial osteoarticular fragment. The frequency and morphology of this fracture pattern remains largely undescribed.

Advances in fracture fixation include percutaneous surgery and fixed-angle screw/plate implants. The tibial Less Invasive Stabilization System (LISS) (Synthes, Paoli, PA) is representative of these advances. The relationship between the tibial plateau fracture morphology and the LISS fixed screw trajectories remains essentially unknown.

The primary purposes of this paper are to describe the frequency and morphology of the posteromedial articular fragment in the setting of bicondylar tibial plateau fractures using computed tomographic scanning. Using three-dimensional computer modeling, we will secondarily assess the ability of the tibial LISS to engage this fragment.

Materials and Methods

Between May 2000 and March 2003, 170 OTA C-type bicondylar tibial plateau fractures were identified using an orthopaedic database. One hundred and forty-six salvageable fractures had computed tomographic (CT) scans performed prior to definitive fixation, and were reviewed using the picture archiving and communication system (PACS).

The CT scans of all 146 fractures were reviewed by two observers using PACS. A medial articular injury was defined by the presence of a fracture line involving the medial tibial plateau articular surface on the axial CT images. Sixty-six (45.2%) injuries involved the medial articular surface. Nine with suboptimal CTs were excluded, leaving fifty-seven injuries for review.

Morphologic Assessment

All fifty-seven CT scans were interpretable and reviewed by two observers. In patients treated with temporary external fixation (49%), the post-manipulation CT scan was used. CT scans were performed using a standard protocol on a General Electric CT scanner. Axial images with sagittal and coronal reformations were available for all 57 fractures.

Using PACS, the major medial tibial plateau articular fracture line was identified on the axial CT image at the level of the articular surface. The angle subtended by the major medial articular fracture line and the posterior femoral condylar axis (PFCA) was considered the major medial articular fracture angle (MAFA) (Figure 1). This angle was given a positive value if the major medial articular fracture line was internally rotated relative to the PFCA, or a negative value if the major medial articular line was externally rotated relative to the PFCA. These angles were then plotted on a scatter diagram. A clustering of MAFAs was identified with an apparent maximum and minimum angle range. Injuries that demonstrated MAFAs within this range were further evaluated and considered as coronal plane fractures of the medial plateau generating a posteromedial fragment.

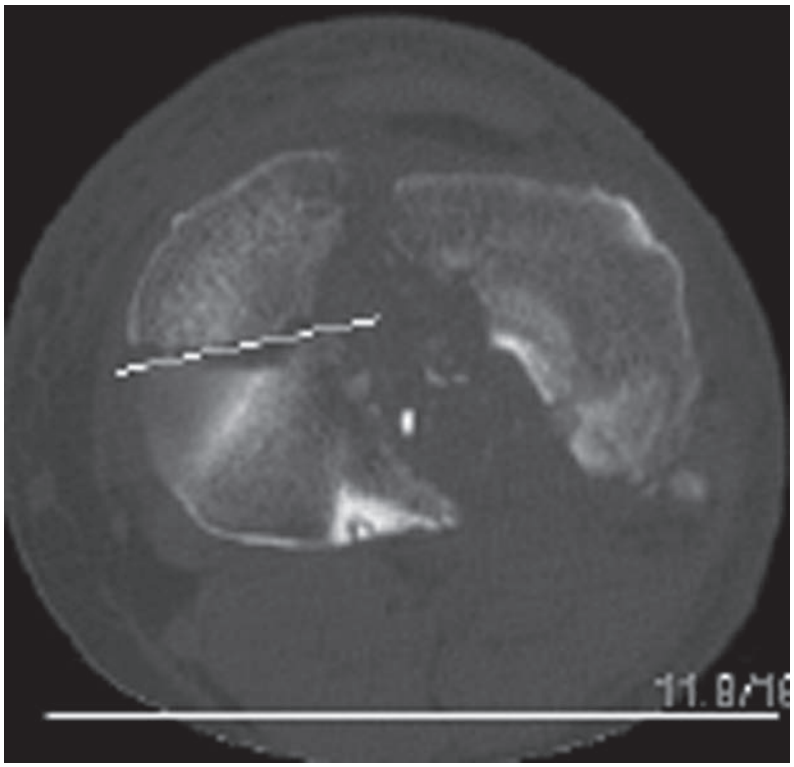

Figure 1: The major medial articular fracture line is identified on this bicondylar tibial plateau injury pattern.

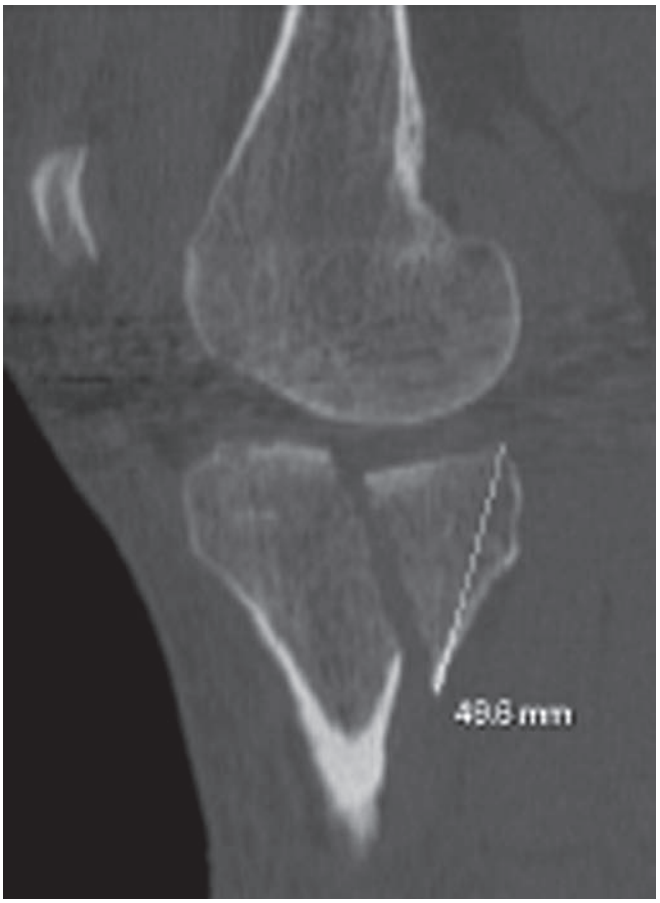

Figure 2: Posterior cortical height (PCH).

Morphologic evaluation included: articular surface area, maximum posterior cortical height (PCH) (Figure 2), and sagittal fracture angle (SFA).

Major fracture displacement of the posteromedial fragment was defined as any posterior translation of the posteromedial fragment relative to the posterolateral margin of the tibial plateau and/or the tip of the fibular head beyond 5mm. Translational displacements less than 5mm were considered minor.

Virtual Surgery

LISS Preparation

All five proximal ("alpha") screw holes of a 9-hole left-sided tibial LISS plate (Synthes, Paoli, PA) were filled with the maximum length LISS screws. The LISS plate and screws were then digitally photographed and CT scanned. A three-dimensional digital virtual LISS plate was created and uniformly applied to a three-dimensional left normal human tibia (NIH Human Body Project).

Fracture Preparation

The DICOM CT images of all fractures with posteromedial fragments were converted into three-dimensional digital fractures. The three-dimensional digital images were then mapped to the three-dimensional digital left normal human tibia (NIH Human Body Project) and LISS plate amalgamation using the fibular head and posterolateral tibial plateau as a primary reference point to initiate mapping.

Determination of Screw/Fragment Interaction

On each three-dimensional "plated" tibial plateau digital model, the posteromedial fracture fragment was identified and digitally isolated. The plated tibial plateau fracture models were viewed circumferentially as translucent three-dimensional objects to accurately ascertain screw penetration with the posteromedial fragment. We arbitrarily defined screw engagement into the posteromedial fragment as 5 or more millimeters of screw penetration (Figure 3A and B).

Statistical Analysis

A regression model evaluated the interaction of posteromedial fragment morphologic variables and the virtual LISS.

Results

Posteromedial Fragment Morphology

Thirty-nine of 57 fractures (68%) demonstrated a posteromedial fragment defined using the medial articular fracture angle range of –42° to 20° obtained from the scatter diagram. The mean MAFA in this group was -11.4° (range, 18.7° to -41.1°). The mean PCH was 43mm (range, 16-59mm), and the mean SFA was 82° (range, 33° to 112°). The mean articular surface area of the posteromedial fragment was 23% of the entire tibial plateau, and ranged from 7.7% to 46.7%. Seven of thirty-nine fractures were identified as having major posterior translational displacements of the posteromedial fragment.

Virtual LISS Surgery

Twenty-six of thirty-nine fractures (66.6%) demonstrated ≥5mm of penetration of at least one LISS screw. The remaining thirteen bicondylar fractures failed to demonstrate any screw engagement of the posteromedial fragment.

Major fracture displacement ($p=0.148$), posterior cortical height ($p=0.152$), sagittal fracture angle (0.06), medial articular fracture angle (MAFA) ($p=0.198$), absolute articular surface area of the posteromedial fragment ($p=0.116$), and absolute surface area of the entire tibial plateau at the level of the articular surface ($p=0.247$) failed to demonstrate any statistically significant association with LISS screw penetration. The articular surface area of the posteromedial fragment as a percentage, or ratio, of the surface area of the entire tibial plateau at the level of the articular surface, however, was statistically significant ($p=0.013$).

Discussion

Nearly half of our bicondylar tibial plateau fractures demonstrated a fracture line traversing the medial tibial plateau articular surface. Of these, approximately two-thirds were considered as having a posteromedial

A.

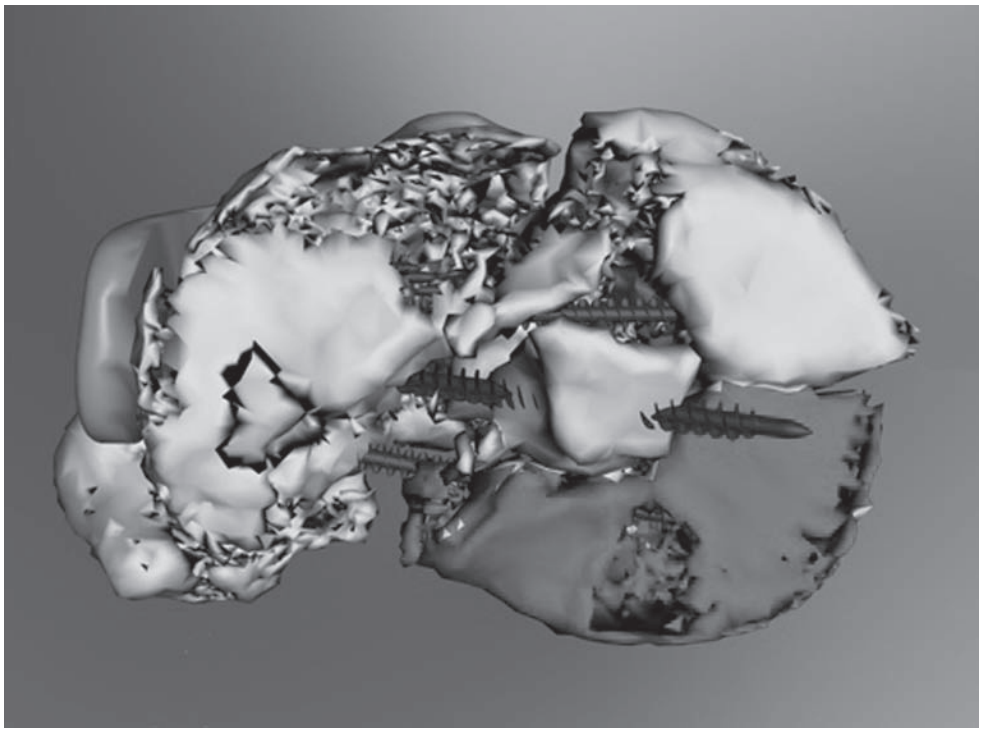

B.

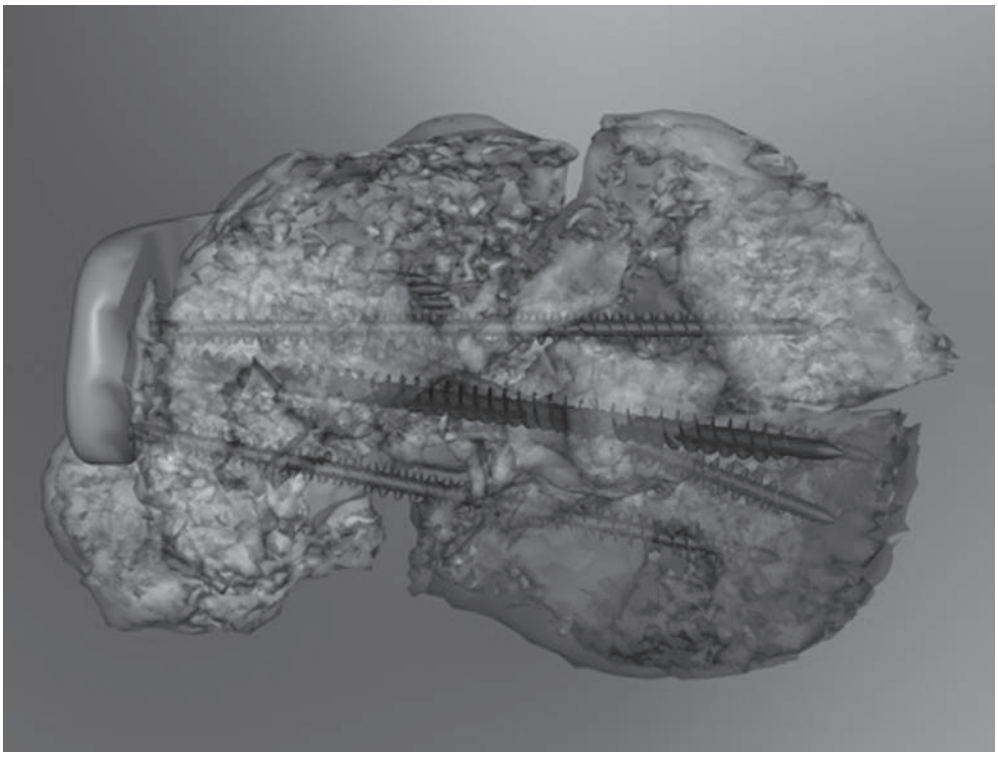

Figure 3: (A). Surface rendering of a left bicondylar tibial plateau fracture, viewing the articular surface from the superior vantage point. The posteromedial fragment has been digitally colored pink to facilitate visualization. The proximal portion of the tibial LISS plate is identified on the lateral aspect of the lateral plateau, immediately anterior to the fibular head. Note that the normal human tibia has been digitally subtracted at this point. (B). The same image and viewing vantage point as Figure 3 (A), however the proximal tibia has been rendered translucent while keeping the LISS screws opaque. Circumferential viewing subsequently allowed accurate identification of screw engagement within the posteromedial fragment.

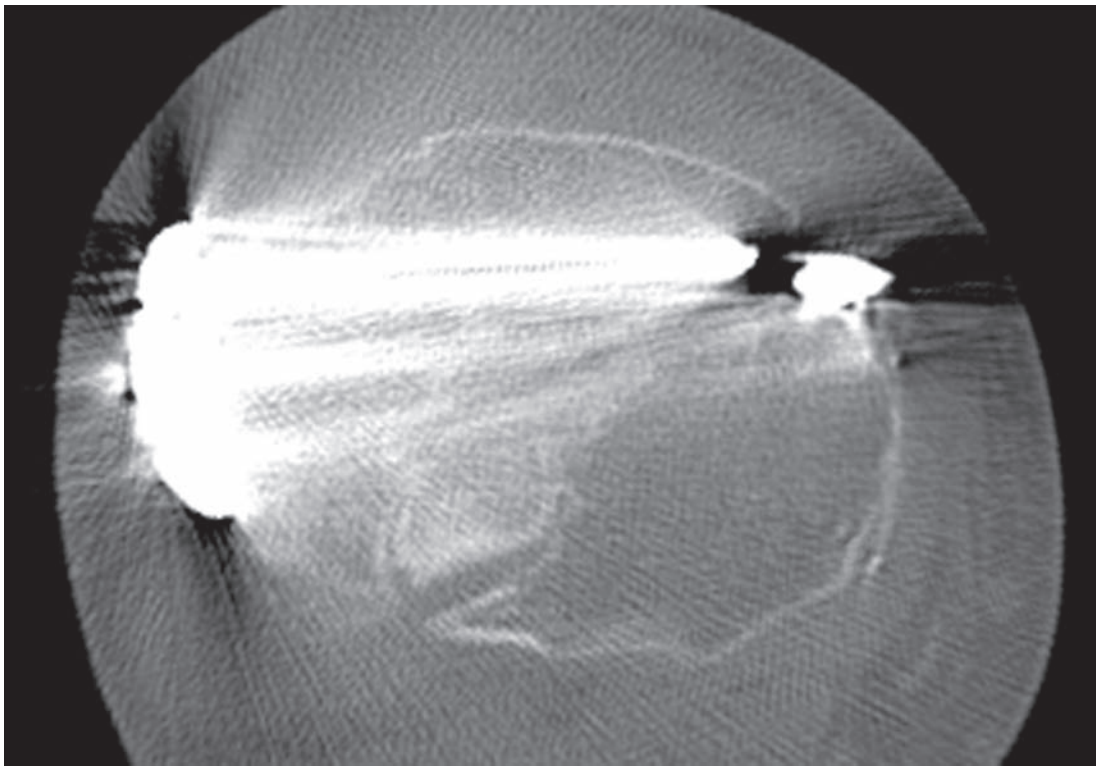

Figure 4: Axial CT image of a bicondylar tibial plateau fracture treated with a fixed-angle laterally applied implant. Note the suboptimal relationship of the locking screws to the relatively large posteromedial fragment.

fragment, according to our definition. This inverted, cone-shaped osteochondral fragment averaged approximately one-quarter of the articular surface of entire plateau at its base, and averaged approximately 4.5cm in height. Using computer-modeling techniques, penetration of the posteromedial fragment by the tibial LISS screws was significantly associated with an increasing articular surface area of the posteromedial fragment as a percentage of the overall plateau articular surface area. However, no other fragment parameter was associated with screw penetration in these bicondylar tibial plateau fracture variants.

The unreliability of LISS to engage these fragments are likely fracture-related and implant-related; specifically, the inverted conical shape of the fragment and the distally-oriented LISS screw trajectory. Together, these factors result in a screw trajectory that aims towards a smaller osseous component of the posteromedial fragment. The findings in this study have recently been illustrated clinically in a series of bicondylar tibial plateau fractures treated with LISS plating. In that series, Gosling identified three patients with loss of reduction secondary to failure to reduce and/or stabilize a posteromedial articular fracture fragment.

While these results should not necessarily be extrapolated to other implants, the complex interactions of fracture and implant variables should be appreciated by the treating surgeon (Figure 4). While LISS plating has demonstrated excellent early results for the management of the high-energy bicondylar tibial plateau fracture, alternate methods, such as supplemental medial exposures and implants, should be considered for this injury pattern.

Recommended Reading

Watson, J. T.: High-energy fractures of the tibial plateau. Orthop Clin North Am, 25(4): 723-52, 1994.

Hohl, M.: Tibial condylar fractures. J Bone Joint Surg Am, 49(7): 1455-67, 1967.

Bendayan, J.; Noblin, J. D.; and Freeland, A. E.: Posteromedial second incision to reduce and stabilize a displaced posterior fragment that can occur in Schatzker Type V bicondylar tibial plateau fractures. Orthopedics, 19(10): 903-4., 1996.

Bhattacharyya, T.; McCarty, L. P., 3rd; Harris, M. B.; Morrison, S. M.; Wixted, J. J.; Vrahas, M. S.; and Smith, R. M.: The posterior shearing tibial plateau fracture: treatment and results via a posterior approach. J Orthop Trauma, 19(5): 305-10, 2005.

De Boeck, H., and Opdecam, P.: Posteromedial tibial plateau fractures. Operative treatment by posterior approach. Clin Orthop Relat Res, (320): 125-8, 1995.

Quantifying Foot Bone Motion Via Magnetic Resonance Imaging

Michael Fassbind, M.S., Eric S. Rohr, M.S., Yangui Hu, Ph.D., David R. Haynor, M.D., Bruce J. Sangeorzan, M.D., and William R. Ledoux, Ph.D.

Previous researchers have quantified foot bone motion using X-ray stereophotogrammetry and magnetic resonance imaging (MRI). These studies were limited by the necessary radiation exposure, the need to implant tantalum beads into the foot bones, the restrictive nature of the input motion and/or the time involved in analyzing the data. The present study uses MRI scans to develop an objective three-dimensional (3-D) method for foot bone motion quantification. Feet are moved through a range of motion unique to each subject while bone motion is tracked. The information gained from this study will provide a better understanding of the movement of the foot bones. Furthermore, the methods employed avoid the invasive nature of X-ray stereophotogrammetry, allowed for patient specific motion and required less processing time than previous MRI based studies.

Methods

Five subjects (53.4 ± 4.4 years) were enrolled in this IRB (Human Subject Division, University of Washington) approved study. Subjects were included if they had a neutrally aligned foot (classified by an orthopedic surgeon) and were free of any lower extremity pathology. Exclusion criteria included the inability to self ambulate, current ulceration and partial foot amputation. There were four steps involved in the measurement of subjects: 1) determining modified Ankle Flexibility Tester (AFT) settings, 2) scanning subjects, 3) processing data and 4) analyzing data. (The AFT was designed to hold a foot in different positions in six degrees of freedom in an MRI scanner; we modified the device to increase the allowable range of motion.)

Determining Test Apparatus Settings

To determine how to position a foot during the MRI scanning, the subject's foot was strapped to a foot plate and held in end ranges of motion while angle measurements were recorded from an electromagnetic sensor system (Polhemus Liberty). Three positions were recorded: 1) maximum plantar flexion, inversion, and internal rotation, 2) anatomical neutral and 3) maximum dorsiflexion, eversion, and external rotation. The output was given in direction cosines and was converted to the appropriate Cardan angles that could be dialed into the AFT inputs. Finally end range of motion positions were tested to see if they were within AFT movement limitations.

Scanning Subject

The subject's foot was scanned (Phillips Intera gyroscan 1.5, slice thickness 1.4, repetition time 5.87, echo time 1.83, flip angle 25 degrees) eight times incremented between the two end range of motion positions and traveling through the neutral position. Included in the MRI scans was a high resolution (hi-res) scan in the neutral position.

Processing Data

Data were processed using Multi-Rigid, a highly automated segmentation and registration software system developed by Yangqiu Hu, Ph.D. candidate. The hires MRI scan was segmented by growing bone volumes from seed lines placed in each bone in 3-D space (Figure 1). The other seven MRI positions were registered by the software to the single segmented hires scan.

Analyzing Data

Relative motions between the bones of interest (calcaneus, talus, navicular, cuboid, three cuneiforms, and five metatarsals) were described using finite helical axes (FHA). We chose FHA as they represent the axis that the joint is rotating about, they are more anatomically meaningful than Cardan angles and they do not involve the subjectivity that can be associated with Grood and Suntay parameters.

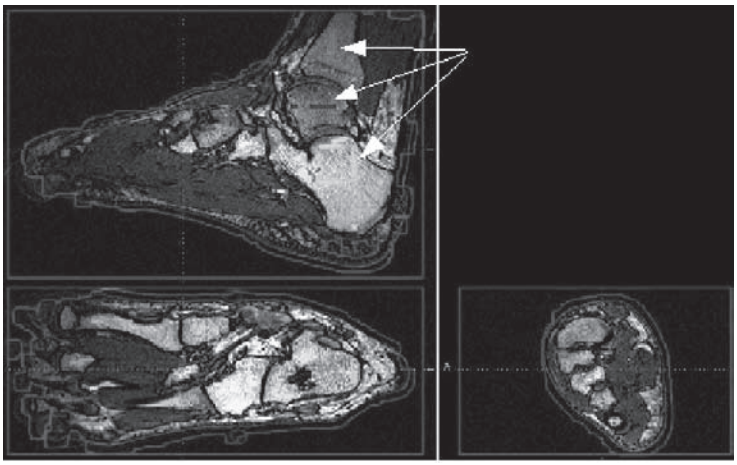

Figure 1: Segmenting foot bones using Multi-Rigid. Arrows show darker lines that were the initial seed lines used to begin the segmentation process. The lighter colors show the resulting segmented bone volumes.

Results

FHA were determined between the bones of interest for the five subjects, e.g., the navicular relative to the talus (Figure 2) and the calcaneus relative to the talus (Figure 3). Only 1 hour of user interaction, and an additional 6 hours of computer time, was required to segment and register the eight MRI scans. The characteristics of the FHA were shown to be similar to those published. For instance the subtalar

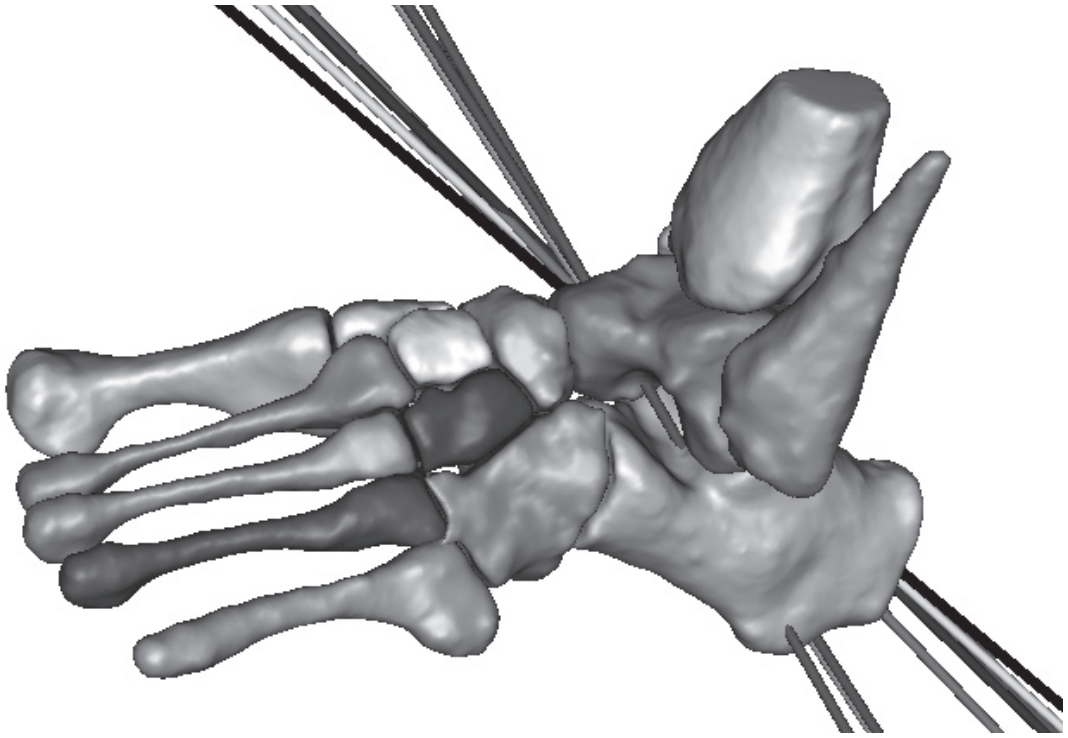

Figure 2: Output from Multi-Rigid after segmentation and registration of the MRI data. FHA's shown are for the talonavicular joint (navicular relative to talus). This is a left foot viewed from the lateral, superior direction.

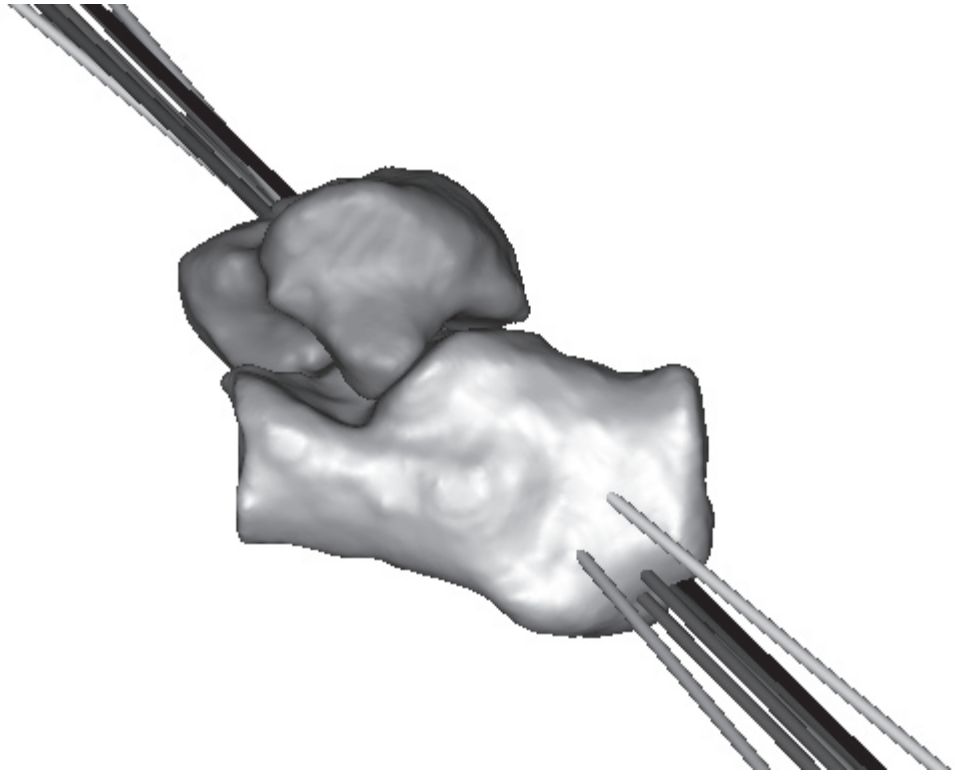

Figure 3: FHA for subtalar joint of a neutrally aligned subject. This is a left foot viewed laterally.

	Sagittal	Transverse	Frontal
Manter	42	16	N/A
Inman	42 ± 9	23 ±11	N/A
FHA 1>8	41.4 ± 5.9	18.1 ± 5.5	69.9 ± 4.9

Table 1: Subtalar joint axis orientation relative to cardinal planes.

joint axis orientation of the FHA from position 1 to position 8 (Table 1) was shown to be very similar to those published by Inman and Manter.

Discussion

Through the use of modern medical imaging technology and software, information from MRI scans of the foot in different positions can be processed to describe foot bone motion via finite helical axes. This methodology allows for the objective and accurate quantification of the motion of the bones of the foot without the need for invasive methods. Further, the analysis is rapidly completed and allows for subject specific positions.

Recommended Reading

Hu, Y., S. K. Mirza, et al. (2005). MR and CT image fusion of the cervical spine: a noninvasive alternative to CT-Myelography, San Diego, CA, United States, International Society for Optical Engineering, Bellingham, WA 98227-0010, United States.

Inman, V. T. (1976). The joints of the ankle. Baltimore, Williams and Wilkins.

Lundberg, A., I. Goldie, et al. (1989). "Kinematics of the ankle/foot complex: Plantarflexion and dorsiflexion." Foot and Ankle 9(4): 194-200.

Manter, J. T. (1941). "Movements of the subtalar and transverse tarsal joints." The Anatomical Record 80(4): 397-410.

Siegler, S., J. K. Udupa, et al. (2005). "Mechanics of the ankle and subtalar joints revealed through a 3D quasi-static stress MRI technique." J Biomech 38(3): 567-78.

Stindel, E., J. K. Udupa, et al. (2001). "An in vivo analysis of the motion of the peri-talar joint complex based on MR imaging." IEEE Trans Biomed Eng 48(2): 236-47.

Udupa, J. K., B. E. Hirsch, et al. (1998). "Analysis of in vivo 3-D internal kinematics of the joints of the foot." IEEE Trans Biomed Eng 45(11): 1387-96.

Acknowledgements

This work was supported by the Dept. of Veterans Affairs, Rehabilitation Research & Development Service grant numbers A2661C and A3030R.

The Latent Failure: Analysis of Capsulorraphy Arthropathy in Patients Presenting After Failed Shoulder Stabilizations

Christopher J. Wahl, M.D., Erin E. Seifert, B.A., Evan D. Ellis, M.D., Sarah E. Matt, B.A., and Frederick A. Matsen III, M.D.

Failure after shoulder stabilization is most commonly defined as recurrent instability; however, failure by latent arthropathy occurring months to years after the index procedure is less-readily acknowledged. This study characterizes a subgroup of patients with capsulorraphy arthropathy (CA) from among a large cohort of patients presenting with dissatisfaction following surgical stabilization procedures.

Methods

342 patients presenting with shoulder complaints following stabilization procedures were evaluated. Information was collected regarding the number and types of previous shoulder procedures and previous shoulder stabilization procedures. Prospective clinical, operative, and self-assessment data (SF-36, Simple Shoulder Test) from these patients were compared to patients presenting with primary instability (PI, N=310) and primary osteoarthritis (OA, N=537). In addition, of those patients undergoing surgical salvage procedures, the number and type of procedure(s) performed were evaluated.

Results

Of 342 "failed" stabilization procedures, 196 (57%) presented with complaints related to recurrent instability and 109 (32%) with refractory shoulder stiffness. In all, 82 patients (24%) demonstrated radiographic evidence of capsulorraphy arthropathy (CA) (Figure 1). Pain (94%) and refractory stiffness (88%) were common complaints. Complaints of recurrent dislocations (2%) or subluxation (15%) were rare. Open capsulorraphy (33%), Bristow (20%) and open Bankart (20%) were the most common index procedures performed. The average time from index surgery to presentation was 18.2 years; the average age at presentation was 46.5 years. The CA group was significantly younger than a 537-patient cohort presenting with OA (46.5y vs. 64.2y, $p < 0.001$), yet there were no significant differences in self-assessed function as measured by SST (4.8 vs 4.4). The CA group reported significantly worse self-assessed shoulder function than individuals presenting with primary shoulder instability (4.8 vs 7.8, respectively, $p < 0.001$) (Figure 2).

When comparing physical function domain of the SF-36, the CA group was significantly worse than patients with primary instability (67.13 vs. 81.88, $p < 0.001$), but were slightly better than the OA group (67.13 vs. 60.74, $p = 0.04$). With regard to pain, the CA group was significantly worse than the PI group (39.73 vs. 54.96, $p < 0.001$), but not significantly different from the OA group (39.73 vs. 38.76, $p = 0.07$). With respect to the physical component summary, the CA group was markedly worse than the instability group (37.74 vs. 43.49, $p < 0.001$) but slightly better than the OA group (37.74 vs. 35.31, $p = 0.04$) (Figure 3).

In 62 patients offered salvage treatment, 31 (48%) underwent total shoulder arthroplasty, 22 (33%) hemiarthroplasty, and 9 (17%) surgical release. Thirteen (16%) secondary and eight (8%) tertiary revisions were performed. Including procedures performed prior to presentation to the senior author, 230 procedures were performed in 82 patients (avg 2.8 procedures/patient).

Discussion

Numerous reports document excellent clinical results following surgical shoulder stabilization procedures; however, this literature

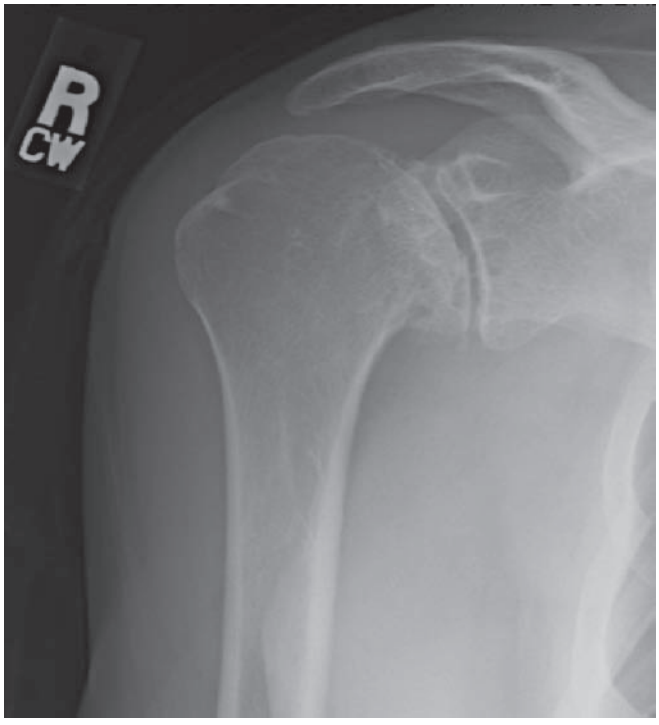

Figure 1: Antero-posterior radiograph of a 44-year old male 18 years following an open Bankart procedure for recurrent anterior shoulder instability.

may not portray the conditions under which the patient deems the procedure unsatisfactory. Failures have been reported by many authors, but the most common criteria used to define failure include recurrent instability and complications due to hardware placement. A few authors, notably Meehan, Magnusson, and Rosenberg have correlated motion losses with poor outcomes or the development of degenerative changes at the glenohumeral joint.

This study attempted to gain a better understanding of the factors that contribute to failure of a shoulder stabilization procedure by reviewing a large cohort of patients who presented dissatisfied with their surgical result. While it is impossible to define with this study what percentage of procedures will result in failure, it gives us a better understanding of failure from the patient's perspective.

While recurrent instability is still the most common mode of failure, refractory stiffness and the latent development of capsulorraphy arthropathy are not uncommon, occurring in 32% of persons. It is clear that the self-reported assessment function and quality of life are significantly worse in the subgroup of patients who develop capsulorraphy arthropathy than in persons who have instability, such that a surgical failure is far more debilitating than the initial pathology. In addition, surgical procedures that act to constrain the shoulder joint (open capsulorraphy and Bristow) accounted for 53% of the index procedures leading to arthropathy. Significant morbidity is associated with these failures, such that patients underwent an average 2.8 procedures (range 1 to 16). The most common salvage procedure performed in those who elected further intervention was a total shoulder arthroplasty.

In summary, procedures to restore glenohumeral stability may lead to the devastating long-term sequela of capsulorraphy arthropathy. Patients with capsulorraphy arthropathy have much worse self-assessed function and quality of life indices than those who have shoulder instability. Stabilization procedures need to restore normal anatomy and avoid excessive restrictions in range of motion to avoid poor subjective outcomes.

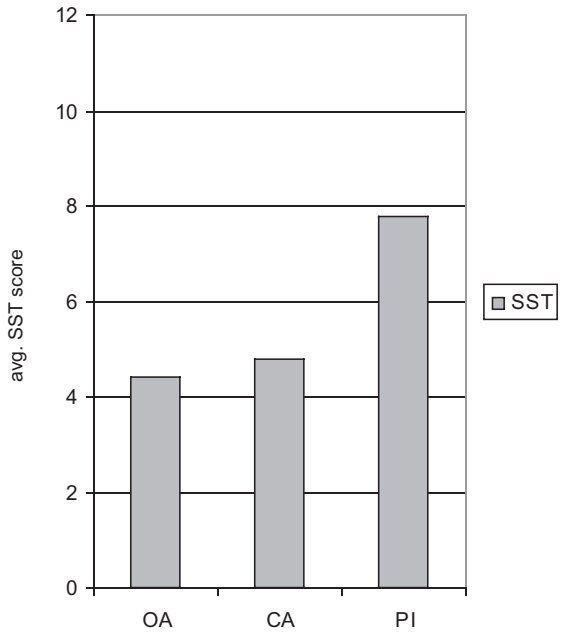

Figure 2: Average SST scores for capsulorraphy arthropathy (CA), primary osteoarthritis (OA) and primary instability (PI) groups. The CA group is significantly younger than the OA group, but no significant differences in self-assessed function between capsulorraphy arthropathy and osteoarthritis groups were present. Both CA and OA groups demonstrated significantly worse self-assessed functional SST scores than a group of patients presenting with primary shoulder instability (PI).

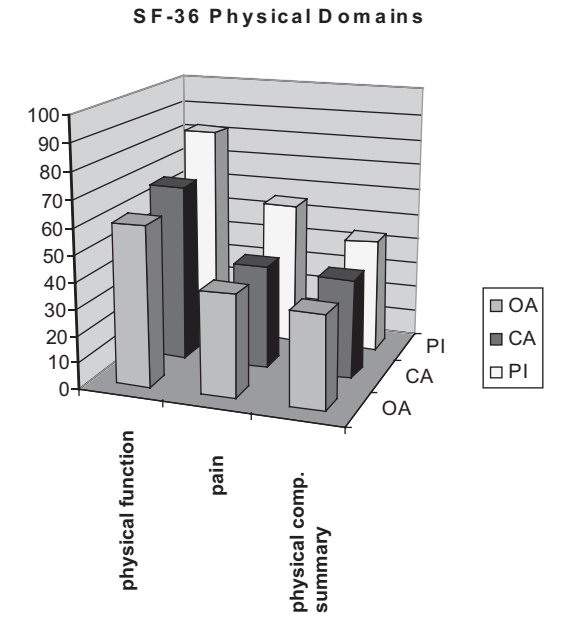

Figure 3: Self-assessed quality of life as measured by the physical domains of the SF-36 scale. With respect to physical function, the CA group fared significantly worse than the PI group, but slightly better than the OA group. With respect to physical pain, there were no significant differences between OA and CA groups, but both were significantly worse than the PI group. Significant differences existed between all groups with respect to the physical component summary domain.

Recommended Reading

Zabinski SJ, Callaway GH, Cohen S, Warren RF. Revision shoulder stabilization: 2- to 10-year results. J Shoulder Elbow Surg. Jan-Feb 1999;8(1):58-65.

Mologne TS, McBride MT, Lapoint JM. Assessment of failed arthroscopic anterior labral repairs. Findings at open surgery. Am J Sports Med. Nov-Dec 1997;25(6):813-817.

Levine WN, Arroyo JS, Pollock RG, Flatow EL, Bigliani LU. Open revision stabilization surgery for recurrent anterior glenohumeral instability. Am J Sports Med. Mar-Apr 2000;28(2):156-160.

Kim SH, Ha KI, Kim YM. Arthroscopic revision Bankart repair: a prospective outcome study. Arthroscopy. May-Jun 2002;18(5):469-482.

Rowe CR, Zarins B, Ciullo JV. Recurrent anterior dislocation of the shoulder after surgical repair. Apparent causes of failure and treatment. J Bone Joint Surg Am. Feb 1984;66(2):159-168.

The EWS/FLI-1 Tumor Protein Inhibits Senescence of Ewing's Sarcoma Cells

Hsien-Ming Hu, Ph.D., Anna Zielinska-Kwiatkowska, M.S., and Howard A. Chansky, M.D.

In over 85% of Ewing's Family Tumors (EFTs) a specific chromosomal translocation t(11;22) results in a chimeric oncogenic product fusing the N-terminal domain of the RNA-binding protein EWS with the C-terminal DNA-binding domain of the ETS family transcription factor FLI-1. EWS/FLI-1 has been shown to be necessary and sufficient to induce transformation both in vivo and in vitro. The EWS/FLI-1 fusion protein functions in part as an aberrant transcription factor contributing to malignant transformation via transcriptional deregulation of target genes. Studies from our laboratory and others have shown that alternative mechanisms involving pre-mRNA splicing and chromatin remodeling also contribute to malignant transformation. Despite a number of downstream biological pathways proposed for EWS/FLI-1, a detailed mechanism through which the oncogenic fusion protein transforms the cells and maintains the malignant phenotype is still elusive.

We have previously demonstrated that synthetic small interfering RNA (siRNA) can specifically suppress EWS/FLI-1 expression in SK-ES Ewing's sarcoma cells. Most importantly, EWS/FLI-1 knockdown results in decreased cell proliferation and invasiveness in the SK-ES Ewing's sarcoma cell line. To further characterize the phenotype of EWS/FLI-1 knockdown, we have developed an adenoviral vector capable of efficient delivery of siRNA into a variety of Ewing's tumor cell lines. In this report, we describe that sustained and near-complete knockdown of EWS/FLI-1 by virus-mediated RNAi induces a senescence-like phenotype in the tumor cells. The senescence is accompanied by activation of the pRb tumor suppressor, which may result from alterations in the expression levels of several upstream G1/S cell cycle regulators. We hypothesize that the EWS/FLI-1 fusion protein blocks cellular senescence and promotes uncontrolled cell proliferation through modulation of G1/S regulatory proteins in Ewing's sarcoma.

Results

Knockdown of EWS/FLI-1 by adenovirus-mediated RNAi in SK-ES and RD-ES Ewing's sarcoma cell lines

SK-ES and RD-ES, Ewing's sarcoma cell lines possessing the type 2 translocation, were infected with adenovirus encoding siRNA targeting EWS/FLI-1 (Ad-siFli-1) or luciferase (Ad-siGL2), a gene not normally present in Ewing's tumor cells. Immunoblotting was performed to analyze the level of EWS/FLI-1 at different time points after infection. As shown in Figure 1, near-complete knockdown of EWS/FLI-1 was achieved by day 2 and the suppression remained for at least 6 days, and as long as 10 days (data not shown).

EWS/FLI-1 depletion induces senescence-like phenotype

To evaluate the effect of EWS/FLI-1 knockdown on the proliferative capacity of SK-ES and RD-ES Ewing's cell lines, cells were counted daily following viral infection. No significant apoptosis was seen by microscopy or flow cytometry. In both cell lines, a comparable growth rate with a doubling time of about 24 hours was observed in non-treated cells or cells infected with the control virus. In contrast, cells infected with Ad-siFli-1 showed a complete growth arrest within 24 hours, and maintained similar cell counts over the 6 day time course. This indicates that the cells survived but ceased to proliferate. We then examined the effect of EWS/FLI-1 suppression on cell cycle by flow cytometry. SK-ES and RD-ES cells were grown for 48 hours following viral infection and then they were fixed and stained with propidium iodide. Compared to the untreated cells, SK-ES and RD-ES cells treated with Ad-siFli-1 targeting EWS/FLI-1 contained an increased G1 population (62% to 78%), a decreased S phase (9% to 2%) and a decreased G2/M (29% to 20%) population. This effect was specific since infecting cells with the control virus Ad-siGL2 showed no effect on the cell cycle profile. These results indicate that knockdown of EWS/FLI-1 results in a growth arrest in the G1 phase.

Knockdown of EWS/FLI-1 in both SK-ES and RD-ES cells also led to a profound change in cell morphology concomitant with G1 growth arrest. Cells infected with Ad-siFli-1 assumed an enlarged and flattened morphology with increased cytoplasm to nucleus

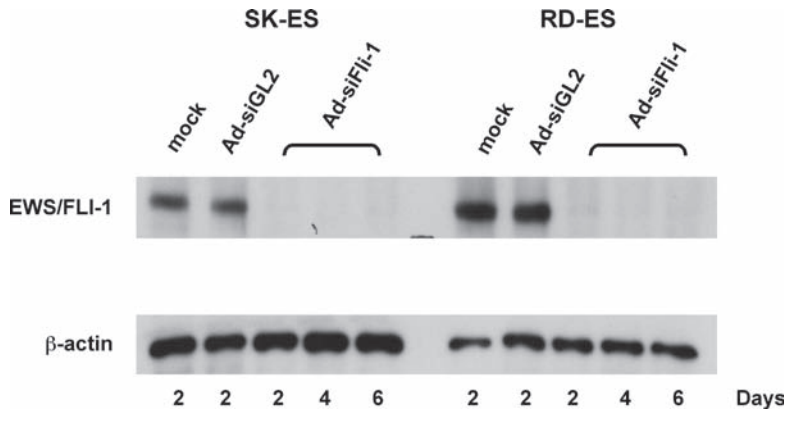

Figure 1: Knockdown of EWS/FLI-1 by adenovirus-delivered shRNA in Ewing's sarcoma cell lines. Whole cell lysates were harvested from SK-ES and RD-ES, both type 2 Ewing's sarcoma cells, at different times after infected with specific shRNA-expressing adenovirus, and analyzed by immunoblotting with an anti-Fli-1 antibody. The same lysates were also blotted with an anti β-actin antibody for a loading control.

ratio and cytoplasmic inclusions, whereas cells infected with control virus were compact and spindle-like, resembling their untreated counterpart. The observation that EWS/FLI-1-depleted Ewing's sarcoma cells assume a senescence-like morphology prompted us to investigate whether SA-beta-galactosidase (SA-beta-gal) activity, a hallmark for cellular senescence, can be detected in these cells. SA-beta-gal-positive cells were readily identified in SK-ES cells infected with Ad-siFli-1 but not in those infected with the control virus. On day 6 post infection, the percentage of SA-beta-gal-positive cells was estimated to be 75% in EWS/FLI-1-depleted cells and 3% in the control cells. RD-ES cells behaved similarly when they were analyzed for SA-beta-gal activity.

Discussion

There is growing evidence that cellular senescence, a physiological program leading to a state of permanent growth arrest, functions in part as a tumor suppressor mechanism. The senescence pathway appears to be reversibly suppressed in some human tumors and it has been proposed that escape from chemotherapy-induced senescence is an important cause of clinical relapse. In this report we show that depletion of the oncogenic fusion protein EWS/FLI-1 in Ewing's sarcoma cells restores or activates a senescence pathway leading to cell cycle arrest.

We now believe that the Ewing's fusion protein EWS/FLI-1 bypasses cellular senescence and promotes cell proliferation through modulation of G1-S phase regulatory proteins (preliminary data not shown). The treatment of Ewing's tumors has remained essentially unchanged despite 13 years having elapsed since identification of the fundamental mutation that causes these potentially fatal malignancies. The observation that depletion of EWS/FLI-1 leads to cell cycle arrest and assumption of a senescent phenotype offers new avenues of investigation and potential targets for molecular therapies.

Recommended Reading

Chansky HA, et. al: Targeting of EWS/FLI-1 by RNA interference attenuates the tumor phenotype of Ewing's sarcoma cells in vitro. J Orthop Res. 2004 Jul;22(4):910.

Martinez N, et. al: The oncogenic fusion protein RUNX1-CBFA2T1 supports proliferation and inhibits senescence in t(8;21)-positive leukaemic cells. BMC Cancer. 2004 Aug 06;4(1):44.

Matrilin-3 is Present in Normal Amounts in Articular Cartilage from a Patient with the T303M MATN3 Genetic Variant Linked to Osteoarthritis

L. Stefan Lohmander, M.D., Ph.D., Jiann-Jiu Wu, Ph.D.,
Thorvaldur Ingvarsson, M.D., Ph.D., and David R. Eyre, Ph.D.

Matrilins are a 4-member family of extracellular matrix proteins found in cartilage and other connective tissues. They form fibrillar structures, are often associated with collagens, and may mediate interactions between collagen fibrils and other extracellular matrix components. Mutations in the matrilin-3 gene and in collagen IX, COMP and DTDST genes can all cause multiple epiphyseal dysplasia (MED), a skeletal variable phenotype that includes early onset osteoarthritis (OA). A polymorphism in the matrilin-3 gene (MATN3), resulting in a threonine-to-methionine substitution in a highly conserved sequence in the EGF domain (Figure 1) was linked to hand OA but not MED in an Icelandic population. Since RER retention and dominant negative effects are found with MED-causing mutations in MATN3, we analyzed for abnormalities of matrilin-3 (matn3) protein in joint cartilage of genotyped patients and a control requiring hip joint replacement for OA.

Materials and Methods

Joint cartilage was dissected from femoral heads obtained after IRB approval of patients with severe hip OA. A male aged 55 at hip joint replacement was homozygous for the polymorphism (M/M), and had bilateral hip, knee and hand OA. A female 40y was heterozygous (M/T) and had bilateral hip, knee and hand OA, while a male 65y with bilateral hip OA lacked the polymorphism (T/T). Cartilage slices were digested with chondroitinase ABC. After removing soluble material (chondroitinase extract), the residues were further extracted with 4M guanidine HCl, 0.05M Tris-HCl, pH 7.5 (guanidine extract). The extracts were dialyzed against distilled water and freeze-dried. Extracted proteins were resolved by SDS-PAGE, blotted to PVDF and matn3 was detected with a specific antiserum raised against peptide sequences within VWF and C-terminal domains of matn3.

Results

Western blots showed that intact matn3 tetramer and monomer were detected mainly in the denaturant extracts from all three genotypes T/T, T/M and M/M (Figure 2). Significant amounts of degraded matn3 fragments were detected, particularly in the chondroitinase extracts of all three OA patients, migrating near the buffer front under reducing condition on SDS-PAGE (Figure 2B, lanes 1-3). Similar levels of matn3 tetramer were found in 4M guanidine HCl extracts of joint cartilage from each of the genotypes T/T, T/M, M/M (Figure 2A, lanes 4-6). Variation in relative amounts of degradation products of the matn3 protein was evident, but no consistent difference that could be related to genotype. The yield of matn3 judged from the monomer band after disulfide cleavage (Figure 2B, lanes 4-6) was similar for all 3 genotypes. Using CNBr-digestion to cleave methionine and detect fragments unique to the M variant, both heterozygous and homozygous tissue samples prominently displayed this protein product in the matrix extract (not shown).

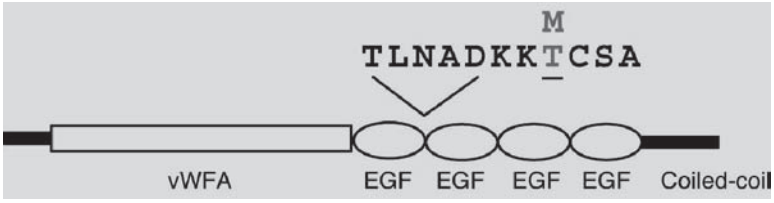

Figure 1: Domain structure of matrilin-3 showing the polymorphic gene variation (M) linked to increased risk of OA.

Discussion

The finding of apparently normal amounts of matn3 in OA joint cartilage extracts of the mutation-carrying individuals suggests that cellular export of the M allelic variant was unimpaired. Risk of OA for carriers may therefore be from consequences of an abnormal protein in the extracellular matrix. The methionine for threonine substitution (Figure 1) occurs next to a cysteine residue which is involved in intrachain disulfide bonding in the EGF-repeat domain. Whether this polymorphism has any effect on conformation or other properties of the matrix form of matn3 is unknown but possible.

Additional families carrying this mutation have been identified subsequent to the original report. Interestingly, members of these families often have OA of the hip or knee, suggesting that the mutation may be associated not only with hand OA, but also large joint OA (Ingvarsson, unpublished).

Recommended Reading

Wagener R, Ehlen HW, Ko YP, et al. (2005) The matrilins – adaptor proteins in the extracellular matrix. FEBS Lett. 579:3323-9.

Hecht JT, Hayes E, Haynes R, Cole WG. (2005) COMP mutations, chondrocyte function and cartilage matrix. Matrix Biol. 23:525-33.

Briggs MD, Chapman KL. (2002) Pseudoachondroplasia and multiple epiphyseal dysplasia: mutation review, molecular interactions, and genotype to phenotype correlations. Human Mutation. 19:465-78.

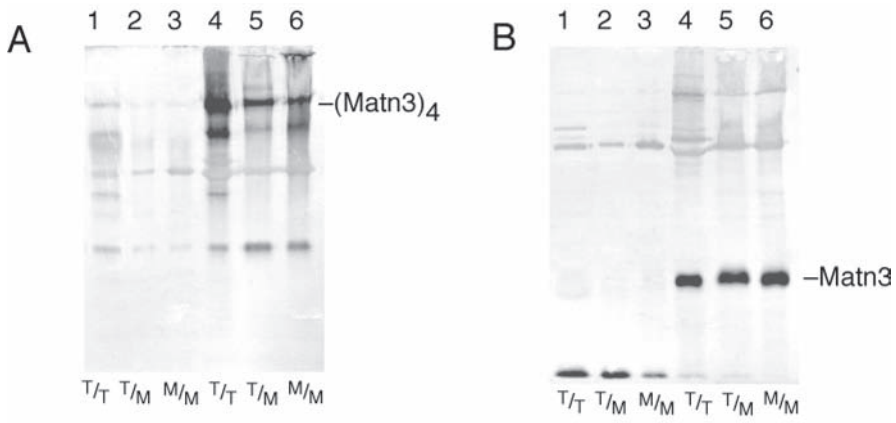

Figure 2: Western blot for matn3 in extracts of joint cartilage from genotypes T/T, T/M and M/M. Lanes 1-3, chondroitinase extracts, lanes 4-6, 4M guanidine HCl extracts. Matrilin samples run under non-reducing condition on SDS-6% PAGE (A), and under reducing condition on 7.5% PAGE (B) were blotted to PVDF membrane and developed with the anti-matrilin-3 serum.

Mabuchi A, Haga N, Maeda K, et al. (2004) Novel and recurrent mutations clustered in the von Willebrand factor A domain of MATN3 in multiple epihyseal dysplasia. Human Mutation 24(5):439-40.

Stefansson SE, Jonsson H, Ingvarsson T, et al.(2003) Genomewide scan for hand osteoarthritis: a novel mutation in matrilin-3. Am J Hum Genet. 72:1448-59.

Wu J-J, Eyre DR. (2001) Identification of matrilin-3 in adult human articular cartilage. Trans Ortho Res Soc. 26:382.

Processing of Collagen Type IX by RCS-LTC Chondrocytes: Evidence for an Effect of Retinoic Acid Through Stimulated MMP9 Expression

Maximillian A. Rogers, B.S., Dennis A. Hanson, Ph.D., David R. Eyre, Ph.D., and Russell J. Fernandes, Ph.D.

Cartilage is a unique tissue characterized by an extensive extracellular matrix. The molecular mechanisms that enable chondrocytes to assemble and maintain a functional cartilage matrix from a complex mix of collagens, proteoglycans and matrix proteins in the correct proportions are not well understood. In the cartilage matrix three tissue-specific collagens, types II, IX and XI, co-polymerize to form a fibrillar framework that is stabilized by inter-molecular cross-links. Type IX collagen molecules are covalently linked to the surface of the type II collagen fibril with type XI collagen forming a filamentous template within the core. How the heteropolymeric collagen fibrils can grow laterally and mature into the cross-linked network that typifies cartilage matrix is a challenge to understand.

An attractive hypothesis is that type IX collagen is selectively removed by proteases from the surface of the growing type II collagen fibril allowing the fibrils to grow laterally. Candidate proteases are MMP3 and the gelatinases. We have begun to explore this question, using the Swarm rat chondrosarcoma chondrocyte cell line RCS-LTC, which assembles type II N-procollagen, type IX and type XI molecules into nacent heterofibrils that are stabilized by the characteristic covalent cross-links typical of cartilage collagen.

Here we investigated type IX collagen proteolysis and matrix metalloproteinase expression in the cell line following treatment with retinoic acid (RetA). Retinoic acid is known to play a role in normal skeletal development participating in the morphogenesis of limbs and growth plate maturation. RetA has also been shown to modulate matrix metalloproteinase expression in cartilage explants and chondrocyte cultures.

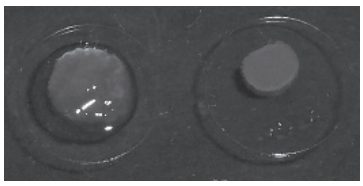

Figure 1: Morphology of RCS-LTC micromass cultures after 1 week of RetA treatment. Untreated (left), Treated (right).

Methods

Cell culture

Following a week in micromass or high density monolayer culture in DMEM containing calf serum and ascorbate, the RCS-LTC chondrocytes were treated with 3uM retinoic acid (RetA) in the absence of serum. Control cultures were treated with ethanol vehicle alone.

Collagen extraction and Western blotting. On days 2 and 4, following treatment with RetA, collagen in the medium and extracted from the matrix with Tris buffered 1M NaCl, was analyzed . The various collagen chains were then resolved by SDS-PAGE, transferred onto PVDF and probed with a polyclonal antibody specific for the N-terminal NC4 domain of the α1(IX) chain of type IX collagen. This antibody is able to detect the full-length α1(IX) chain and any C-terminally degraded products on western blots. A chemiluminescence detection system was used. Partially purified types II and IX collagens were used as standards.

Gene expression analysis

After 24 and 48 hr treatment with RetA, total RNA was extracted from RCS-LTC cultures using Qiagen QIAshredder and RNeasy kits. Equal aliquots of RNA from control and experimental cultures were DNase treated, the mRNA reversed transcribed and the expression of cartilage collagen and metalloproteinase genes of interest analyzed by PCR using exon specific primers.

Results

Within a week in micromass culture the RCS-LTC chondrocytes elaborated a highly hydrated extracellular matrix rich in proteoglycans and collagen. After treatment with RetA the morphology of the cultures changed dramatically. Figure 1 shows that by day 7 in culture with RetA the height of the cell/matrix micromass collapsed compared with the control suggesting a loss of water and proteoglycans.

Western blotting, using an antibody specific for the α1(IX) NC4 domain identified intact α1(IX) collagen chains in the medium (Figure 2) and matrix (not shown) of both treated and

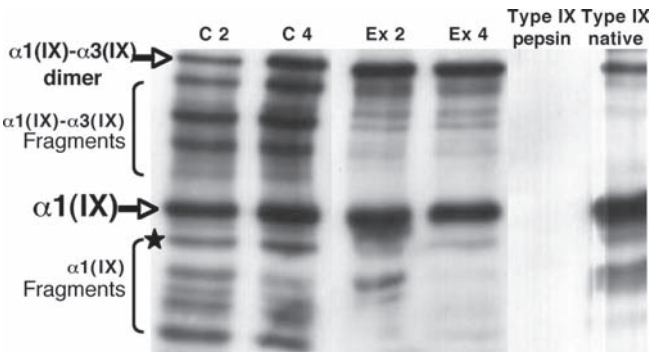

Figure 2: Western blot showing reactivity of α1(IX) chains and fragments in medium of control (C) and RetA (Ex) treated cultures after 2 and 4 days of treatment.

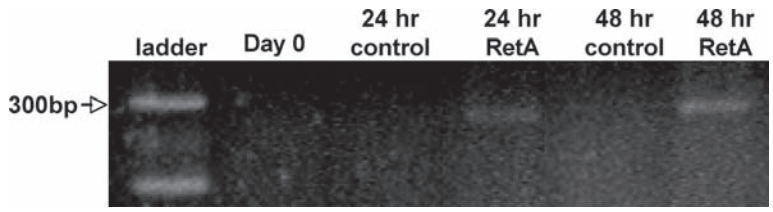

Figure 3: RCS-LTC chondrocytes turn on MMP9 expression following RetA treatment.

control cultures. The antibody also strongly reacted with fragments of degraded α1(IX) chains in control cultures suggesting turnover of type IX collagen. Following treatment with RetA, reactivity to these fragments was lost or reduced, indicative of further degradation of these fragments. For example there is a reduced reactivity to the fragment below the α1(IX) band (indicated by a star in Figure 2) following treatment with RetA. Based on the molecular size, this band is the α1(IX) chain minus the COL 1 domain. Interestingly, reactivity to the intact α1(IX) chain persisted, implying that a proportion of type IX collagen molecules was spared from proteolysis. The data imply activation and/or synthesis of new proteases, most likely gelatinases following RetA treatment.

Gene expression analysis showed that MMP9 (gelatinase B) expression was turned on following 24 hour treatment with RetA (Figure 3). Expression of MMP3 (stromelysin 1) and MMP13 (collagenase 3) was unchanged. The RCS-LTC cell line did not express MMP1, MMP2 and MMP7 and these proteases were not turned on in response to RetA. ADAMTS-4 expression was increased compared to control but ADAMTS-5 seemed unchanged.

The chondrocyte phenotype was maintained and type II collagen, type IX collagen (α1(IX) chain) and type XI collagen (α1(XI) chain), continued to be expressed even after 48 hours of RetA treatment.

Discussion

The change in the gross morphology of the cultures can be explained by the degradation of proteoglycan and the concomitant loss of water from the extracellular matrix. It has been shown that ADAMTS-4 is induced in Swarm rat chondrosarcoma cultures in response to RetA.

The results show that the RCS-LTC cells express MMP3 under normal culture conditions. MMP3 has been shown to selectively cleave type IX collagen in the NC2 domain (C-terminal end of the molecule) invitro. Such a cleavage would generate α1(IX) chain fragments consistent with our observations. MMP3 is implicated in early limited proteolysis of type IX collagen in these cultures. The data also shows that the gelatinases, MMP2 and MMP9, are not normally expressed by the RCS-LTC cell line. This could explain why the α1(IX) fragments are not further degraded in these cultures. Following induction of MMP9 by RetA, antibody reactivity to the α1(IX) fragments is lost implicating this enzyme in the further degradation of these fragments. We speculate that the NC4 domain, which is specifically recognized by the antibody is proteolytically cleaved off with resultant loss of reactivity. The gelatinolytic activity of MMP9 synthesized by RetA stimulated cultures is under analysis by gelatin zymography.

The data support the hypothesis that MMP3 and MMP9 are important in the turnover of type IX collagen. MMP9 may play a role in clearing type IX collagen fragments from the surface of the growing type II collagen fibril, a process thought to be needed for lateral growth of the type II collagen fibril.

Recommended Reading

Eyre DR. Collagens and cartilage matrix homeostasis. Clin Orthop Relat Res. 2004 Oct;(427 Suppl):S118-22.

Fernandes RJ, Schmid TM, Eyre DR. Assembly of collagen types II, IX and XI into nascent hetero-fibrils by a rat chondrocyte cell line. Eur J Biochem. 2003 Aug;270(15):3243-50.

Shingleton WD, Ellis AJ, Rowan AD, Cawston TE. Retinoic acid combines with interleukin-1 to promote the degradation of collagen from bovine nasal cartilage: matrix metalloproteinases-1 and -13 are involved in cartilage collagen breakdown. J Cell Biochem. 2000 Sep 14;79(4):519-31.

Sandy JD, Gamett D, Thompson V, Verscharen C. Chondrocyte-mediated catabolism of aggrecan: aggrecanase-dependent cleavage induced by interleukin-1 or retinoic acid can be inhibited by glucosamine. Biochem J. 1998 Oct 1;335 (Pt 1):59-66.

Brown DJ, Bishop P, Hamdi H, Kenney MC. Cleavage of structural components of mammalian vitreous by endogenous matrix metalloproteinase-2. Curr Eye Res. 1996 Apr;15(4):439-45.

Wu JJ, Lark MW, Chun LE, Eyre DR. Sites of stromelysin cleavage in collagen types II, IX, X, and XI of cartilage. J Biol Chem. 1991 Mar 25;266(9):5625-8.

Acknowledgements

NIH, NIAMS grants AR37318 and AR052896.

Comparison of Pullout Button Versus Suture Anchor for Zone I Flexor Tendon Repair

Wren V. McCallister, M.D., Heidi C. Ambrose, M.D., Leonid I. Katolik, M.D., and Thomas E. Trumble, M.D.

Avulsions or complete disruptions of the flexor digitorum profundus tendon in zone I are repaired commonly using a pullout suture tied over a button. This technique is based on the original description by Bunnell in 1948. The choice of suture material is limited and requires a smooth suture that is nonlocking so that it can be pulled out. The nonlocking suture technique has been shown to be weaker than a locking suture technique. Infection can result from communication with the external environment and pain and discomfort can result from the button pressing on the nail. Damage can occur to the nailbed, which can lead to permanent nail deformity and skin necrosis can result from the pressure of the button. The pullout suture is vulnerable to rupture and the button construct can catch on clothing while dressing or on objects in the environment. The use of suture anchors to repair zone I flexor tendon avulsions or complete disruptions is an alternative treatment method that avoids the morbidity associated with the pullout button technique. In addition to the advantages of avoiding an external suture construct, suture anchors placed into the distal phalanx also allow the surgeon to use a biomechanically superior locking suture. This retrospective cohort investigation was designed to test the global null hypothesis that there is no difference in the clinical outcome after zone I flexor tendon avulsion or complete disruption repaired with the pullout button technique or suture anchors placed in the distal phalanx.

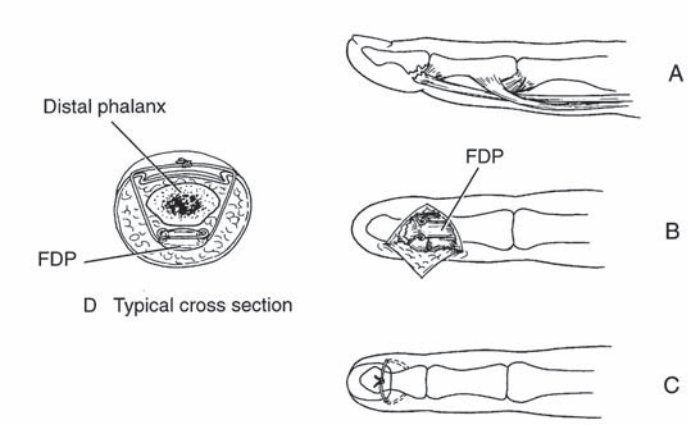

Figure 1: Lateral (A) and volar (B and C) views showing avulsed flexor digitorum profundus tendon and surgical exposure. (D) Volar and cross-sectional views showing pullout button technique modified using the fingernail as a button.

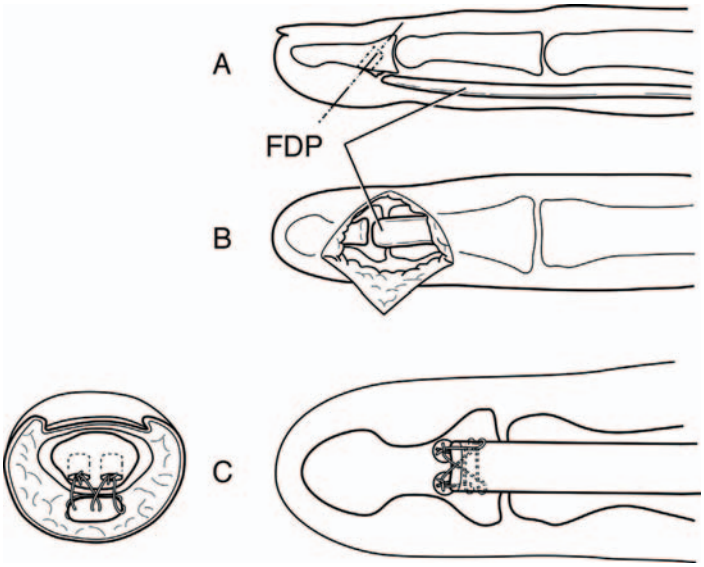

Figure 2: (A) Lateral and (B) volar views showing avulsed flexor digitorum profundus tendon and surgical exposure. (C) Volar and cross-sectional views showing suture anchor placement in the distal phalanx and suture technique.

Methods

Between 1998 and 2002 there were 26 consecutive zone I flexor tendon injuries identified at our institution. Group A (n=13) had repairs from 1998 to 2000 using a standard pullout button technique (Figure 1) and group B (n=13) had repairs from 2000 to 2002 using suture anchors placed in the distal phalanx (Figures 2 and 3). Patient characteristics are shown in Table 1. The same postoperative flexor tendon rehabilitation protocol (based on the Indianapolis protocol described by Cannon and Strickland) and follow-up schedule were used for both groups regardless of whether there was a nerve injury. All patients initially entered in the study completed one year of follow-up evaluation.

Evaluation, by an independent hand therapist, included measurement of the active proximal and distal interphalangeal joint ranges of motion using a goniometer on the dorsum of the joint. Sensibility was evaluated using Semmes-Weinstein monofilament testing and static 2-point discrimination. Grip strength

was measured with a dynamometer and compared with the contralateral uninjured tendon.

For statistical purposes the nonrandomized cohort groups were treated as two retrospective cohort groups with Cox regression analysis. A pre hoc power analysis determined the number of subject in each group.

Results

There were no failures of the tendon repair and no repeat surgeries in either group. Two patients in group A had a superficial infection that resolved with oral antibiotics. There were no infections in group B. Range of motion, sensibility and grip strength are reported in Table 2.

All patients returned to their pre-injury jobs. Patients in group A returned to work an average of 12.23±3.68 weeks (range, 8–18 wk) after surgery and patients in group B returned to work an average of 9.77±2.01 weeks (range, 8–13 wk) after surgery. This was a statistically significant difference ($p < .05$).

Discussion

The morbidity associated with the pullout button technique is well documented. A search for successful and less-morbid means of treating zone I flexor tendon avulsions or complete disruptions is warranted to improve patient outcomes. The suture anchor technique is attractive because it avoids problems associated with an externalized suture construct and also offers the opportunity to use the biomechanically superior locking suture. The use of two mini–bone suture anchors placed in the distal phalanx enables an optimal four-strand repair pattern. We chose the hemi-modified Kessler core suture pattern because investigations have shown that four-strand repairs are significantly stronger than two-strand patterns.

The results of this investigation show that there is no significant difference in the clinical outcome for range of motion and grip strength after repair of zone I flexor tendon avulsions or complete disruptions using either the pullout button technique or the suture anchor technique. Sensibility, when stratified by nerve injury and subsequent repair, also showed no significant difference between the two groups. There was a statistically significant improvement in patient satisfaction and time to return to work for patients treated using the suture anchor technique. The suture anchor technique is not associated with any adverse effects on outcome (there was no evidence of flexion contracture) and avoids the morbidity associated with the pullout button technique.

A.

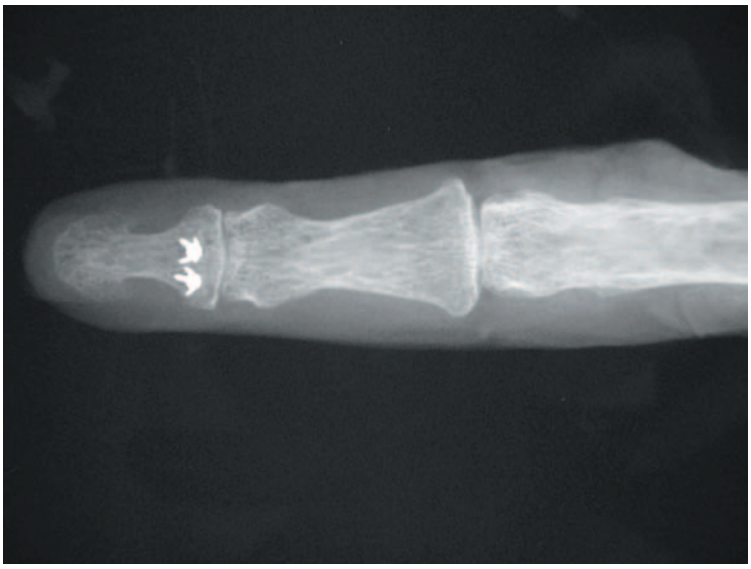

B.

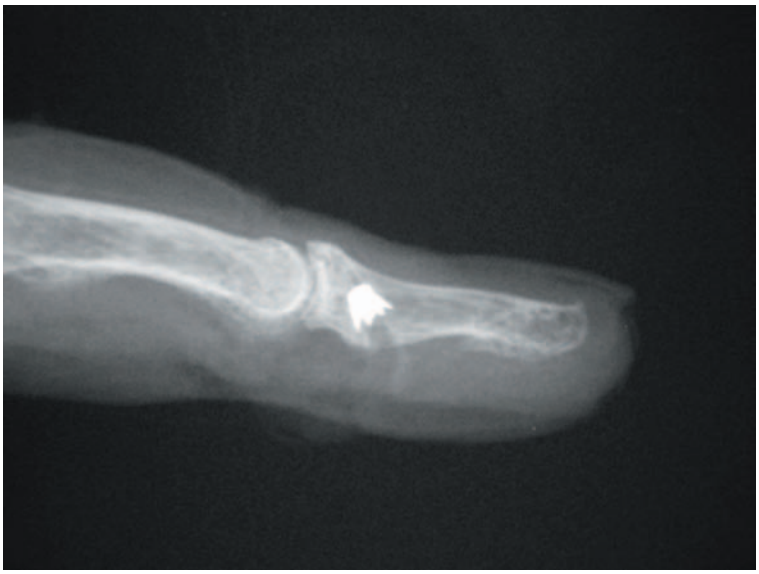

Figure 3: (A) Anteroposterior and (B) lateral radiographs of microsuture anchors placed in the distal phalanx. The trajectory from distal volar to dorsal proximal enables bony purchase in the largest portion of the proximal phalanx.

Recommended Reading

Bunnell S. Surgery of the hand. 2nd ed. Philadelphia: JB Lippincott, 1948:381– 466.

Silva MJ, Hollstien SB, Brodt MD, Boyer MI, Tetro AM, Gelberman RH. Flexor digitorum profundus tendon-to-bone repair: an ex vivo biomechanical analysis of 3 pullout suture techniques. J Hand Surg 1998;23A:120–126.

Skoff HD, Hecker AT, Hayes WC, Sebell-Sklar R, Straughn N. Bone suture anchors in hand surgery. J Hand Surg 1995; 20B:245–248.

	Group A	Group B
Mean age	28 ± 8 years	29 ± 9 years
Male	9	9
Female	4	4
Dominant hand	7	8
Lacerations	7	7
Avulsions	6	6
Unilateral digital nerve injuries	5	6
Delay to surgery	3.6 days	4.2 days

Table 1: Patient Characteristics.

	Group A	Group B	p-value
Mean range of motion (°)			
PIP	99.23 ± 9.09	104.23 ± 4.49	0.11
DIP	57.31 ± 3.88	56.54 ± 4.27	0.69
PIP+DIP	156 ± 10.68	160.77 ± 5.34	0.25
Mean flexion contracture (°)			
PIP	4.62 ± 2.22	3.08 ± 2.29	0.08
DIP	9.54 ± 4.84	8.23 ± 3.79	0.50
PIP+DIP	14.15 ± 5.43	11.31 ± 3.59	0.16
Sensibility			
SW	3.32 ± .87	3.42 ± .89	0.75
Nerve injury (SW)	4.10 ± 1.02	7.20 ± 2.28	0.92
2-point	5.23 ± 2.09	5.54 ± 2.18	0.70
Nerve injury (2-point)	4.12 ± 0.91	7.33 ± 2.07	0.97
Grip strength (%)	97.76 ± 24.95	101.96 ± 13.99	0.65

Table 2: Clinical Outcomes. PIP = proximal interphalangeal joint, DIP = distal interphalangeal joint, SW = Semmes Weinstein monofilament, 2-point = two-point discrimination. Grip strength is reported as a percentage of the contralateral uninjured tendon.

Brustein M, Pellegrini J, Choueka J, Heminger H, Mass D. Bone suture anchors versus the pullout button for repair of distal profundus tendon injuries: a comparison of strength in human cadaveric hands. J Hand Surg 2001;26A:489–496.

Silva MJ, Hollstien SB, Fayazi AH, Adler P, Gelberman RH, Boyer MI. The effects of multiple strand suture techniques on the tensile properties of repair of the flexor digitorum profundus tendon to bone. J Bone Joint Surg 1998;80A:1507–1514.

The Effect of Achilles Tendon Overpull on a Cadaveric Flatfoot Model

Andrew J. Blackman, B.S., Joanna J. Blevins, M.S., Bruce J. Sangeorzan, M.D., and William R. Ledoux, Ph.D.

Flatfoot deformity (pes planus) involves not only loss of the medial longitudinal arch of the foot, but is also characterized by forefoot abduction and hindfoot eversion. Many cases, especially those that are severe or longstanding, are associated with Achilles tendon contracture. In recent years, much research has been devoted to creating and testing physiological flatfoot models in cadavers. We are unaware of a model that has examined the effects of Achilles tendon contracture (equinus deformity) on the flatfoot. One goal of this study was to determine if Achilles tendon overpull in a cadaveric flatfoot model is associated with increased pes planus severity.

Most current cadaveric models rely on substantial sectioning of ligaments and/or tendons, which simulates complete rupture, to create the flatfoot deformity. MRI data has shown that complete soft tissue ruptures do not usually occur in pes planus feet. Thus, another objective of this study was to develop and validate a new cadaveric flatfoot model that includes selective ligament attenuation, rather than sectioning, followed by cyclic axial compression with tendons loaded. We believe that this will better simulate the physiological conditions that lead to the development of a flatfoot.

Methods

Ten fresh-frozen human cadaver feet (76 ± 13 years; range, 56 to 88 years; eight female, two male) with no gross or radiographic evidence of previous surgery or deformity were used for this IRB-approved study. The tibialis posterior, peroneus longus, peroneus brevis, flexor digitorum longus, flexor hallucis longus and Achilles tendons were preserved during dissection and fitted with plastic tendon clamps.

A custom-designed acrylic foot-loading frame was used to apply compressive forces to the tibia and fibula and tensile forces to the tendons (Figure 1). Physiological muscle forces for midstance (30% gait cycle) were calculated using physiological cross-sectional area, EMG measurements, specific tension, and pennation angle. Forces were scaled to 25% of normal due to loading constraints. A 7º wedge was also used to dorsiflex the foot to simulate the midstance. The Fastrak® electromagnetic motion analysis system was used to measure the 3D orientation and track the movements of the tibia, calcaneus, first metatarsal, navicular, cuboid, medial cuneiform, and talus with motion sensors secured via carbon fiber bone rods (4.0-4.6 mm diameter) in each bone. Normal bone orientations were taken in three conditions: unloaded, normal tendon loads, and 50% Achilles overpull.

A flatfoot model was created by attenuating ligaments involved in flatfoot deformity followed by cyclic axial loading an average of 17,600 cycles (range 14,000-20,000) at 2 Hz with a maximum force of 600 N. During cyclic loading, the tendons continued to be loaded in tension, except the tibialis posterior tendon, which was unloaded to simulate PTT dysfunction. Flatfoot 3D bone orientations were acquired in the unloaded, normal tendon loads, and Achilles overpull conditions, and all data were normalized to the normal foot unloaded condition.

Linear mixed effects models were used to determine if rotation differed by

	Sagittal plane (°) Plantar flexion (+) Dorsiflexion (-)	Frontal plane (°) Inversion (+) Eversion (-)	Transverse plane (°) Abduction (+) Adduction (-)
Navicular-to-talus	-1.47 ± 2.07	-2.98 ± 1.74	3.02 ± 2.20
Calcaneus-to-talus	NS	-1.26 ± 1.38	1.08 ± 2.32
First metatarsal-to-talus	-4.89 ± 3.59	NS	3.98 ± 3.30
Talus-to-tibia	1.33 ± 2.71	-2.77 ± 3.01	1.27 ± 1.91
Calcaneus-to-tibia	NS	-4.01 ± 2.66	1.78 ± 1.90
Cuboid-to-calcaneus	-0.96 ± 1.01	-0.58 ± 0.91	1.32 ± 0.94
First metatarsal-to-calcaneus	-4.32 ± 3.27	0.68 ± 0.76	2.90 ± 1.63
Calcaneus	1.44 ±1.76	-4.74 ± 2.83	-3.27 ± 2.01
First metatarsal	-2.89 ± 1.82	-4.06 ± 2.98	NS
Talus	2.00 ± 2.37	-3.49 ± 3.09	-4.35 ± 2.95
Medial Cuneiform	-1.09 ± 1.13	-4.92 ± 3.92	-1.69 ± 1.51
Cuboid	NS	-5.33 ± 3.00	-1.94 ± 1.58
Navicular	NS	-6.47 ± 3.41	-1.33 ± 1.81

Table 1: Differences in bone-to-bone rotations (top) and absolute bone rotations (bottom) between normal feet and surgically created flat feet; $p<0.05$ for all values reported; NS indicates no statistically significant difference between normal and flat conditions.

	Sagittal plane (°) Plantar flexion (+) Dorsiflexion (-)	Frontal plane (°) Inversion (+) Eversion (-)	Transverse plane (°) Abduction (+) Adduction (-)
Navicular-to-talus	-1.23 ± 1.12	NS	0.96 ± 0.87
Calcaneus-to-talus	NS	NS	NS
First metatarsal-to-talus	-2.39 ± 1.19	NS	NS
Talus-to-tibia	1.36 ± 1.12	NS	NS
Calcaneus-to-tibia	0.98 ± 0.57	NS	NS
Cuboid-to-calcaneus	NS	-0.54 ± 0.70	0.52 ± 0.76
First metatarsal-to-calcaneus	-1.77 ± 0.43	NS	0.96 ± 0.59
Calcaneus	1.55 ± 0.64	NS	-0.91 ± 0.75
First metatarsal	NS	NS	NS
Talus	2.17 ± 1.25	NS	NS
Medial Cuneiform	NS	NS	NS
Cuboid	1.61 ± 0.88	-1.20 ± 1.03	NS
Navicular	0.94 ± 0.50	NS	NS

Table 2: Differences in bone-to-bone rotations (top) and absolute bone rotations (bottom) between normal tendon loading and Achilles tendon overpull; $p<0.05$ for all values reported; NS indicates no statistically significant difference between normal and overpull conditions.

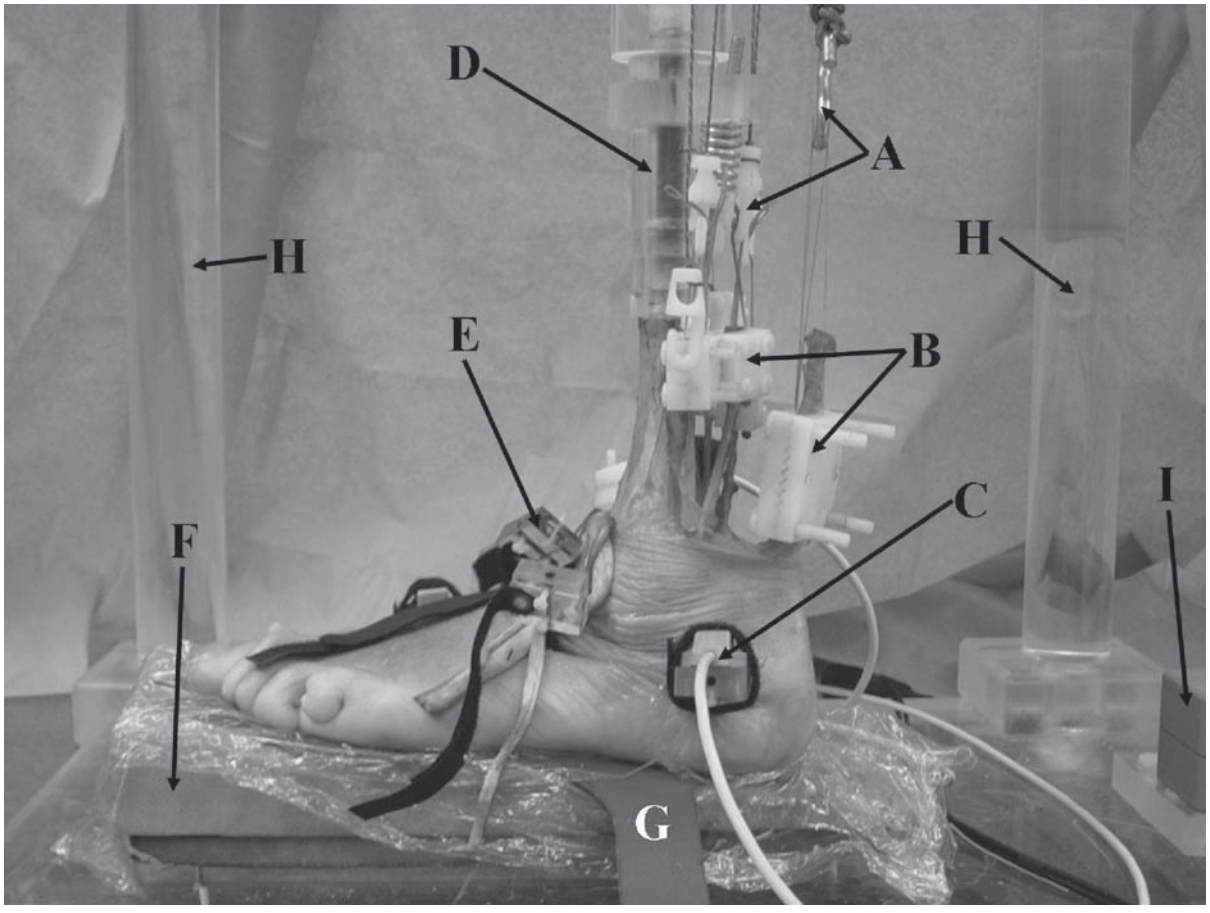

Figure 1: A foot specimen loaded in the static loading frame. (A) hooks attached to tension actuators cylinders above (not seen) and (B) tendon clamps below, (C) Fastrak motion analysis sensor mounted to acrylic block with Velcro, (D) compression rod attached to a compression actuator above (not seen) and inserted into tibial intramedullary shaft below, (E) Fastrak sensor mounting block secured to the bone via a carbon fiber rod, (F) 7° dorsiflexion wedge to simulate midstance, (G) the Pedar plantar pressure sensor wrapped in plastic wrap, (H) support column for acrylic loading frame, and (I) Fastrak motion analysis transmitter.

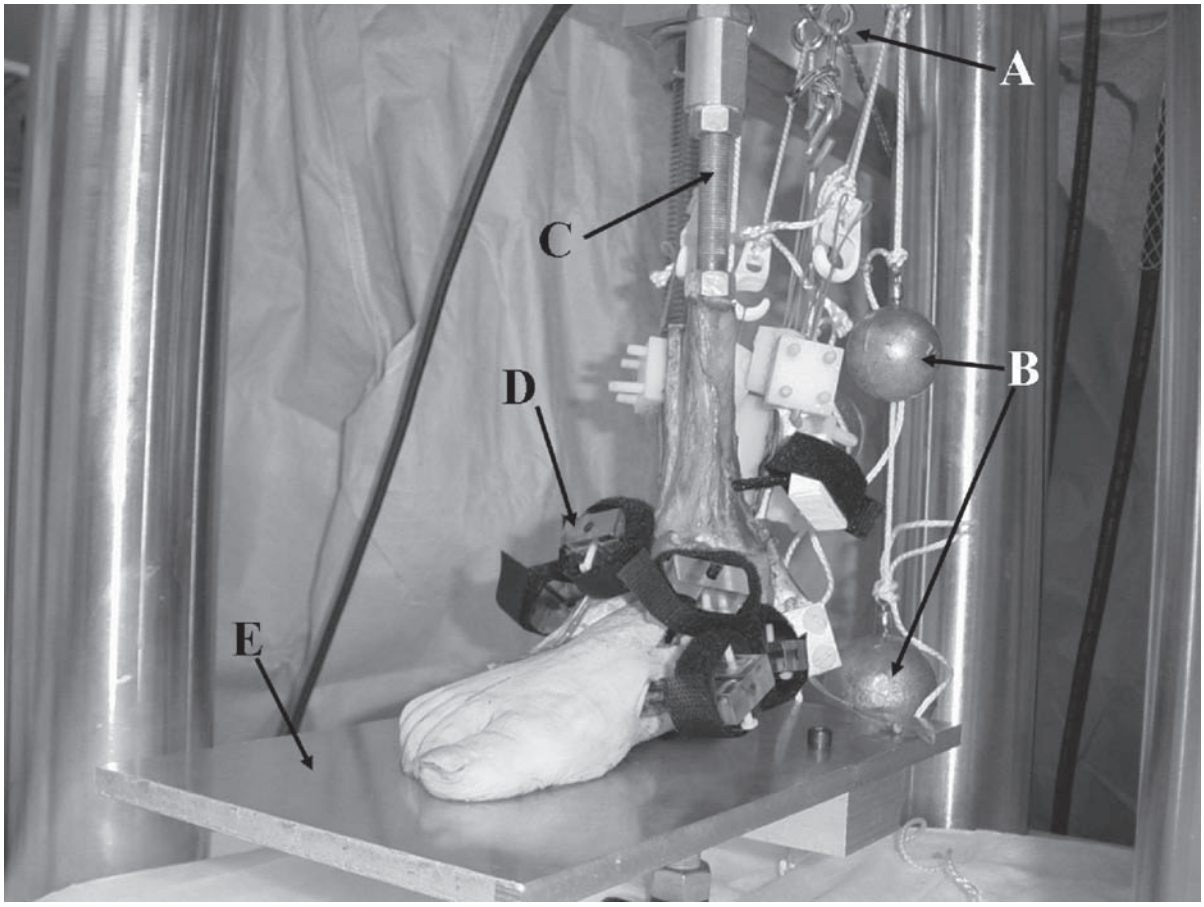

Figure 2: A foot specimen loaded in the cyclic loading frame. (A) eyehooks used to suspend (B) weights that are attached to the tendon clamps, (C) tibial intramedullary rod, (D) Fastrak sensor mounting blocks remained in place during cyclic loading, and (E) aluminum plate attached to actuator to produce cyclic loading.

foot type (normal vs. flat) and/or tendon loads (normal vs. Achilles overpull). Interactions between foot condition and tendon loads were estimated to determine if the relationship between these factors and rotation was other than additive.

Results

Changes seen between normal feet and the created flat feet were consistent with those seen clinically with the pes planus deformity. The first metatarsal dorsiflexed and abducted relative to the talus. The navicular dorsiflexed, everted, and abducted relative to the talus. The calcaneus everted relative to the tibia. The talus plantar flexed and adducted. Complete results are summarized in Table 1.

Achilles tendon overpull resulted primarily in changes in the sagittal plane, which included talar plantar flexion, first metatarsal-to-talus dorsiflexion, and navicular-to-talus dorsiflexion. There were also significant changes in the transverse plane, namely navicular-to-talus abduction and first metatarsal-to-calcaneus abduction. There was a small trend towards calcaneal eversion, but it did not reach statistical significance ($p=0.2$). Complete results are summarized in Table 2.

Analysis of the plantar pressure data showed that maximum force under the heel significantly decreased with Achilles tendon overpull while force underneath all metatarsal heads increased. Comparing flat feet to normal feet showed decreased force under the hindfoot and increased force under the first metatarsal head.

Discussion

The cadaveric model developed for this study resulted in significant changes in 3D bone position that are consistent with those of a physiologic pes planus deformity. Calcaneal eversion, talonavicular joint abduction, forefoot dorsiflexion, forefoot abduction, talar adduction, and talar plantar flexion are all common features of flatfoot and were all seen in the current model.

Overloading the Achilles tendon in the flatfoot model resulted in significant changes in the sagittal plane, including talar plantar flexion, first metatarsal-to-talus dorsiflexion, and navicular-to-talus dorsiflexion, that are consistent with flattening of the longitudinal arch. Navicular-to-talus and first metatarsal-to-calcaneus abduction show that Achilles tendon overpull also increases forefoot abduction in this model. However, no significant hindfoot eversion was seen in the Achilles tendon overpull condition compared to normal tendon loads.

In conclusion, this study indicates that ligament attenuation followed by cyclic axial loading with tendons loaded can create a cadaveric flatfoot model that is consistent with the in vivo deformity. This study also indicates that the Achilles tendon contracture seen in many patients

with flat feet may contribute to the severity of the deformity, particularly in longitudinal arch depression and forefoot abduction.

Acknowledgements

This work was supported in part by the Medical Student Research and Training Program at the University of Washington, and the Department of Veterans Affairs, Rehabilitation R&D Service grant number A2661C.

Recommended Reading

Deland, J. T., R. J. de Asla, et al. (2005). "Posterior tibial tendon insufficiency: which ligaments are involved?" Foot Ankle Int 26(6): 427-35.

Fukunaga, T., R. R. Roy, et al. (1996). "Specific tension of human plantar flexors and dorsiflexors." J Appl Physiol 80(1): 158-65.

Imhauser, C. W., S. Siegler, et al. (2004). "The effect of posterior tibialis tendon dysfunction on the plantar pressure characteristics and the kinematics of the arch and the hindfoot." Clin Biomech (Bristol, Avon) 19(2): 161-9.

Kitaoka, H. B., Z. P. Luo, et al. (1998). "Three-dimensional analysis of flatfoot deformity: Cadaver study." Foot Ankle Int 19(7): 447-51.

Olson, S. L., W. R. Ledoux, et al. (2003). "Muscular imbalances resulting in a clawed hallux." Foot & Ankle International 24(6): 477-485.

Perry, J. (1992). Gait analysis: Normal and pathological function. Thorofare, NJ, SLACK Incorporated.

Pierrynowski, M. R. (1982). A physiological model for the solution of individual muscle force during normal human walking. Vancouver, British Columbia, Simon Fraser University.

Loading Induced Osteoblastic Activity is Modulated by Signaling in Osteocyte Networks

Sundar Srinivasan, Ph.D., Brandon J. Ausk, M.S., and Ted S. Gross, Ph.D.

The site-specificity of bone's response to mechanical loading may provide critical insights in how mechanotransduction functions within bone. For example, if osteocytes serve as mechanotransducers within bone, it could be expected that mechanically activated osteocytes effect osteoblast activity only within a localized area, and have limited effect upon remote osteoblasts. While previous studies have attempted to relate site specific surface responses with aspects of the induced strain environment (e.g., strain magnitude or strain gradients), these relations have demonstrated, at best, only moderate predictive abilities. Here, we examine the fundamental hypothesis that localized osteoblastic activity induced by tissue strains is modulated by the signaling within the osteocytic network. We examined this hypothesis using a novel agent based model (ABM) for real-time signaling amongst bone cells.

Methods

Extending a previously developed ABM, we examined real-time signaling when an anatomically scaled, murine tibia mid-shaft cross-section was subjected to bending. To model the cellular network topology, mid-shaft tibia cross-sections of 16 wk C57BL/6 mice (n=5) were imaged (200X, 90 μm thick; Figure 1a) and mean osteocyte numbers determined within 384 sub-sectors (96 circumferential and 4 radial). A Mersenne-Twister pseudo random number generator was used to determine osteocyte spatial locations within each sub-sector (for each simulation, the network was therefore unique in terms of cellular spatial proximity). Osteoblastic cells were generated along bone surfaces and functionally coupled to neighboring cells located within a canalicular length of 30 μm. In the ABM, real-time signaling was induced in either osteocytes and/or osteoblasts when tissue strains were elevated beyond a threshold ($T^{\varepsilon}max$, $T^{\varepsilon}min$). Cell activity within localized cellular neighborhoods was propagated and influenced activity in recipient cells when above a threshold ($T^{C}max$, $T^{C}min$). Finally, real-time cellular activity was constrained by molecular stores (M) and their rates of recovery (R^{t}). We explored the network response to a previously calibrated loading regimen (1-Hz, 100 cycle, 1300 με cyclic waveform). Based on the defined force and moment boundary conditions, tissue strains at the level of each cell were determined via beam theory. Simulations were first performed for a network in which homogeneous osteoblasts served as mechanosensors and were functionally uncoupled from osteocytes (Ob). Second, a model in which homogeneous osteocytes served as mechanosensors and were functionally coupled to each other and to homogeneous osteoblasts was explored (Oc). Finally, simulations were performed for heterogeneous populations in both scenarios (where function values assigned individual cells were assumed to be normally distributed about the population mean; Ob_H, Oc_H). Real-time signaling was determined in periosteal osteoblasts at 16 equal angle pie sectors for 10 simulations/condition (Figure 1b and c). At periosteal locations where induced strains were above thresholds for osteoblastic activation (determined in vivo to be > 800 με at 1-Hz), peak real-time responses were correlated to induced tissue strains.

Results

Similar to in vitro Ca2+ signaling, real-time signaling induced in periosteal osteoblastic cells consisted of a large

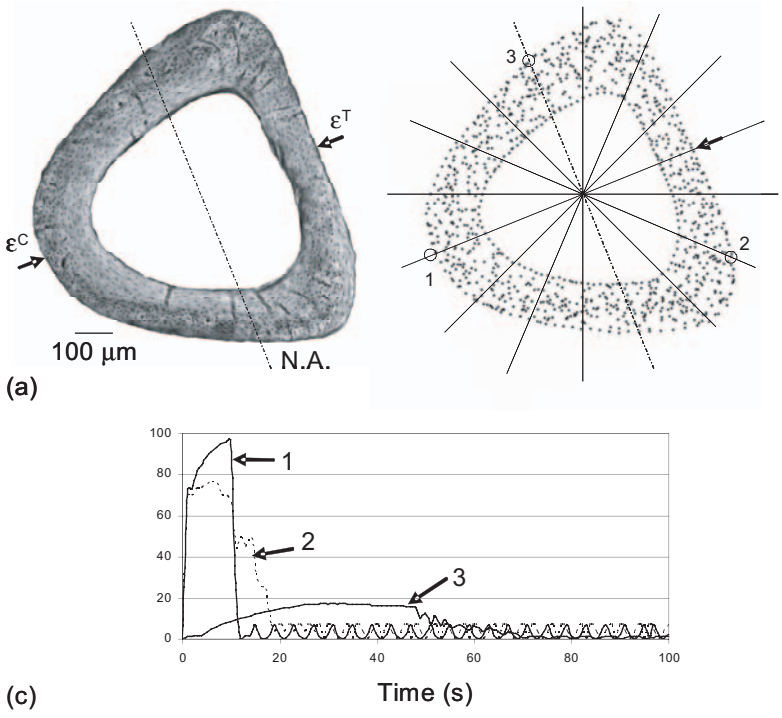

Figure 1: Image of a mid-shaft cross-section (a) and modeled osteocyte-osteoblast network configuration illustrated (black dots; b). The induced strain environment is also noted (neutral axis N.A., peak tension εT, compression εC). Real-time activity was determined in periosteal osteoblasts located at 16 equal angle sectors (b) and illustrated for 3 representative osteoblasts (c).

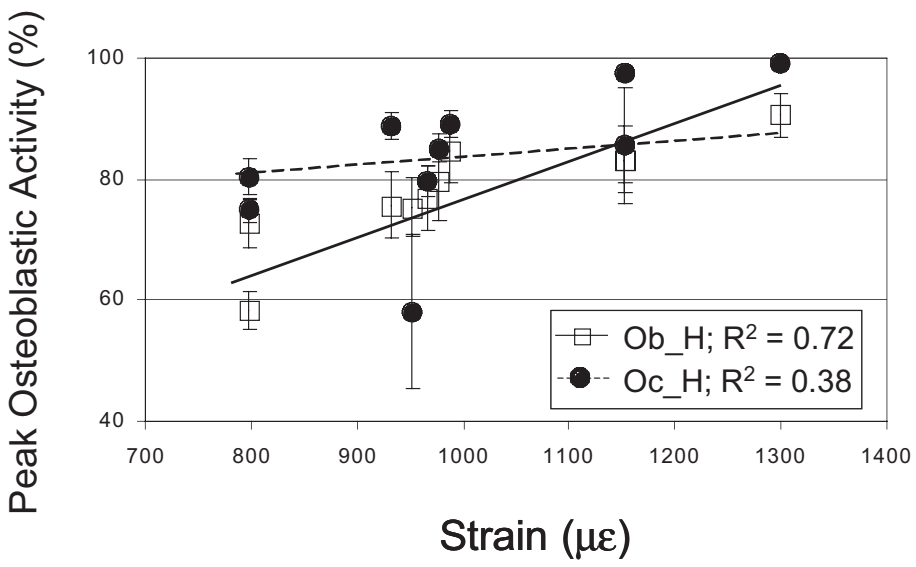

Figure 2: Relation between induced strains and osteoblastic activity (± s.e.) in heterogeneous networks in which osteoblasts served as the sole mechanosensor (Ob_H) or osteocytes served as a coupled mechanosensor (Oc_H). Variability in the predicted response arose due to heterogeneity, but the relation between predicted osteoblast activity and strain magnitude was substantially diminished when heterogeneous osteocytes and osteoblasts were coupled.

transient followed by low level steady state fluctuations (Figure 1c). When homogeneous osteoblasts served as mechanosensors, osteoblastic activity was directly correlated with strain distribution (R2 = 1.0). This relation was only slightly diminished when homogenous osteocytes served this role (R2 = 0.83). Heterogeneity in osteoblasts serving as mechanosensors, further diminished the relation between activation and the induced strain environment (R2 = 0.72). Interestingly, when all bone cells were fully heterogeneous and osteoblasts were capable of activation via osteocytes, the relation between the strain distribution and site-specific osteoblastic activity was substantially weakened (R2 = 0.38, Figure 2).

Discussion

In this study, we developed an ABM framework to examine real-time signaling between osteocytes and osteoblasts stimulated by mechanical loading. We used this framework to explore potential modalities underlying the poor predictive power of strain environments in forecasting site specific osteoblastic activity. In support of our hypothesis, our studies indicated that localized osteoblastic activity arises (at a minimum) via the dynamic interplay between the induced strain environment, the topology of the underlying osteocytic network (i.e., how close cells are to one another and their ability to communicate) and the heterogeneity of cells within bone. The most physiologic results arose when osteocytes were heterogeneous in their ability to sense and respond (which is likely) and were coupled together with osteoblasts (also likely). While this study examined induced tissue deformations, the ABM framework would readily permit incorporation of additional mechanocoupling events (e.g., fluid flow distributions) and, uniquely, interactions between these varied mechanical stimuli

Acknowledgements

Funding from the Whitaker Foundation and NIAMS (AR48102) is gratefully acknowledged.

Recommended Reading

Kotha, S.P., Y.F. Hsieh, R.M. Strigel, R. Muller, and M.J. Silva, Experimental and finite element analysis of the rat ulnar loading model-correlations between strain and bone formation following fatigue loading. J Biomech, 2004. 37(4): p. 541-8.

Gross, T.S., J.L. Edwards, K.J. McLeod, and C.T. Rubin, Strain gradients correlate with sites of periosteal bone formation. J Bone Miner Res, 1997. 12(6): p. 982-8.

Ausk, B.J., T.S. Gross, and S. Srinivasan, An agent based model for real-time signaling induced in osteocytic networks by mechanical stimuli. J Biomech, In Press.

Srinivasan, S., D.A. Weimer, S.C. Agans, S.D. Bain, and T.S. Gross, Low magnitude mechanical loading becomes osteogenic when rest is inserted between each load cycle. J Bone Miner Res, 2002. 17(9): p. 1613-1620.

Hung, C.T., S.R. Pollack, T.M. Reilly, and C.T. Brighton, Real-time calcium response of cultured bone cells to fluid flow. Clin Orthop, 1995(313): p. 256-69.

Donahue, S.W., C.R. Jacobs, and H.J. Donahue, Flow-induced calcium oscillations in rat osteoblasts are age, loading frequency, and shear stress dependent. Am J Physiol Cell Physiol, 2001. 281(5): p. C1635-41.

Outcomes Assessment of Corrective Osteotomies for Distal Radius Malunions

Seth D. Dodds, M.D. and Thomas E. Trumble, M.D.

When distal radius fractures heal in a malunited position, the kinematics of wrist motion and function are affected. While loss of motion is not always a presenting complaint, patients will frequently experience wrist pain or loss of grip strength. A number of previously reported clinical studies of distal radius malunions have focused on the technique of fixation or objective parameters related to the patient's outcome after corrective osteotomy. We report a combination of subject and objective outcomes for a retrospectively collected case series of 47 patients who were followed for a minimum of 2 years. The purpose of our study was to assess specific objective parameters and to understand which parameters contributed to subjective outcome. Our hypothesis was that correction of radiographic parameters, such as radial inclination, palmar tilt, and radial length would affect not only patient range of motion and grip strength, but also visual analog pain and DASH questionnaire scores.

Materials and Methods

Over a 5 year time period, the senior author performed 47 corrective osteotomies for dorsally-angulated, extra-articular distal radius malunions (Figure 1). There were 20 men and 27 women, all with an average age of 36.5 years (SD 10.8, range 15 to 63 years old). All patients were either non-smokers or had quit smoking prior to the surgical procedure. Post-operative follow up consisted of an average of 33 months (SD 8, range 24-56 months).

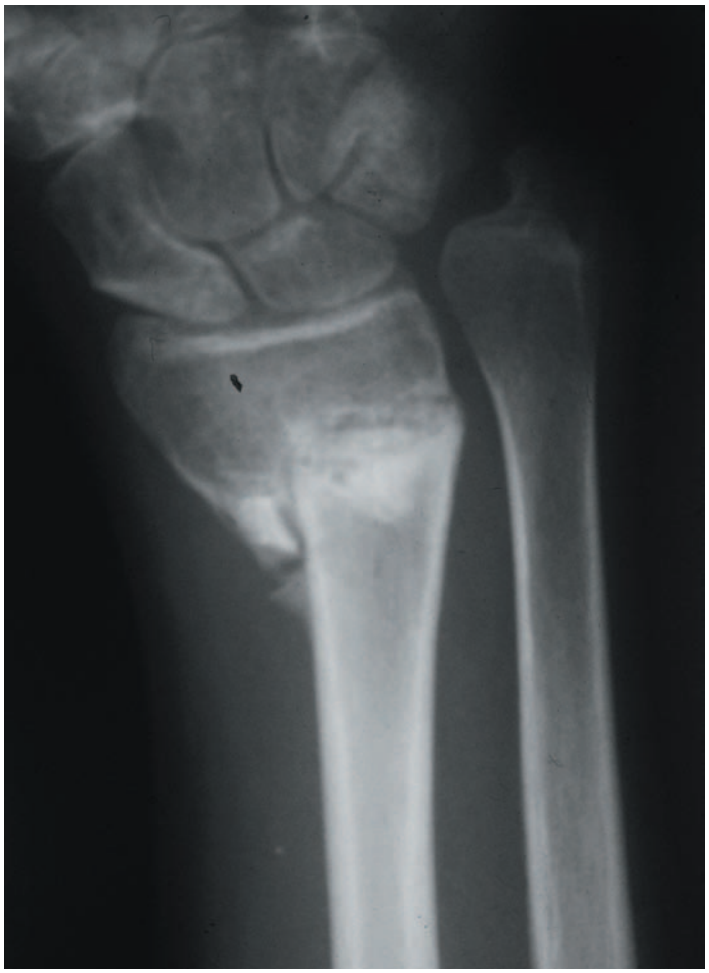

Figure 1: This pre-operative PA radiograph demonstrates an extra-articular distal radius malunion with loss of radial inclination and radial length.

Operative Procedure

Prior to the surgical procedure, each patient's radiographs were templated to create an intra-operative plan for the location and total correction desired. Under tourniquet control, a dorsal approach to the distal radius was performed between the third and fourth dorsal compartments. The osteotomy was planned and then executed according to the pre-operative template. Next, a structural wedge of autologous iliac crest bone graft was placed in the reduced osteotomy site and provisionally fixed with one or two radial styloid Kirschner wires. A non-locking dorsal T-shaped plate was used for definitive fixation in all cases. All patients returned to the operating room after union at the osteotomy site was confirmed clinically and radiographically for a removal of hardware (Figure 2).

Data Collection

Subjective data collection consisted of disabilities of the arm, shoulder, and hand (DASH) scores, pain scores ranking pain on a 1 to 10 scale based on the visual analogue pain scale, and a satisfaction score based on a 1 to 10 ranking with 1 being the least satisfied and 10 being the most satisfied. Patients underwent standardized physical exams of bilateral wrists measuring wrist range of motion and grip strength with a dynamometer. Standard posteroanterior and lateral radiographs were measured for radial inclination, palmar tilt, and radial length at three specific time points: pre-operatively, post-reduction, and at final follow-up. Time to union was documented as the post-operative week from the osteotomy when there was significantly diminished tenderness at the osteotomy site and bridging bone on radiographs. Data was assessed

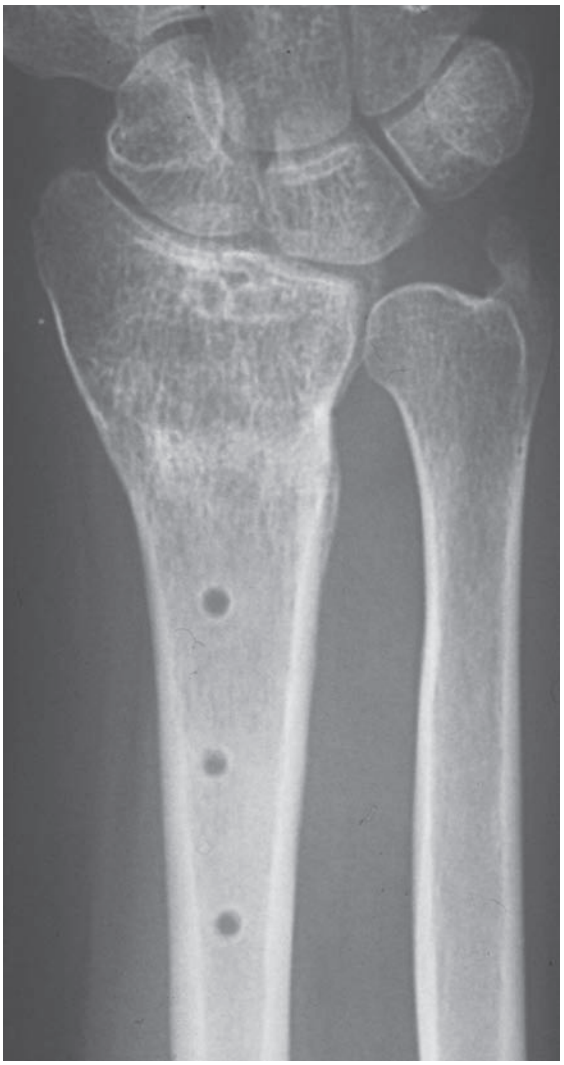

Figure 2: This post-osteotomy PA radiograph shows restoration of radial inclination, radial length, and congruency of the distal radioulnar joint after removal of internal fixation.

using an analysis of variance for parametric data, a Kruskal-Wallis tests for non-parametric data, and Pearson correlation coefficients between outcome variables ($p < 0.05$).

Results

The average time to union for all patients was 8.0 ± 1.6 weeks. There was one case of a delayed union (healing time of greater than 3 months), with a time to union of 13 weeks. At final follow-up 46 patients reported a return to their same level of activity prior to their injury and all returned to some form of work. Specific subjective and objective data are presented in Table 1.

Significant Pearson correlation coefficients were found between the following pre-operative variables: palmar tilt and patient satisfaction ($r = 0.295$, $p < 0.04$); flexion/extension and patient satisfaction ($r = 0.451$, $p < 0.01$); flexion/extension and grip strength ($r = 0.407$, $p < 0.01$); and, lastly, age and pain score ($r = 0.299$, $p < 0.04$). Significant correlations were demonstrated between the following post-operative variables: radial length and grip strength ($r = 0.308$, $p < 0.04$), flexion/extension and grip strength ($r = 0.406$, $p < 0.01$), and final pain scores and grip strength ($r = -0303$, $p < 0.04$). Additionally, final radial length was correlated inversely with final DASH scores ($r = -0.288$, $p < 0.05$) and final pain correlated with time to union ($r = 0.440$, $p < 0.01$).

Complications

A total of 7 patients (15%) suffered complications directly related to their surgery. These complications included two superficial pin-related infections, one extensor pollicis longus rupture treated with an extensor indicis proprius transfer, one transient median nerve neurapraxia, 2 median nerve neuropraxias that required carpal tunnel release, and one case of radial sensory nerve hypersensitivity.

Discussion

This relatively large series of 47 patients with dorsally angulated distal radius malunions that underwent corrective osteotomy offers both subjective and objective data assessment of patient outcome. Expected mean improvements in radiographic parameters, range of motion, and grip strength were all maintained at final follow up (mean, 33 months). In realigning the distal radius, it is critical to maintain the correction achieved at surgery. Patients with minor residual deformity after osteotomy for distal radius malunion fare better than patients who suffered subsequent collapse and persistent deformity.

The unique purpose of our study was not only to assess specific objective parameters, but also to understand which parameters contributed to subjective outcome. Our hypothesis that correction of radiographic parameters would correlate with improvements in objective clinical measures and subjective patient outcomes was upheld in a few circumstances. For example, improvements in radial length from the pre-operative, shortened position correlated with improvements in grip strength and DASH scores. In the management of acute distal radius fractures radial shortening closely correlates with final functional outcome. It is not surprising, then, that restoration of radial length in distal radius malunions correlated with improved grip strength and DASH scores.

In summary, extra-articular distal radius malunions can be effectively treated with corrective osteotomy using a dorsal approach for the osteotomy, reduction of the malaligned joint surface, and subsequent internal fixation. The data from this series of

	Pre-op	Post-op	Final	ANOVA	Post-hoc analysis Pre-op vs. Final	Post-hoc analysis Post-op vs. Final
Rad Inclination (degrees)	8.6 ± 6.0	20.2 ± 1.5	19.7 ± 1.6	$p < 0.01$	$p < 0.01$	$p = 0.81$
Palmar Tilt (degrees)	-26.6 ± 11.9	6.5 ± 4.8	6.1 ± 5.1	$p < 0.01$	$p < 0.01$	$p = 0.97$
Radial Length (mm)	-5.6 ± 1.6	-0.3 ± 0.9	-0.5 ± 0.9	$p < 0.01$	$p < 0.01$	$p = 0.66$
	Pre-op	Contr.	Final	ANOVA	Post-hoc analysis Pre-op vs. Final	Post-hoc analysis Contr. vs. Final
Flex/Ext (degrees)	100.0 ± 17.6	113.9 ± 14.7	122.5 ± 12.0	$p < 0.01$	$p < 0.01$	$p = 0.02$
Rad/Uln Dev. (degrees)	35.0 ± 9.3	42.2 ± 9.0	48.1 ± 7.6	$p < 0.01$	$p < 0.01$	$p < 0.01$
Pron/Sup (degrees)	132.1 ± 16.4	141.4 ± 13.8	145.9 ± 11.7	$p < 0.01$	$p < 0.01$	$p = 0.28$
Grip Strength (kg)	22.4 ± 8.7	29.5 ± 12.6	36.4 ± 14.2	$p < 0.01$	$p < 0.01$	$p = 0.02$
	Pre-op	Final		Kruskal-Wallis		
VAS Pain Scale (1-10)	6.4 ± 12	0.8 ± 0.8		$p < 0.01$		
Satisf. Scale (1-10)	3.0 ± 1.3	8.2 ±1.7		$p < 0.01$		
DASH Score (0-150)	105.6 ± 22.6	54.1 ± 14.0		$p < 0.01$		

Table 1: Comparison of Pre-operative and Post-operative Mean Values with Standard Deviations after Corrective Osteotomy.

patients demonstrates that reductions assessed by radiographic parameters were maintained at final follow up. Restoration of radial length was found to correlate with improvements in functional outcome, specifically grip strength and DASH scores. Reconstruction of extra-articular distal radius malunions should focus on restoration of the anatomic position of the radiocarpal joint to maximize patient outcome.

Recommended Reading

Trumble TE, Schmitt SR, Vedder NB. Factors affecting functional outcome of displaced intra-articular distal radius fractures. J Hand Surg Am. 1994;19(2):325-340.

Bronstein AJ, Trumble TE, Tencer AF. The effects of distal radius fracture malalignment on forearm rotation: a cadaveric study. J Hand Surg [Am]. 1997;22(2):258-262.

Moore DC, Hogan KA, Crisco JJ, 3rd, Akelman E, Dasilva MF, Weiss AP. Three-dimensional in vivo kinematics of the distal radioulnar joint in malunited distal radius fractures. J Hand Surg [Am]. 2002;27(2):233-242.

Ring D, Roberge C, Morgan T, Jupiter JB. Osteotomy for malunited fractures of the distal radius: a comparison of structural and nonstructural autogenous bone grafts. J Hand Surg [Am]. 2002;27(2):216-222.

Jupiter JB, Ring D. A comparison of early and late reconstruction of malunited fractures of the distal end of the radius. J Bone Joint Surg Am. 1996;78(5):739-748.

Prommersberger KJ, Van Schoonhoven J, Lanz UB. Outcome after corrective osteotomy for malunited fractures of the distal end of the radius. J Hand Surg [Br]. 2002;27(1):55-60.

Percutaneous Pins vs. Volar Plates for Unstable Distal Radius Fractures: A Biomechanical Study Using a Cadaver Model

Jeffrey Knox, B.A., Heidi C. Ambrose, M.D., Wren V. McCallister, M.D., and Thomas E. Trumble, M.D.

Distal radius fractures are common and can occasionally be a challenge to treat. Many methods are available to treat distal radius fractures, each with their own benefits and potential complications which must be weighed when choosing which treatment to use. The treatment method chosen should provide an accurate and stable reduction and allow early rehabilitation while minimizing soft tissue trauma.

Two commonly used methods of fixation are open reduction with internal fixation using plates and percutaneous pin fixation. Percutaneous pins allow for a low cost fixation of unstable fractures with minimal soft tissue dissection. Internal fixation provides a very stable fixation that allows early active movement. Because of the incidence of extensor tendon rupture with dorsal plates, volar plating has been introduced as an alternative with which tendon rupture is a rare event. A recent clinical trial comparing percutaneous pinning vs. internal fixation demonstrated improved clinical outcomes in patients treated with percutaneous pins.

To date, no studies have been identified that compared the biomechanical stability of Kirschner wires vs. plate fixation for distal radius fractures. Because of the potential benefits of using percutaneous pins in managing distal radius fractures, a formal biomechanical study was done comparing the stability of pins vs. volar plates in treating unstable distal radius fractures using a cadaver model.

Methods

This study was performed on 7 fresh frozen cadaver arms from cadavers in which an AO type C1 fracture with dorsal comminution was created as follows. The soft tissue was removed from the specimens, leaving the 5 primary motor tendons of the wrist (ECRB, ECRL, ECU, FCU, and FCR), pronator teres, pronator quadratus, dorsal retinaculum, wrist capsule, elbow capsule, and the interosseous membrane. The fracture was created by first removing a 30º dorsal wedge centered 2cm proximal to the distal end of the radius while maintaining the integrity of the volar cortex. This was initiated with a pneumatic saw and completed with an osteotome. Secondly, a sagittal cut was created between the scapho-lunate fossae that extended from the dorsal wedge to the distal tip of the radius penetrating the volar cortex with the pneumatic saw.

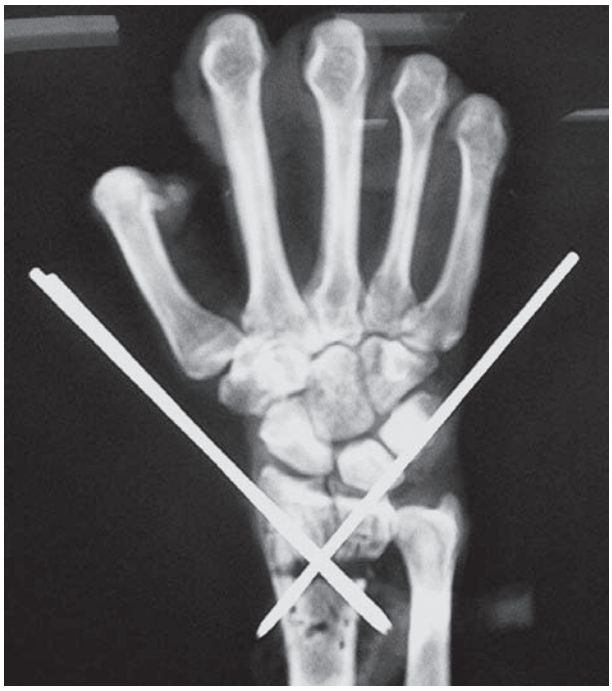

Figure 1: X-ray of fracture with pin fixation.

The fracture was held with two 1.27mm Kirschner wires inserted through the radial fragment then held with one pin through the ulnar fragment in a crossed fashion (Figure 1). The specimens were then tested after which the pins were removed and a DVR volar plate (Hand Innovations, Miami, FL) was inserted onto the fracture site and testing was repeated (Figure 2). This pinning pattern was demonstrated to be the most stable by Naidu et al for fixing unstable distal radius fractures. The DVR plate was found to be three times as strong as the other plates tested for distal radius fractures with a segmental dorsal defect. This is the reason that this pin configuration and this plate were chosen for this study.

The humerus of each specimen was fixed into the loading device with the elbow at 90º and each of the five tendons was then attached to the loading device (Figure 3). Four 1.27mm Kirschner wires were inserted across the fracture site to be used as measurement pints, one in each distal fragment and one directly below each of these both located in the proximal fragment. These were used to measure the movement across the extra-articular fracture site before,

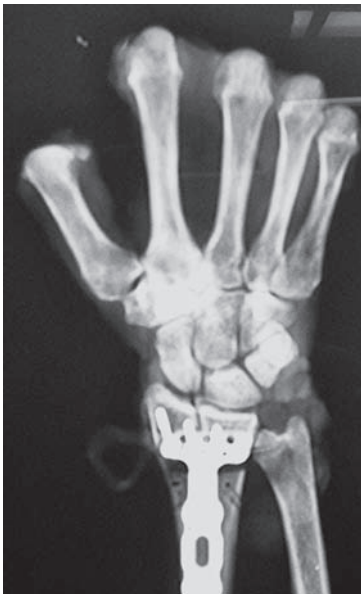

Figure 2: X-ray of fracture with plate fixation.

during, and after stressing using digital calipers (Mitutoyo, Aurora, IL). Measurement was done at the same site on the Kirschner wires each time. This could then provide a measurement of translational motion across the fracture site.

The specimens were then incrementally tested at loads starting with 36N, increasing in 16N increments up to 100N in extension and 68N in flexion. Testing was halted at 68N during flexion as the initial specimens' pins began to fatigue so the study was designed to stress but not fatigue the pin fixation. During testing, all five motor tendons were loaded in the device but tension was created only on the tendons in the desired tendon group. At each level of force, the force was applied once to allow for viscoelastic deformation. The force was then applied three more times with measurements made after each time. If the volar cortex fractured during dissection or testing, the specimen was eliminated from consideration. All testing was done by a single researcher to eliminate inter-observer variation. Institutional IRB approval was obtained for this research study.

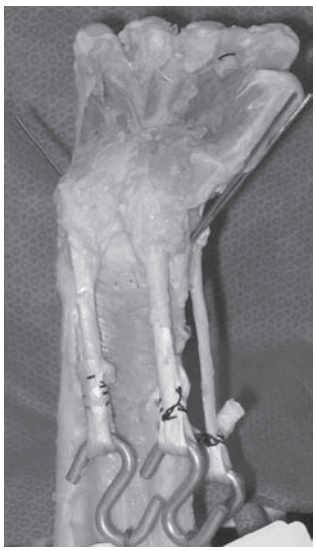

Figure 3: Cadaver forearm loaded with pneumatic testing device.

Sample	Pin (mm)	Plate (mm)	Difference
1	3.565	1.101	2.464
2	4.395	1.678	2.717
3	1.694	0.481	1.213
4	4.345	1.406	2.939
5	0.911	0.484	0.427
6	1.207	1.416	-0.209
7	1.420	0.936	0.484
Average	2.505	1.072	1.433

Table 1: Average Displacement Across Fracture Site.

A mean of all measurements for each specimen were then calculated individually for each level of force individually for flexion and extension to assess the behavior of each fixation method at different forces. These values were then averaged to create a single mean total displacement figure for each method of fixation. The two means were then analyzed using the student t test testing the null hypothesis that pins were equally stable to plates in fixing unstable distal radius fractures. Providing an average displacement serves to provide a summary figure that helps minimize intra-observer variation while providing a description of the overall motion with each method of fixation.

Results

Volar plating was found to be significantly more stable than pinning with an average movement across the fracture site of 1.1mm +/- 0.5mm compared to 2.5mm +/- 1.3mm when pins were attached (P=0.024) (see Table 1, Figure 4). The pins also demonstrated a significant degree of slipping after repeated stressing. With successive stressing, the fracture site experienced increasing displacement. This increase was not seen after pins were removed and plates were added.

Discussion

These results demonstrate that volar plate fixation results in less displacement of intra-articular distal radius fractures with dorsal comminution compared with K-wire fixation. Although no previous studies have compared these two methods, previous studies have looked at the biomechanics of the individual methods. Naidu et al studied the biomechanics of K-wire fixation for extra-articular distal radius fractures, demonstrating superior stability with the pin configuration used in this study.

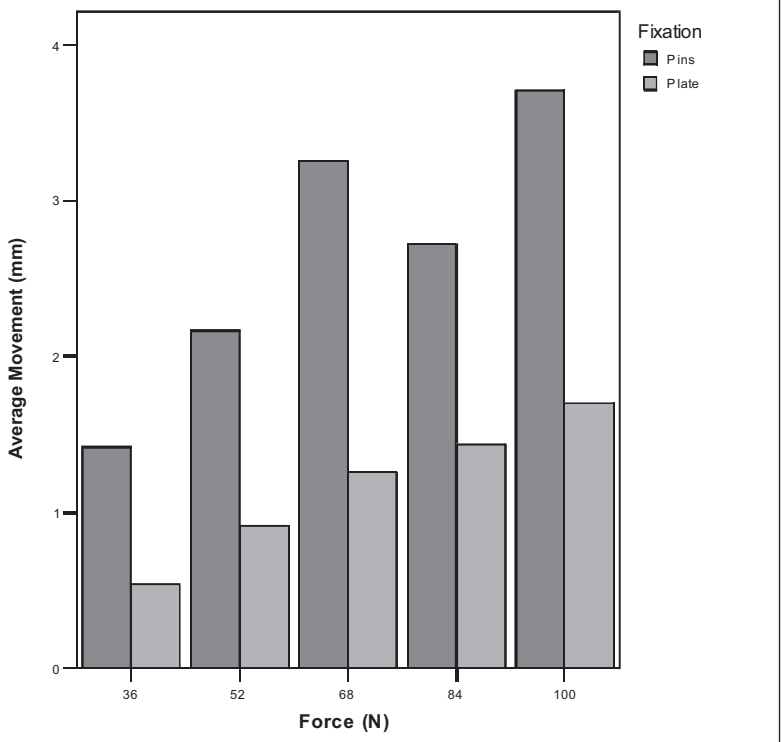

Figure 4: Average movement / Force table.

This was, however, done in an extra-articular model and only one study was identified that investigated the stability of Kirschner wires for intra-articular distal radius fractures.

Although multiple studies exist that investigate the biomechanical strength of distal radius plates, no studies have been published that looked at the DVR distal radius plate. This plate has been stated to be three times stronger than other plates when used in a distal radius fracture with a dorsal segmental defect although no supporting studies have been published to support this.

While percutaneous pinning can be a successful method of treating unstable distal radius fractures, it is difficult to obtain an accurate reduction using pins, especially for more complex fracture patterns. The pins may also slip thus making it difficult to maintain accurate alignment and articular incongruity.

Recommended Reading

Orbay JL, Fernandez DL: Volar fixation for dorsally displaced fractures of the distal radius: a preliminary report. J Hand Surg [Am] 2002:27:205-215.

Naidu SH, Capo JT, Moulton M, Ciccone W, 2nd, Radin A: Percutaneous pinning of distal radius fractures: a biomechanical study. J Hand Surg [Am] 1997:22:252-257.

Orbay JL, Fernandez DL: Volar fixed-angle plate fixation for unstable distal radius fractures in the elderly patient. J Hand Surg [Am] 2004:29:96-102.

Leung F, Zhu L, Ho H, et al. Palmar plate fixation of AO type C2 fracture of distl radius using a locking compression plate- A biomechanical study in a cadaveric model. J Hand Surg [Br] 2003: 28B: 3: 263-266.

Oblique Ulnar Shortening Osteotomy with a New Plate and Compression System

Anthony J. Lauder, M.D. and Thomas E. Trumble, M.D.

The ulnar shortening osteotomy has become the gold standard for correcting positive ulnar variance. Ulnar variance is defined as the difference in length between the distal ulnar corner of the radius and the distal most aspect of the dome of the ulnar head. Positive ulnar variance occurs when the dome of the distal ulna is more distal than the ulnar corner of the distal radius. This positive variance leads to ulnar sided wrist pain and degenerative processes due to the overloading that occurs between the ulnar head and the ulnar carpus. Thus, the goals of the shortening procedure are to relieve pain and prevent arthritis by reestablishing a neutral or slightly negative ulnar variance. The typical indications for the osteotomy include ulnar impaction syndrome, non-repairable tears of the triangular fibrocartilage complex (TFCC), previous radial head excision and associated Essex-Lopresti lesions, attritional luno-triquetral ligament tears, ulnar nonunions, radial malunions, and early post-traumatic distal radioulnar joint (DRUJ) arthritis. Numerous authors have introduced methods and systems for performing, and hopefully simplifying, the osteotomy. This study compares the results of shortening ulnas with a new plate and compression system to a previously described and accepted method.

Material & Methods

Dynamic Compression Plating

Thirty-seven patients underwent an ulnar shortening osteotomy using a dynamic compression plate and an AO compression/distraction device (Synthes, Paoli, PA) as described by Chen and Wolfe. Sixteen patients were male and twenty-one were female. Average patient age at the time of the shortening osteotomy was 36 years. Six of the osteotomies were carried out for prior distal radius fractures that healed with some degree of shortening. Thirty-one of the osteotomies were performed for degenerative, non-repairable tears of the TFCC.

This technique implements a 3.5 mm 6 hole dynamic compression plate (Synthes, Paoli, PA). Perfectly parallel freehand osteotomies must be made at 45-degree angles to the plate. This is followed by the placement of a lag screw inserted perpendicular to the approximated osteotomies. After completing the osteotomy the AO compression/distraction device is used to further reduce and compress the distal and proximal bone ends.

New Ulnar Shortening Osteotomy System

Seventeen patients underwent an ulnar shortening osteotomy utilizing a new system manufactured by Trimed (Valencia, CA). Seven of the patients were male and ten were female. Average patient age at the time of surgery was 38 years. Three of the osteotomies were performed to relieve systems stemming from distal radius malunions that had healed shortened. The remaining fourteen osteotomies were performed for degenerative TFCC tears.

This new system, designed by the senior author (TET), implements a new plate allowing for compression at the osteotomy site with a Bone Compression Clamp™ and lag screw (Figure 1). In this system the lag screw is placed through a guide ensuring perpendicular placement of the screw to the osteotomy. Dissimilar to the Chen and Wolfe technique which requires moving the plate prior to osteotomizing the ulna, this system utilizes a slotted hole so that the plate is firmly affixed prior to performing the osteotomy (Figure 2). Furthermore, the system has cutting guides that attach directly to plate, eliminating the need for freehand osteotomies (Figure 3).

Outcome Measures

All patients were evaluated for pre- and postoperative range of motion and grip strength. These measures were recorded for the surgical side and then compared as a percentage to the contralateral arm. Pain levels were recorded according to the Visual Analog Scale where a score of zero is no pain and a score of ten is the worst pain that individual has ever experienced. Patient function was established using the Disabilities of the Arm, Shoulder

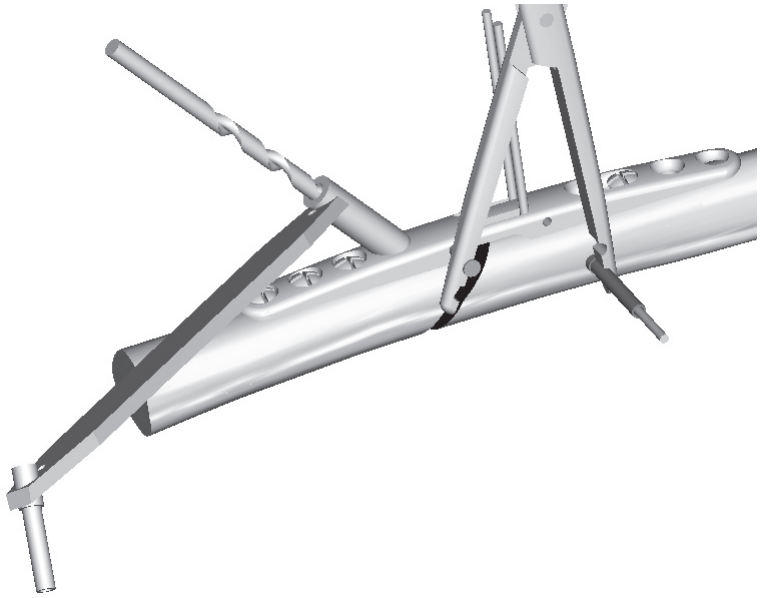

Figure 1: Graphic illustration demonstrating Bone Compression Clamp™ spanning compressing osteotomy during insertion of lag screw.

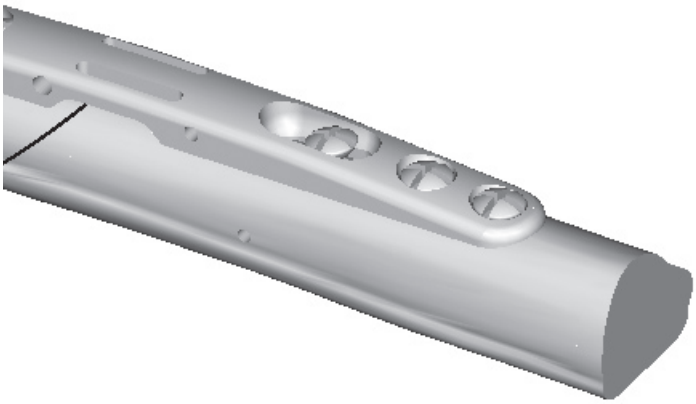

Figure 2: Graphic illustration demonstrating finished osteotomy and plate construct. Note the slotted hole on the side of the plate with 3 screws. This hole eliminates the need to remove the plate during the saw cuts and allows for compression at the osteotomy site.

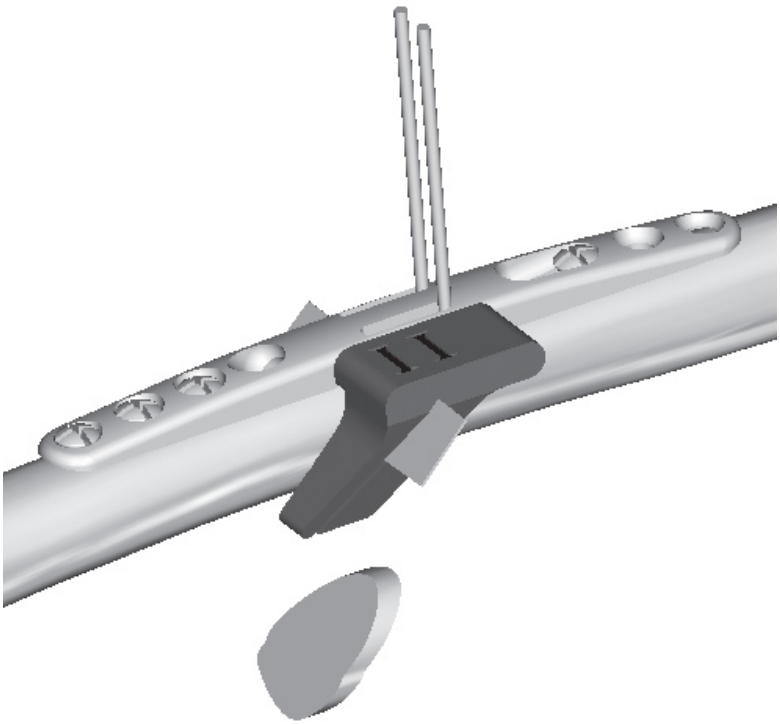

Figure 3: Graphic illustration demonstrating one of the osteotomy guides attached directly to plate. This eliminates the need for freehand cuts.

and Hand (DASH) Outcome Measure. This is a 30 item self-administered questionnaire designed to measure function of the upper extremity. The test is scored from 1-100 with a higher score representing increased disability.

Results

All patients were followed for a minimum of 12 months. Bony union, defined as bridging of the trabecular bone and cortical margin blurring was achieved at an average of 7.43 weeks for the dynamic compression system and 7.41 weeks for the new Trimed system. Shortening of the ulna averaged 3.95 mm and 4.12 mm for the dynamic compression group and the Trimed group respectively. Pain scores decreased from an average of 5.97 preoperatively to 0.78 after surgery in the dynamic compression group. The patients in the Trimed group had a similar experience with their scores changing from 5.88 to 0.71.

Pre- and postoperative range of motion, grip strength, pain and DASH scores are tallied in Tables 1 and 2.

Complications were few. In the dynamic compression group ten plates were removed for prominence and two cases of carpal tunnel syndrome developed in the non-immediate postoperative period. Four plates were removed in the Trimed group and one patient developed carpal tunnel syndrome in the postoperative period. There were no infections, delayed unions, or nonunions in either group.

Discussion

The ulnar shortening osteotomy has proven benefits for patients with ulnar sided wrist pain stemming from positive ulnar variance. Presumably, pain is relieved through a decompression effect provided by the correction of the radio-ulnar length discrepancy. Many methods for correcting this overloading of the distal ulnar and triquetrum have been proposed. In 1941 Henry Milch was the first to describe a shortening technique using nothing more than a wire and plaster immobilization. Plate and screw fixation of an osteotomy was not proposed until the early 1970's. Since that time several plating systems have been developed to make a technically demanding procedure more facile while simultaneously decreasing complication rates.

This study compared the patient outcomes of ulnar shortening osteotomies made with two different surgical systems and techniques. The first system (dynamic compression) has been used in the past with good results. However, this technique requires osteotomy cuts be made perfectly parallel to assure good alignment and opposition of the cut bone ends. Furthermore, the plate

Feature	Preop	Postop	% Contralateral
Wrist Flexion/Extension (°)	107.76	116.41	96.11
Wrist Radial/Ulnar Deviation (°)	34.00	40.27	92.15
Wrist Pronation/Supination (°)	134.46	143.78	96.88
Grip Strength (kg)	25.95	32.46	94.57
Pain (Visual Analog 1-10)	5.97	0.78	NA
DASH Scores	65.1	11.3	NA

Table 1: Qualitative Outcomes Dynamic Compression System. (NA: Not Applicable).

Feature	Preop	Postop	% Contralateral
Wrist Flexion/Extension (°)	110.00	116.47	98.26
Wrist Radial/Ulnar Deviation (°)	36.47	43.82	95.92
Wrist Pronation/Supination (°)	133.24	136.76	96.70
Grip Strength (kg)	26.41	34.06	93.69
Pain (Visual Analog 1-10)	5.88	0.71	NA
DASH Scores	65.4	10.4	NA

Table 2: Qualitative Outcomes Trimed System. (NA: Not Applicable).

must be moved during the procedure to complete the osteotomy. This adds both time and room for error. With the new system (Trimed) osteotomies are made through guides attached to the plate, thus, eliminating freehand cuts and plate reapplication.

Our data show that patients improved rather dramatically both quantitatively and qualitatively after undergoing an ulnar shortening with either system. Postoperative range of motion and grip strength increased to nearly 100% of the contralateral non-operative side. Furthermore, DASH scores demonstrated that patients felt they were functioning at much higher levels after surgery while Visual Analog pain scores dropped to near negligible levels. This illustrates the utility of this procedure in appropriately selected patients. Importantly, the similar results for both systems demonstrates our new system works as well as a proven technique. We believe our system offers several technical advantages, however, helping to eliminate surgical time and postoperative complications.

Recommended Reading

Palmer AK, Werner FW. Biomechanics of the distal radioulnar joint. Clin Orthop 1984;187:26-35.

Chen NC, Wolfe SW. Ulna shortening osteotomy using a compression device. J Hand Surg 2003;28A:88-93.

Deitch MA, Stern PJ. Ulnocarpal abutment. Hand Clin 1998;14:251-263.

Open Distal Femur Fractures Treated with Lateral Locked Implants: Union, Secondary Bone Grafting, and Predictive Parameters

Craig C. Greene, M.D., David P. Barei, M.D., F.R.C.S.C., Daphne M. Beingessner, M.D., F.R.C.S.C., Lisa A. Taitsman, M.D., M.P.H., and Sean E. Nork, M.D.

Treatment complications of supracondylar-intercondylar distal femur fractures include nonunion, secondary loss of reduction, and the need for subsequent procedures. Preservation of osseous viability using indirect reduction methods, however, has led to an increase in fracture union rates without the need for supplemental bone grafting procedures. Similarly, advances in distal fragment fixation appear to have decreased secondary reduction loss.

Open distal femur fractures represent a unique subgroup of injuries that present additional challenges. Specifically, the magnitude of associated soft tissue injury and traumatic bone loss creates an exceptionally unfavorable environment for bone healing, particularly in the supracondylar region. These factors are often worsened as a result of the necessary surgical debridement to assure removal of foreign and devitalized material from the traumatized area. Because of the typically longer duration required to achieve osseous union, secondary loss of reduction is often an anticipated event, necessitating surgical intervention to expedite or assure union. Given the large spectrum of injury to both the soft tissue envelope and magnitude of bone loss, parameters to identify clinically relevant bone loss and guide surgical decision-making regarding the need for bone grafting is lacking.

We hypothesize that indirect reduction and stabilization of open supracondylar femur fractures using fixed-angle screw/plate implants decrease the need for subsequent bone grafting while avoiding secondary loss of reduction. We further hypothesize that the radiographic features at the time of definitive fixation may predict union despite apparent bone loss.

Methods

Between January 2001 and December 2004 inclusive (forty-eight months), all patients sustaining a supracondylar-intercondylar fracture of the distal femur were identified from our institution's orthopaedic trauma database. Fractures are entered and coded according to the AO/OTA Fracture Classification System by orthopaedic trauma fellows trained in this classification system. This search identified 51 skeletally mature patients with 54 open supracondylar-intercondylar distal femur fractures, classified as OTA 33 C-type injuries, eligible for review. One patient died prior to definitive fixation and was excluded from further review. Additional exclusions included twelve fractures treated with nonlocking screw/plate implants, and 4 patients with less than 3 months of followup. The remaining 34 adults with 36 open AO/OTA C-type distal femur fractures were considered the study group and were retrospectively reviewed.

There were 23 male and 11 female patients. The average age was 45 years (range, 17-82 years). Two patients had bilateral injuries. Twenty-five injuries were caused by motor vehicle or motorcycle collisions. Six patients were injured after a fall from a height, and three additional patients were injured by other mechanisms. Thirty-three fractures were Type IIIA, one Type IIIB, and one Type IIIC fracture according to Gustilo. Additionally, there were two Type II fractures and one Type I fracture.

Following appropriate initial debridements, all fractures were treated with minimally invasive fixed angle screw/plate implants, specifically, 35 fractures were stabilized with the distal femoral Less Invasive Stabilization System (LISS), and three fractures were stabilized with Locking Condylar Plates (LCP). Twenty-five fractures were treated acutely with manipulative reduction and application of knee spanning temporary external fixation. Eight fractures were managed with acute ORIF, and three fractures were temporized with proximal tibial skeletal traction. Thirty-three patients underwent operative fracture debridement within 24 hours of their presentation to hospital. In patients treated with temporary external fixation or skeletal traction, the average time to definitive fixation was 3.4 days. Definitive bone stabilization was performed through a lateral based incision using a minimally-invasive technique.

Fracture union was defined as bridging callus on 2 of 4 cortices on biplanar radiographs combined with a lack of patient symptoms. Radiographic data was available using the picture archiving and communication system (PACS) and were reviewed by two trauma fellowship trained Orthopaedic attending surgeon. Agreement was obtained by consensus. Initial and united anatomic lateral distal femoral angles (aLDFA=81°±5°) were evaluated on the AP view. Sagittal plane reductions were evaluated on the lateral view. Clinically significant bone loss was defined as the radiographic presence of antibiotic beads (beads) within a cavitary metaphyseal defect. All patients had minimum 3-month followup.

Results

The average length of follow-up was eleven months. Nine patients were followed between three and six months, 14 patients were followed between six and 12 months, and 13 patients had greater than one year of follow-up. Twenty fractures had polymethylmethacrylate antibiotic beads (PMMA beads) placed within a metaphyseal defect, while 16 fractures did not receive beads. Of those fractures treated initially with PMMA beads, 11 (55%) underwent staged bone grafting to achieve union. Conversely, of the 16 fractures that were not treated

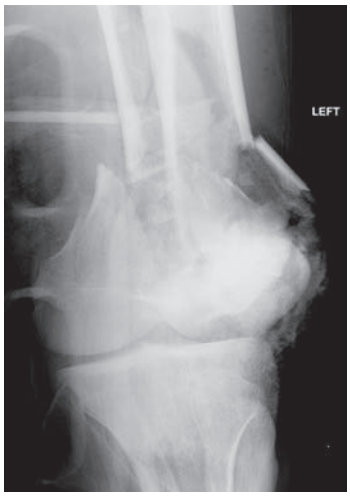

A.

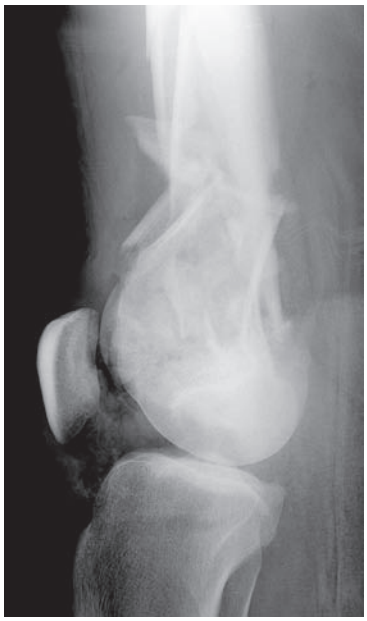

B.

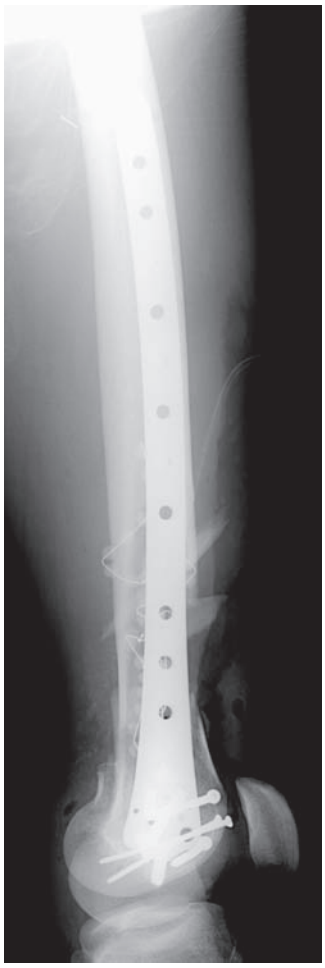

C.

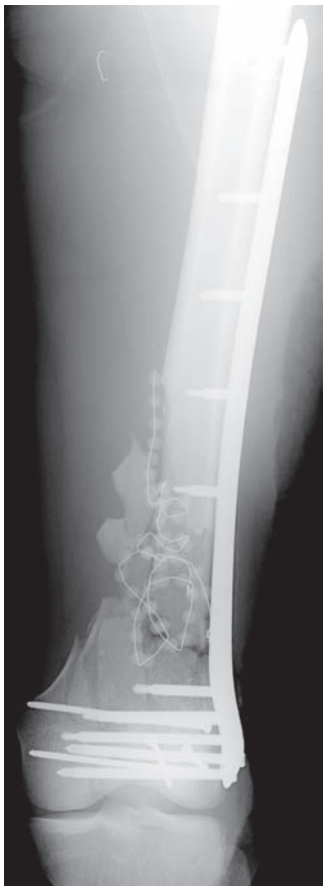

D.

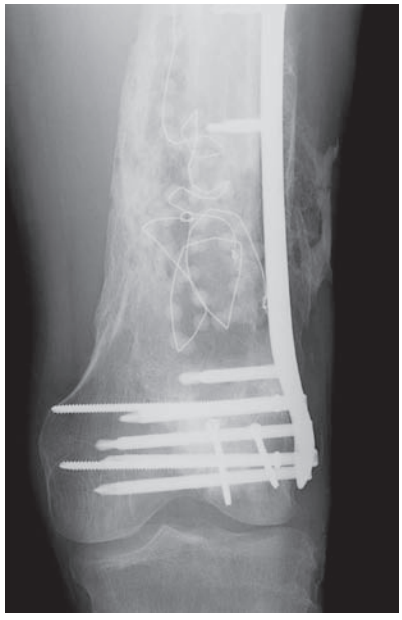

E.

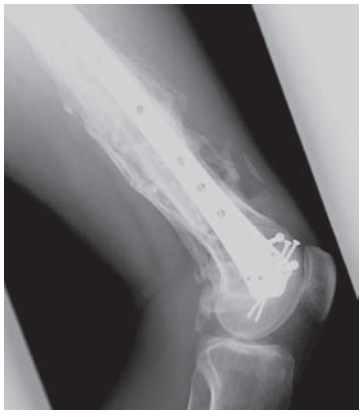

F.

Figure 1: This 19 year-old male was involved in a high-speed motor vehicle collision. The physical examination demonstrated an open anterolateral distal thigh wound with exposed bone fragments. A) and B). Injury anteroposterior and lateral plain radiographs of the distal femur demonstrating supracondylar comminution with intra-articular involvement. After resuscitation, initial orthopaedic treatment consisted of operative debridement of the open wound with application of knee-spanning temporary external fixation. C) and D). Six days later, definitive treatment consisted of direct reduction and stabilization of the articular injury followed by indirect meta-diaphyseal reduction and stabilization using a 13-hole distal femoral LISS plate. PMMA beads were inserted into the substantial metaphyseal defect. Immediate post-operative radiographs demonstrate the presence of posterior cortical continuity on the lateral radiograph with deficient continuity noted along the medial cortex. No further surgical interventions were performed. E) and F). Anteroposterior and lateral plain radiographs one year later demonstrate satisfactory union with maintenance of sagittal and coronal plane alignment.

with PMMA beads, only 2 (13%) were bone grafted to achieve union. Not surprisingly, the presence of PMMA beads was significantly associated with subsequent staged bone grafting to obtain union ($p<0.01$). Of those with PMMA beads and staged bone grafting, three had posterior cortical bone loss, three had medial and posterior cortical bone loss, and 5 had segmental defects. Of the nine fractures with beads not requiring bone graft, all had radiographic appearance of posterior cortical contact; 7 of these had radiographic appearance of medial cortical contact. Using the Chi-square statistic, the radiographic appearance of posterior ($p<0.001$) and medial ($p<0.025$) cortical continuity were strongly associated with injuries not requiring bone graft, despite the presence of PMMA beads. There were 2 nonunions, One of these occurred in a patient with segmental bone loss treated with staged bone grafting. Despite this, the fracture required revision plating and additional bone grafting to ultimately obtain union. The second nonunion occurred in a patient treated without PMMA beads or staged bone grafting. This patient ultimately developed an oligotrophic nonunion successfully treated with revision plating and supplemental bone grafting. Thirty-four of 36 fractures had accurate frontal plane reductions, and 35 of 36 had adequate sagittal plane reductions. Reduction loss (5° varus) occurred in 1 patient.

Discussion

Fixed-angle screw/plate implants with indirect reduction techniques have been demonstrated to be successful in the treatment of supracondylar distal femur fractures without requiring supplemental bone graft to achieve union. The limits of obtaining fracture union and maintaining fracture stability with fixed-angle screw/plate devices however may be taxed in situations of overt bone loss and worsening soft tissue injury, as encountered in the open supracondylar distal femur fracture. Identification of parameters that may aid in the determining fracture patterns that may or may not heal, particularly in the face of overt bone loss, however, is lacking. Accordingly, this study has demonstrated that fixed-angle screw/plate implants applied using indirect reduction techniques are successful in treating these challenging injury patterns. The insertion of PMMA beads at the time of definitive fixation was felt to reflect clinically important metaphyseal bone defects, and was identified as a surrogate for bone loss. However, in our investigation, 35% of those fractures with PMMA beads did not require subsequent bone grafts, suggesting that not all bone defects require subsequent bone grafting (Figure 1).

The radiographic appearance of posterior cortical contact and/or medial cortical contact strongly correlates with union and may obviate the need for staged bone grafting, despite the lack of anterior or lateral bone. Osseous presence in these areas suggests maintenance of the posteromedial soft tissue envelope critical for obtaining union. The maintenance of frontal and sagittal plane alignments also suggests that adequate early fracture stability is obtained. It is likely that the ensuing bridging callus in the posterior and/or medial regions enhances fracture stability and considerably negates the stresses subsequently incurred by the lateral implant.

Union rates of distal femur fractures, both open and closed, treated with LISS plates range from 91% to 93%. To date, no investigation has isolated the treatment of open distal femur fractures treated with locked lateral plating applied in a minimally invasive fashion. Our study demonstrates that fixed angle screw/plate implants may decrease the need for staged bone grafting while maintaining alignment even in situations with metaphyseal bone loss, provided that viable posterior and/or medial osseous fragments exist.

Recommended Reading

Bolhofner BR, Carmen B, Clifford P. The results of open reduction and Internal fixation of distal femur fractures using a biologic (indirect) reduction technique. J Orthop Trauma 1996;10(6):372-7.

Kregor PJ, Stannard JA, Zlowodzki M, Cole PA. Treatment of distal femur fractures using the less invasive stabilization system: surgical experience and early clinical results in 103 fractures. J Orthop Trauma 2004;18(8):509-20.

Mize RD, Bucholz RW, Grogan DP. Surgical treatment of displaced, comminuted fractures of the distal end of the femur. J Bone Joint Surg Am 1982;64(6):871-9.

Mize RD. Surgical management of complex fractures of the distal femur. Clin Orthop Relat Res 1989(240):77-86.

Neer CS, 2nd, Grantham SA, Shelton ML. Supracondylar fracture of the adult femur. A study of one hundred and ten cases. J Bone Joint Surg Am 1967;49(4):591-613.

Ostrum RF, Geel C. Indirect reduction and internal fixation of supracondylar femur fractures without bone graft. J Orthop Trauma 1995;9(4):278-84.

Zehntner MK, Marchesi DG, Burch H, Ganz R. Alignment of supracondylar/intercondylar fractures of the femur after internal fixation by AO/ASIF technique. J Orthop Trauma 1992;6(3):318-26.

The Reverse Delta Prosthesis – A New Approach to Combined Arthritis and Instability and Rotator Cuff Deficiency of the Shoulder: Early Experience and Lessons Learned

Frederick A. Matsen III, M.D., Caroline Chebli, M.D., and Alexander Bertlesen, P.A.C.

In the absence of a functioning rotator cuff and supporting coracoacromial arch, the glenohumeral joint may lack sufficient stability for the deltoid to function effectively in elevating the arm. The result is often referred to as 'pseudoparalysis' of the shoulder. The stability required for deltoid function may be lacking in primary cuff tear arthropathy (Figure 1), failed cuff surgery that included surgical sacrifice of the coracoacromial arch (Figure 2), failed shoulder arthroplasty complicated by instability, (Figure 3) and failed fracture surgery where the tuberosities fail to properly unite. In these situations, standard reconstruction by cuff repair and / or conventional arthroplasty cannot restore the needed fulcrum for deltoid function. Until recently, there was no solution to these problems. A creative approach was implemented in Europe by Grammont in which a hemispherical ball was fixed to the glenoid and a concave metaphyseal component was fixed to the humerus (Figure 4). The European results from the last decade have indicated that in the absence of complications this prosthesis was very effective in restoring comfort and function to previously unreconstructable shoulders and that the perioperative complication rate has been high, including such major problems as infection, fracture of the acromion, humerus and glenoid, nerve palsies, and dislocations. In some series the early revision rates have been as high as 60%!

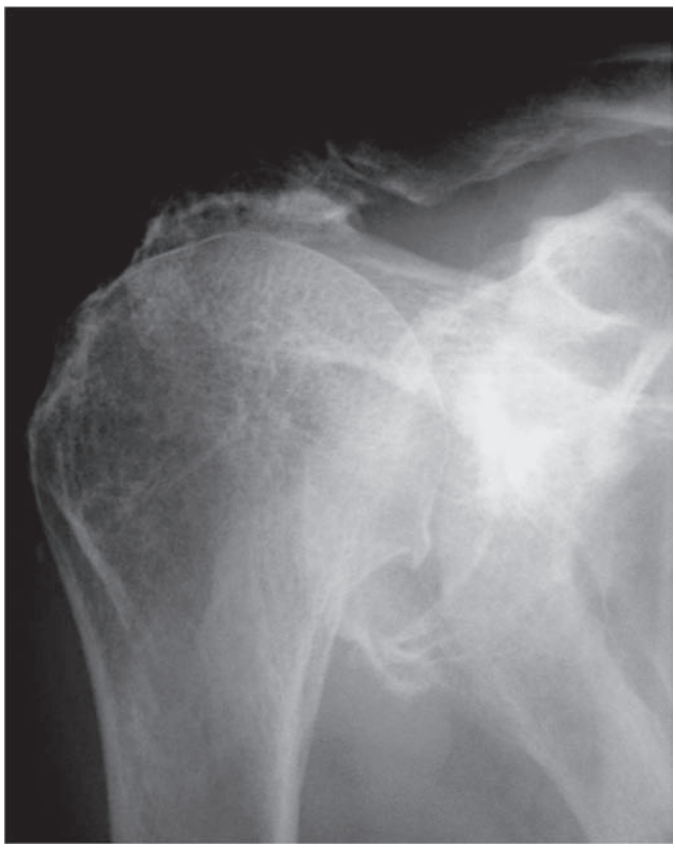

Figure 1: Characteristic radiographic appearance of cuff tear arthropathy.

This reverse prosthesis was recently made available in the United States. A year ago, the Shoulder and Elbow Services at the University of Washington Medical Center trained in this technique and cautiously instated a clinical series with a goal to minimizing the risk of complications. Cadaver dissections and laboratory studies enabled the team to understand the unique geometry of this prosthesis as well as strategies by which it can be most safely applied.

Our technique emphasizes the anterior deltopectoral approach because of its familiarity, ease of glenoid and humeral exposure and its extensile nature. The glenosphere is positioned low on the glenoid to avoid notching and to enable the inferior locking screw to engage the robust bone of the axillary border of the scapula (Figure 5). The tension in the deltoid is carefully controlled by the amount of bone resection and the height of the polyethylene spacer. We strive to achieve no gap between the humeral and glenoid articular surfaces with gentle distraction on the humerus (Figure 6).

To this point we have only short-term follow-up on our patients. Fourteen patients have an average of three months functional data. At this point we have been able to avoid the perioperative complications described above. What we are presenting here is (1) the severe degree of functional compromise of the patients before surgery and (2) the early functional return realized by some patients with this type of surgical reconstruction (see Table 1) (Figure 7).

We are encouraged to continue in applying this method to carefully selected patients and are following

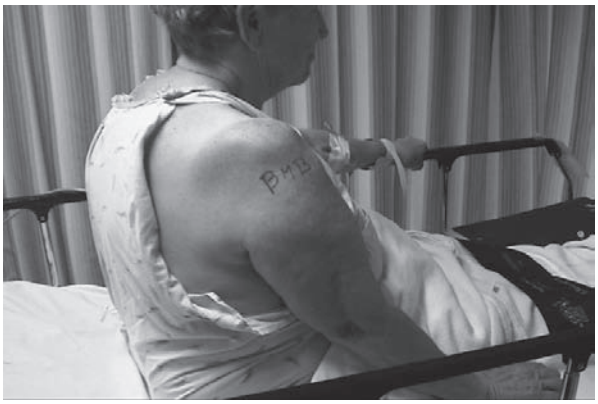

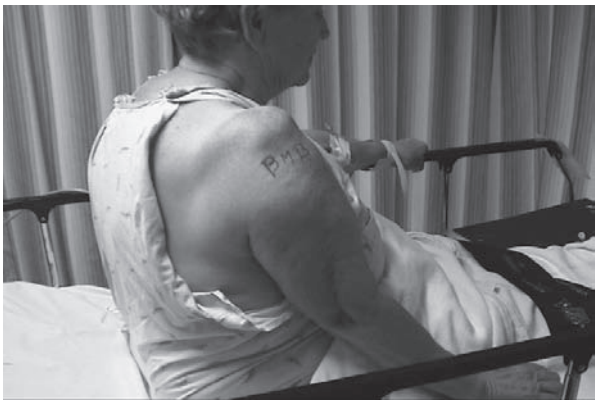

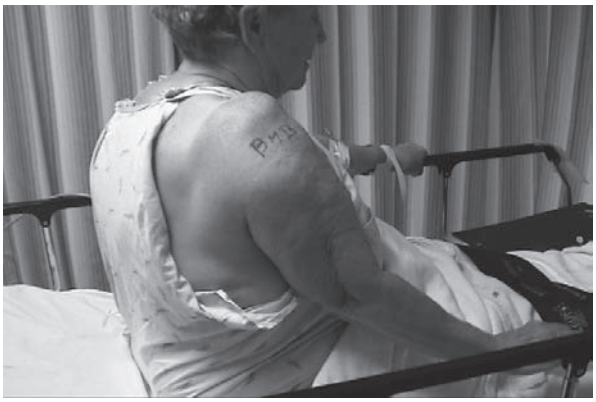

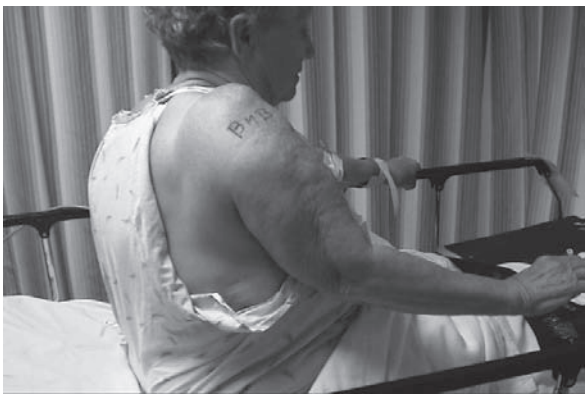

Figure 2: Sequential radiographs showing attempted arm elevation by a patient with a failed rotator cuff repair and acromioplasty. This inability to elevate the arm is referred to as pseudoparalysis.

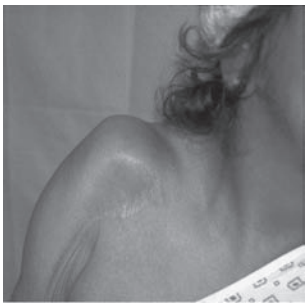

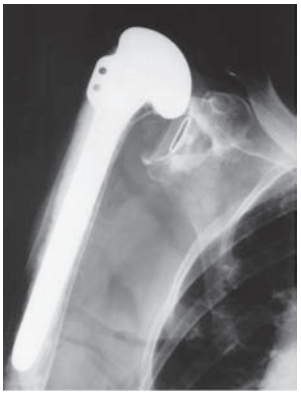

Figure 3: Failed arthroplasty with anterosuperior escape. (clinical and radiographic images.

Figure 4: The reverse Delta prosthesis.

our patients carefully to evaluate their function over time.

Recommended Reading

Werner CML, Steinmann PA, Gilbart M, Gerber C. Treatment of Painful Pseudoparesis Due to Irreparable Rotator Cuff Dysfunction with the Delta III Reverse-Ball-and-Socket Total Shoulder Prosthesis. J Bone Joint Surg Am 2005; 87: 1476-1486.

Frankle M, Siegal S, Pupello D, Saleem A, Mighell M, Vasey M. The Reverse Shoulder Prosthesis for Glenohumeral Arthritis Associated with Severe Rotator Cuff Deficiency. A Minimum Two-Year Follow-up Study of Sixty Patients. J Bone Joint Surg Am 2005; 87: 1697-1705.

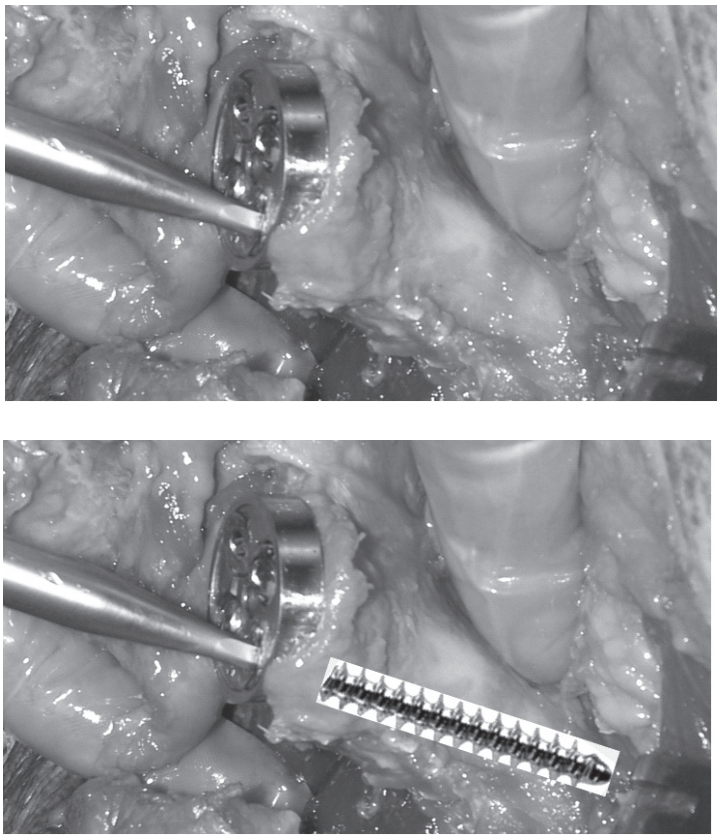

Figure 5: Desired screw placement in the axillary pillar of the scapula.

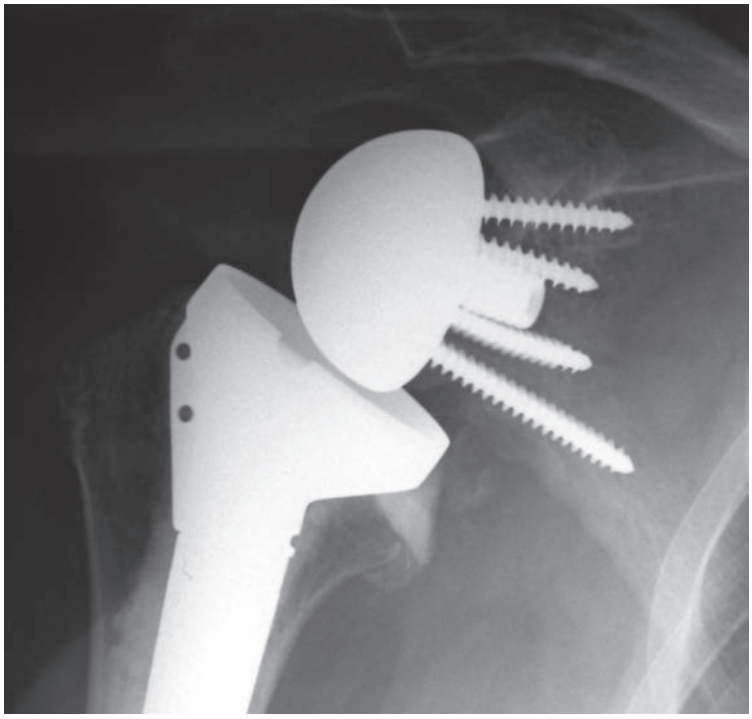

Figure 6: Postoperative radiograph of reverse prosthesis.

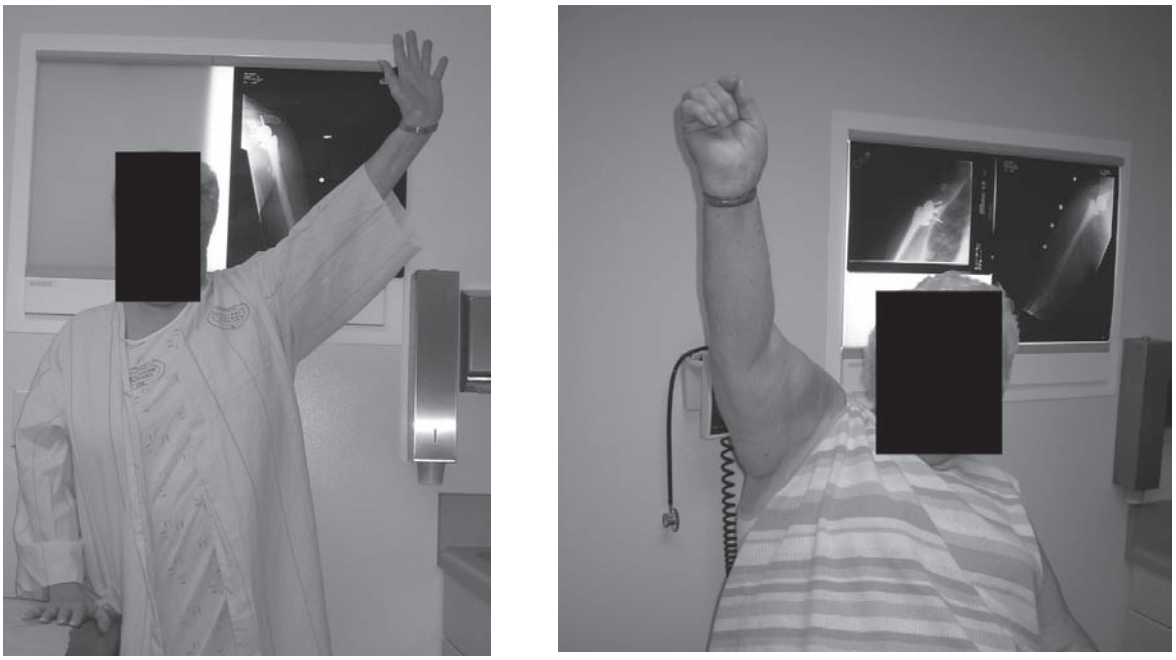

Figure 7: Clinical elevation after reverse prosthesis

Self assessed function	Percent of patients that could perform the function before surgery	Percent of patients that could perform the function at most recent follow-up
Able to sleep comfortably	21%	50%
Tuck in shirt	29%	43%
Wash back of opposite shoulder	7%	64%
Lift hand to shoulder level	43%	86%
Lift one pound to shoulder level	7%	64%

Table 1: Self assessed function table.

Graduating Residents
Class of 2006

Heidi Ambrose, M.D.

After residency, Heidi will be completing an upper extremity fellowship at Allegheny General Hospital in Pittsburgh, PA. Following this, she hopes to return to the Seattle area to practice.

Eric Klineberg, M.D.

In the next academic year, Eric will begin a spine fellowship at The Cleveland Clinic in Cleveland, Ohio. Upon completion, he hopes to return to the Pacific Northwest to practice.

Mel Wahl, M.D.

Mel will move to San Francisco where he will complete a spine fellowship at the San Francisco Spine Institute. Afterwards, he plans on returning home to practice in Eastern Washington.

Stacey Donion, M.D.

Upon graduation, Stacey will be joining Group Health in Tacoma, Washington.

Bill Montgomery, M.D.

In the coming year, Bill and his family will attend a spine fellowship at the Cleveland Clinic with the hope of returning to Hawaii or the Seattle area.

Burt Yaszay, M.D.

Burt will move to New York where he will complete a spine fellowship at New York University / Hospital for Joint Disease. He plans on pursuing an academic career in spine surgery.

Incoming Residents

Sean Amann

Sean is from Denver, Colorado. He got his undergraduate degree at the University of Colorado and his medical degree from the Chicago Medical School. His main area of clinical and research interest is sports medicine and trauma, specifically multi-ligamentous knee injuries. Activities away from work include homebrewing beer, backpacking, skiing, and snowboarding.

Aric Christal

Aric was born and raised in Alaska. He graduated from Harvard with a degree in organismic and evolutionary biology. In 2001, he started medical school at the University of Washington. In his free time, he enjoys backpacking, international travel, and skiing.

Jeremy Bauer

Jeremy is from Ferndale, Washington. He attended the University of Washington as an undergraduate. He went to medical school at Drexel University College of Medicine. Currently, his major interests include hand surgery and pediatric orthopaedics. In his spare time, he likes mountain biking, running, weightlifting, backpacking, and hunting.

Wendy Emerson

Wendy was born in Flower Mound, Texas. She got her undergraduate education at Oral Roberts University. She attended medical school at the University of Texas Medical Branch at Galveston. Her orthopaedic interests include sports medicine and shoulder and elbow injuries. Her extracurricular activies include basketball and spending time with her family.

Incoming Residents

Michael Hwang

Michael graduated magna cum laude from Duke University in 2001 with a BS degree in Biology. He received his MD degree from the University of Chicago Pritzker School of Medicine in 2005. Having spent the majority of his upbringing on the east coast, Michael has now come to Seattle with his wife, Erica, an internal medicine resident, to pursue his residency in orthopaedics. He enjoys basketball, working out, hiking, travelling, and reading.

Christopher Wolf

Christopher graduated from the University of Delaware. He received his MD from Jefferson Medical College in Philadelphia, Pennsylvania. He is most interested in sports medicine and joint replacement at this time. In his spare time, he enjoys hiking, snowboarding, travel, and camping.

Lee Pace

Born and raised in rural Utah. Lee attended Southern Utah University where he majored in chemistry and minored in history. He attended medical school in Boston at Boston University. In his spare time, he likes to snowboard, work out, and he says he is beginning to dabble in the world of business and real estate investing.

Vinko Zlomislic

Vinko is from Arcadia, California. He attended UCLA as an undergraduate and Michigan State University for medical school. At this time, he is most interested in sports medicine and traumatology in orthopaedics. Hobbies included soccer, surfing, adventure racing, weightlifting, and travel.

ACEs

Foot/Ankle

Ian L. D. Le, M.D.

Christian C. Hall, M.D.

Bryan W. Lipinski, M.D.

Spine

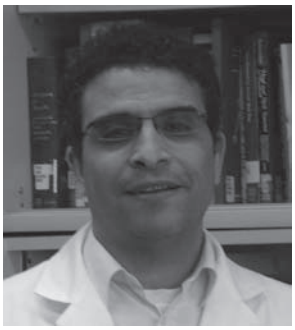

Hossein Elgafy, M.D.

David W. Stevens, M.D.

Trauma

Ginger K. Bryant, M.D.

Matthew L. Graves, M.D.

Craig C. Greene, M.D.

James L. Howard, M.D.

Timothy J. O'Mara, M.D.

Brad J. Yoo, M.D.

ACEs

Hand

Shai Luria, M.D.

Oncology

Joshua C. Patt, M.D.

Shoulder/Elbow

Caroline M. Chebli, M.D.

Pediatrics

Wesley P. Bevan, M.D.

Fellows

Hand

Seth D. Dodds, M.D.

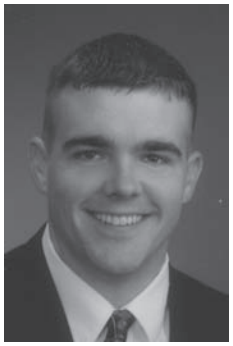

Anthony J. Lauder, M.D.

Wren V. McCallister, M.D.

2006 Department of Orthopaedics and Sports Medicine New Faculty

Robert P. Dunbar, M.D.

Dr. Dunbar received his undergraduate degree from the College of the Holy Cross in Worcester, MA, and then spent two years as a Peace Corps Volunteer in Burkina Faso, West Africa. He returned to the U.S. to pursue medical training at Georgetown University School of Medicine in Washington, DC. He subsequently completed residency training at the Hospital for Special Surgery/Cornell University Medical Center in Manhattan, NY. After serving 4 years of active duty service in the US Navy, including three years overseas in Yokosuka, Japan, Dr. Dunbar completed Advanced Clinical Experience/Trauma training at Harborview Medical Center/ University of Washington. He then served as director of the orthopaedic trauma service for one of the Navy's three residencies in Portsmouth, VA, and for the past two years he has been the Navy's only fellowship trained orthopaedic traumatologist on the East Coast. Dr. Dunbar is returning to Harborview Medical Center, where he will join the staff as an orthopaedic traumatologist.

Daphne M. Beingessner, M.D.

Dr. Beingessner received her undergraduate degrees in Mathematics and Science from the University of Waterloo in Ontario, Canada. She completed her medical degree and Master of Science in Biophysics from the University of Western Ontario. Her internship and residency training in orthopaedic surgery were completed at the University of Western Ontario. Dr. Beingessner then went on to complete her upper extremity fellowship training at the Hand and Upper Limb Centre in London, Ontario, and her Trauma Advanced Clinical Experience at Harborview Medical Center in Seattle, Washington. Dr. Beingessner is currently an acting assistant professor in the Department of Orthopaedics and Sports Medicine at the University of Washington. She will join the Orthopaedics' faculty as an assistant professor at Harborview Medical Center where she will specialize in orthopaedic trauma.

Paul Manner, M.D.

Dr. Paul Manner was born in Boston, Massachusetts. For three years, Paul was enrolled in a five-year, double-degree (Bachelor of Music, Bachelor of Science) program at Tufts University and New England Conservatory of Music, where he attended both schools simultaneously. In September 1985, he elected to withdraw from his studies as a clarinet performance major at NEC to concentrate on and complete his Tufts studies. He received his medical degree from McGill University in Montreal. He was an intern and later on a resident at St. Luke's/Roosevelt Hospital Center in New York City. He completed his residency in orthopaedic surgery back at McGill University. A fellowship at Shriner's Hospital in Montreal followed. Afterwards, he completed a fellowship in adult reconstruction and joint replacement at the University of Pittsburgh Medical Center. In 2001, he was hired as an Assistant Professor at George Washington University in Washington, DC. Dr. Manner will join Seth Leopold on the hip and knee reconstruction service based at the University of Washington Medical Center. He specializes in less invasive techniques for joint replacement.

2006 Department of Orthopaedics and Sports Medicine New Faculty

Jason S. Weisstein, M.D., M.P.H.

Dr. Jason S. Weisstein is a native of California. He graduated with high honors from the University of Pennsylvania with a dual major in Biology and Spanish. He earned his medical degree at the Mount Sinai School of Medicine in New York, NY where he graduated class valedictorian and Alpha Omega Alpha. While in New York, he also completed a master of public health degree at the Columbia University. There, he graduated top of his class receiving the prestigious award for the most outstanding academic achievement and promise in the field of public health.

Dr. Weisstein attended the University of California, San Francisco for internship and orthopaedic surgery residency training. He completed his orthopaedic oncology fellowship under Ernest U. Conrad, III, M.D. at the University of Washington and the Children's Hospital and Regional Medical Center of Seattle.

After fellowship, Dr. Weisstein became the director of musculoskeletal oncology at the Tucson Orthopaedic Institute in Tucson, AZ. This fall, he will be joining the University of Washington orthopaedic oncology service where he will specialize in the full range of both adult and pediatric orthopaedic oncology, benign and malignant bone and soft tissue tumors, metastatic disease, metabolic bone disease, osteomyelitis, and limb salvage.

Klane White, M.D.

Dr. White, a native of California, earned both his undergraduate degree in biological sciences and a master's degree in biological oceanography from the University of Southern California. He received his medical degree from the George Washington University School of Medicine in Washington, DC. His internship in general surgery and residency in orthopaedic surgery were completed at the University of California San Diego, where he also served as an NIH fellow in orthopaedic and basic science research. Dr. White then went on to complete a fellowship in pediatric orthopaedics and scoliosis at Texas Scottish Rite Hospital for Children in Dallas. He is active in orthopaedic research and has published on various subjects in both clinical pediatric orthopaedics and spine biomechanics. Dr. White specializes in pediatric orthopaedic surgery at Children's Hospital and Regional Medical Center, with specific interests in pediatric hip disease, spinal deformity and skeletal dysplasias. He and his wife Amy have two young daughters.

Department Photo

Left to right

Fourth Row: Bruce Sangeorzan, Douglas Hanel, Jason King, David Barei, Evan Ellis, Rick Bransford,, Mark Freeborn, Soren Olson, Jeremy Bauer, Drew Fehsenfeld

Third Row: Sohail Mirza, Dan Stamper, Seth Leopold, Joseph Lynch, Ted Wagner, Jens Chapman, Christopher Howe, Mike Lee, Scott Ruhlman, Robert Dunbar, Stephen Benirschke

Second Row: Jamie Antoine, Addison Stone, Annie Links, Jeremiah Clinton, Gregg Nicandri, Mary Cunningham, Allison MacLennan, Jason Wilcox, Rajshri Maheshwari

First Row: Stacey Donion, Mel Wahl, Heidi Ambrose, Scott Boden, MD - OREF HARK Visiting Professor, Frederick Matsen, Bill Montgomery, Eric Klineberg, Burt Yaszay

Research Grants

National Institutes of Health (NIH)

Augmentation of Peak Bone Mass
Ted S. Gross, Ph.D.

Collagens of Cartilage and the Intervertebral Disc
David R. Eyre, Ph.D.

Collagen Cross-Linking in Skeletal Aging and Diseases
David R. Eyre, Ph.D.

Collagen Type II/IX/XI Heteropolymer Assembly
Russell J. Fernandes, Ph.D.

Disuse Induced Osteocyte Hypoxia
Ted S. Gross, Ph.D.

Imaging of Molecules by Oscillator-Coupled Resonance
John A. Sidles, Ph.D.

Organization of Mechanical Signals in Bone Cells via Membrane
Ted S. Gross, Ph.D.

Safety of Lumbar Fusion Surgery for Chronic Back Pain
Sohail K. Mirza, M.D.

Skeletal Dysplasias
David R. Eyre, Ph.D.

Veterans Affairs Rehabilitation Research and Development Service

Ankle Equinus and Plantar Pressure in Individuals with Diabetes
Bruce J. Sangeorzan, M.D.

Ewing's Sarcoma Fusion Proteins and mRNA Splicing Factors
Howard A. Chansky, M.D.

Gait Simulation: Neutrally Aligned and Pathologic Feet
Bruce J. Sangeorzan, M.D.

Kinematic Models of Normal and Painful Osteoarthritic Feet
Bruce J. Sangeorzan, M.D.

The Epidemiology of Foot Structure and Ulceration in Diabetic Veterans
Bruce J. Sangeorzan, M.D.

VA Center of Excellence in Amputation Prevention and Prosthetic Engineering
Bruce J. Sangeorzan, M.D.

Orthopaedic Research and Education Foundation (OREF)

Melissa Zimel Orthopaedic Research Fellowship
Ernest U. Conrad, M.D.

Reduction of Total Knee Arthroplasty Risk in Morbidly Obese Patients Using Laparoscopic Bariatic Surgery: A Prospective, Controlled Trial
Seth S. Leopold, M.D.

A.O. North America

AO Spine North America Fellowship
Carlos Bellabarba, M.D.

Stability After Pin Versus Dorsal Plate Fixation of Simulated Interarticular Distal Radius Fractures: A Biomechanical Investigation
Thomas E. Trumble, M.D.
Wren V. McCallister, M.D.

Amgen, Inc.

Inhibition of Muscle Paralysis Induced Bone Loss by OPG
Ted S. Gross, Ph.D.

Arthrex, Inc.

Mechanical Testing of Arthroscopic Soft Tissue Anchors
Allan F, Tencer, Ph.D.

BioAxone Therapeutique, Inc.

Cethrin Trial
Jens R. Chapman, M.D.

Centers for Disease Control

Chest Injuries Due to Motor Vehicle Side Impacts
Allan F, Tencer, Ph.D.

Research Grants

Integra Lifesciences Corporation

Comparison of Bioabsorable Tubes for Repair of Nerve Injury
Thomas E. Trumble, M.D.

Johnson & Johnson, Inc.

Clinical Spine Fellowship Grant
Theodore A. Wagner, M.D.

Depuy Mitek Fellowship Grant
Christopher J. Wahl, M.D.

National Science Foundation

University of Washington Engineered Biomaterials
Christopher H. Allan, M.D.
Frederick A. Matsen III, M.D.

Ostex International, Inc.

Molecular Markers of Connective Tissue Degradation
David R. Eyre, Ph.D.

Synthes Spine Co.

PRODISC-C Versus Anterior Cervical Discectomy and Fusion (ACDF)
Jens R. Chapman, M.D.

Spine End-Results Research Fund
Frederick A. Matsen III, M.D.

The Boeing Company

Randomized Clinical Trial of Open versus Endoscopic Carpal Tunnel Release and Hand Therapy Comparing Patient Satisfaction. Functional Outcome and Cost Effectiveness
Thomas E. Trumble, M.D.

US Army Research Office

UW Team-Advance on Single Nuclear Detection and Atomic-Scale Imaging
John A. Sidles, Ph.D.

Washington Woman's Foundation

Strengthening the Femoral Neck to Prevent Hip Fractures caused by Osteoporosis
Frederick A. Matsen III, M.D.

Whitaker Foundation

Examining Processes Underlying the Dramatic Osteogenic Response Elicited by Rest-Inserted Loading
Sundar Srinivasan, Ph.D.

Zymogenetics, Inc.

Recombinant Human Thrombin Trial
Sohail K. Mirza, M.D.

Resident Research Awards

VICTOR FRANKEL RESIDENT RESEARCH AWARD

Presented to these residents in Orthopaedic Surgery for Excellence in Clinical or Basic Science Research

Timothy P. Lovell, M.D. - 1990
Mohammad Diab, M.D. - 1992
P. Brodie Wood, M.D. - 1994
William J. Mills, Jr., M.D. - 1995
Peter T. Simonian, M.D. - 1996
Daniel J. Stechshulte, Jr. M.D. Ph.D. - 1997
Ben DuBois, M.D. - 2002
Wren McCallister, M.D. - 2004
Wren McCallister, M.D. - 2005
William Montgomery, M.D. - 2005

THE EDWIN L. LAURNEN AWARD

Established in 1993 by Edwin L. Laurnen for the Best Resident Paper in Spine Research

Sohail K. Mirza, M.D. - 1994
Peter T. Simonian, M.D. - 1995
Randall W. Viola, M.D. - 1996
Jason Thompson, M.D. - 2003

THE ESTHER WHITING AWARD

Established in 1977 by J. Irving Tuell, M.D. for the Best Resident Paper with an Historical Orientation

William Oppenheim, M.D. - 1977
Stuart Hutchinson, M.D. - 1978
John M. Clark, M.D. - 1981
Joseph Zuckerman, M.D. - 1981
Marc Swiontkowski, M.D. - 1982
Marc Swiontkowski, M.D. - 1983
Richard Barry, M.D. - 1984
James Crutcher, M.D. - 1987
James Crutcher, M.D. - 1988
Nancy Ensley, M.D. - 1988
Eric Vanderhooft, M.D. - 1990
Curt Rodin, M.D. – 1992
James W. Vahey, M.D. - 1993
Timothy C. Beals, M.D. - 1994
David J. Belfie, M.D. - 1997
Andrew Howlett, M.D. - 2003
Alexis Falicov, M.D. - 2004
Waqqar Khan-Farooqi, M.D. - 2005

Faculty Teaching Award

RESIDENT EDUCATION TEACHING AWARD

Presented to faculty members in Orthopaedic Surgery in recognition of Outstanding Resident Education

Frederick A. Matsen III, M.D. - 1990
Robert A. Winquist, M.D. - 1990
Ernest U. Conrad, M.D. - 1991
Michael E. Morris, M.D. - 1991
John M. Hendrickson, M.D. - 1992
Theodore K. Greenlee, M.D. - 1992
Marc F. Swiontkowski, M.D. - 1993
John T. Sack, M.D. - 1993
Jens R. Chapman, M.D. - 1994
Thomas M. Green, M.D. - 1994
M.L. Chip Routt, M.D. - 1995
Richard M. Kirby, M.D. - 1995
Howard A. Chansky, M.D. - 1996
William P. Barrett, M.D. - 1996
Stephen K. Benirschke, M.D. - 1997
Mark C. Dales, M.D. - 1997
M. Bradford Henley, M.D. - 1998
John T. Sack, M.D. - 1998
James D. Bruckner, M.D. - 1999
Dominic Reilly, M.D. - 1999
Kevin L. Smith, M.D. - 2000
John T. Sack, M.D. - 2000
Sean E. Nork, M.D. - 2001
Theodore K. Greenlee, M.D. - 2001
Howard A. Chansky, M.D. - 2002
William J. Mills, M.D. - 2003

Contributors to Departmental Research and Education

April 2005 Through March 2006

We express our appreciation to all who have contributed to the work of the Department of Orthopaedics and Sports Medicine over the past year. Your assistance makes possible special research activities, educational programs, and other projects that we could not offer without this extra support from our alumni, faculty, and friends in the community. We owe a special thanks to the University of Washington Resident Alumni who have made significant contributions to help further the education of our current residents. We have tried to include in this list all who contributed; if anyone was overlooked, please be sure to let us know!

Friends of Orthopaedics

Paul J. Abbott
Christopher Allan
Edward Almquist
Alvarado Orthopedic Medical Group
Marilyn Alvine
Mary Jan B. Anderson
Scott Ian Anderson
Carl Andrews
Nancy Andrews
Marlene Angel
AO Stiftung-ASIF Foundation
Allan Bach
Martha Baker
Samuel Baker
Bank of America Foundation
William Barrett
Timothy Beals
David Belfie
Gary Bergman
Janet Brown
Stephen Bowman
Eric Bowton
Thomas R. Bridges
John F. Burns
Susan Cero
Gary Clancey
Paula Clancey
Todd Clarke
Joseph C. Clifford
Judith Clifford
Michael Coe
Vernon J. Cooley
Richard Conrad
Vernon Cooley
Jay Crary
James Crutcher
Gene Dahlin
Dorothy Davis
Frederick Davis
DePuy
Brenda Dimond
Richard A. Dimond
Oriente Ditano
Ben DuBois
Roberta Dugin
EBI Medical, Inc.
Tom Eiguren
Anne Elliott
Brady Elliott
Leonard Ely
Donald Ericksen
Alexis Falicov
Cynthia Farrar
Edward Farrar
Daniel Flugstad
Trygve Forland
Harold J. Forney
Victor Forni
Jonathan Franklin
Michael K. Gannon
Park Gloyd
Nanci Green
Thomas Green
Sandra Greenlee
Theodore Greenlee
Karen Gritzka
Thomas Gritzka
Scott Hacker
Hand Innovations, LLC
Sigvard Hansen Jr.
Helena Orthopaedic Clinic
Joel Hoekema
Scott Hormel
Fred Huang
Larry Hull
Thomas Weston Hutchinson
Inland Orthopaedics of Spokane
David E. Karges
Carleton Keck
Kinetikos Medicine
Richard Kirby
Jonathan Knight
Walter F. Krengel
Gladys Kretzler
Harry Kretzler
Ronald Kristensen
Judy B. Lalonde
Marie C. Lawrence
David Levinsohn
Carolyn W. Luck
Calvin Reynolds MacKay
Martin Mankey
Vivian E. Marshall
Richard E. Martindale
Frederick Matsen
William H. Matchett
Gregory K. May
Heather D. McAdam
David Medoff
Sandee Mendrysa
Jane Metcalf
Michael Metcalf
Becky Mezistrano
Joseph Mezistrano
John Michelotti
Ralph Miller
Peter W. Mitchell
Mickey Moore
Michael Morris
David Morrow
Susan Moseley
Marr Mullen
Neil J. Wells, Inc.
John A. Neufeld
Sean Nork
Northwest Biomet
William Obremskey
William L. Oppenheim
Pacific Medical, Inc.
Pacific Orthopaedics
Pacific Rim Orthopaedic Surgeons
Dan Page
Lawrence V. Page
Walter Petlow
Mary Pleger
Proliance Surgeons, Inc.
Brett R. Quigley
Timothy Rapp
Steven Ratcliffe
Gregory Rafijah
Jim Reiff
Mark Remington
K. Roberts
Rodney Roberts
Shirley Rodarte
Michael J. Sailer
Ronald Sandler
Kenichi Sato
Sarah Sato
Guy R. Schmidt
Chris Schuldt
The Seattle Foundation
Seattle Hand Surgery Group
Richard Semon
Amy Shafer
Brian L. Shafer
Marilyn Sheldon

Friends of Orthopaedics

Constance Sidles
John Sidles
Simonian Sports Medicine Clinic
Peter Simonian
Kristin Sims
William Sims
Aaron Smith
Carla Smith
James Sobeski
Larry Southern
Patricia A. Spence
Lynn Staheli
The Stephens Group
Susan Smith Stephens
Jeff Stickney
Edward A. Stokel
Stryker
Beth Swiontkowski
Marc Swiontkowski
Synthes USA
Lisa Taitsman
Carol Teitz
John L. Thayer
William T. Thieme
Steven Thomas
TriMed, Inc.
Martin Tullus
United Way King County
Mary Stuart Van Meter
J. Eric Vanderhooft
Joy Vanderwerff
Nicholas B. Vedder
Robert Veith
Theodore Wagner
Charles Wahtola
Michael D. Walsh
Jane Walton
Washington Orthopaedic Center
Webber Law and Yard Care, Inc.
Richard Webber
John D. West III
Doris Wilkinson
Jay Albert Winzenreid
Emma Woodhouse-Graber
Wright Medical

Alumni

1952
Park W. Gloyd, M.D. ★

1954
Trygve Forland, M.D. ★

1955
Robert W. Florence, M.D.

1956
J. Michael Egglin, M.D. ★
John E. Goeckler, M.D.
Robert L. Romano, M.D.

1957
John H. Aberle, M.D. ★
John R. Beebe, M.D.

1958
Harry H. Kretzler, Jr., M.D. ★
James R. Friend, M.D. ★
Kenneth L. Martin, M.D. ★
Samuel L. Clifford, M.D.

1959
James W. Tupper, M.D.

1960
Irving Tobin, M.D. ★
William V. Smith, M.D. ★

1961
Robert C. Colburn, M.D.

1962
Arthur Ratcliffe, M.D.
Marr P. Mullen, M.D. ★

1963
Alfred I. Blue, M.D.
Robert A. Kraft, M.D.

1964
David E. Karges, M.D. ★★★★
Harold J. Forney, M.D. ★
Theodore K. Greenlee II, M.D. ★★★★★
Thomas E. Soderberg, M.D.

1966
F. Richard Convery, M.D. ★
Joseph S. Mezistrano, M.D. ★
William A. Reilly, Jr., M.D.

1967
Ivar W. Birkeland, M.D.
J. Conrad Clifford, M.D. ★
Robert F. Smith, M.D. ★★★★★

1968
Lynn T. Staheli, M.D. ★
Stewart M. Scham, M.D. ★
William T. Thieme, M.D. ★

1969
Edward E. Almquist, M.D. ★★
Edward L. Lester, M.D.
Hugh E. Toomey, M.D. ★★★
Sigvard T. Hansen, Jr., M.D. ★★★★

1970
John C. Brown, M.D. ★
John M. Coletti, Jr., M.D. ★
Malcolm B. Madenwald, M.D. ★
Michael T. Phillips, M.D. ★
Robert D Schrock, Jr., M.D.

1971
Bruce E. Bradley, Jr., M.D.
Franklin G. Alvine, M.D. ★★★★
Jerome H. Zechmann, M.D.
Louis A. Roser, M.D. ★
Nils Fauchald, Jr., M.D.

1972
David J. LaGasse, M.D.
David R. Nank, M.D. ★★
Donald D. Hubbard, M.D. ★
John A. Neufeld, M.D. ★
Thomas L. Gritzka, M.D. ★

1973
Frederick J. Davis, M.D. ★
Larry D. Hull, M.D. ★
Robert P. Watkins, Jr., M.D. ★
Theodore A. Wagner, M.D. ★★★★★

1974
Richard A. Dimond, M.D. ★★
Ronald B.H. Sandler, M.D. ★★★
Samuel R. Baker, M.D. ★★
Robert A. Winquist, M.D. ★★★★★

1975
Donald L. Plowman, M.D. ★★★
Frederick A. Matsen III, M.D. ★★★★★
Gunter Knittel, M.D.
Larry R. Pedegana, M.D. ★
Thomas M. Green, M.D. ★★★★
William M. Backlund, M.D., P.S. ★

1976
Douglas K. Kehl, M.D.
Douglas T. Davidson III, M.D. ★
John F. Burns, M.D. ★
Peter Melcher, M.D.
Richard A. Zorn, M.D. ★

1977
Carl A. Andrews, M.D. ★
Geoffrey W. Sheridan, M.D. ★★
Larry D. Iversen, M.D. ★
Mark C. Olson, M.D. ★
Steven T. Bramwell, M.D.

1978
Arnold G. Peterson, M.D. ★★★★
Gary J. Clancey, M.D. ★★★
John W. Brantigan, M.D.
Richard S. Westbrook, M.D. ★★
Robert J. Strukel, M.D.
William Oppenheim, M.D. ★

1979
Allan W. Bach, M.D. ★★★★★
Gregory M. Engel, M.D. ★★
Jonathan L. Knight, M.D. ★★
Richard L. Semon, M.D. ★★★★

1980
Carol C. Teitz, M.D. ★★★
Douglas G. Norquist, M.D.
John M. Hendrickson, M.D. ★★
Michael A. Sousa, M.D. ★★
Stuart R. Hutchinson, M.D. ★

1981
Dennis J. Kvidera, M.D. ★
John M. Clark, Jr., M.D., Ph.D. ★★★
Martin S. Tullus, M.D. ★★★★★
Robert G. Veith, M.D. ★★★★★

1982
John L. Thayer, M.D. ★
Richard M. Kirby, M.D. ★★★★★
Steven S. Ratcliffe, M.D. ★★
William D. Burman, M.D.

1983
E. Anne O. Elliot, M.D. ★
Edward L. Farrar III, M.D. ★★★★★
Henry K. Yee, M.D.
Joseph D. Zuckerman, M.D. ★★★★
Keith A. Mayo, M.D. ★★★
Robert M. Berry, M.D.

STARS INDICATE TOTAL DONATIONS IN SUPPORT OF THE RESIDENCY

★★★★★ = $10,000 and over
★★★★ = $7,500 - $9,999
★★★ = $5,000 - $7,499
★★ = $2,500 - $4,999
★ = $1 - $2,499

1984
Jeffrey C. Parker, M.D. ★
Jeffrey W. Akeson, M.D. ★★★
Kevin P. Schoenfelder, M.D. ★
Marc F. Swiontkowski, M.D. ★★★★★
Thomas J. Fischer, M.D. ★★★★

1985
Daniel L. Flugstad, M.D. ★★★★
Jeffrey N. Hansen, M.D. ★★★
Paul J. Abbott, M.D. ★★★★
Richard J. Barry, M.D. ★
William P. Barrett, M.D. ★★★★★

1986
Carleton A. Keck, Jr., M.D. ★★★
Gary Bergman, M.D. ★★★★★
Lawrence E. Holland, M.D. ★
Michael E. Morris, M.D. ★★★★

1987
Craig T. Arntz, M.D. ★★
Herbert R. Clark, M.D. ★★
Michael K. Gannon, M.D. ★
Steven L. Reed, M.D. ★

1988
Jonathan L. Franklin, M.D. ★★★★
Michael A. Thorpe, M.D. ★★★★★
Richard V. Williamson, M.D. ★

1989
James P. Crutcher, M.D. ★★★★
Lawrence V. Page, D.O. ★
Martin G. Mankey, M.D. ★★★
Nancy J. Ensley, M.D.
Steve C. Thomas, M.D. ★★★★

1990
David M. Kieras, M.D. ★
J. Roberto R. Carreon, M.D.
Jay A. Winzenried, M.D. ★★
Ken Fujii, M.D. ★
Walter F. Krengel III, M.D. ★★

1991
David H. Bishop, M.D. ★★
Kit M. Song, M.D.
Mark Remington, M.D. ★★★
Mark E. Murphy, M.D., Ph.D. ★
Tim P. Lovell, M.D. ★★

1992
Curt Rodin, M.D.
Don Striplin, M.D. ★★
Eli Powell, M.D. ★
Jeff Stickney, M.D. ★
John D. West, M.D. ★
Michael Sailer, M.D. ★★★

1993
J. Eric Vanderhooft, M.D. ★★★★
Lyle S. Sorensen, M.D. ★★★★★
Philip J. Kregor, M.D. ★★
Susan R. Cero, M.D. ★★★★

1994
Brodie Wood, M.D. ★★
Eric Bowton, M.D. ★★
Jim Vahey, M.D. ★
Sohail K. Mirza, M.D. ★
William Obremskey, M.D. ★★

1995
Ron Kristensen, M.D. ★
Scott Hormel, M.D. ★★
Timothy Beals, M.D. ★
Todd Clarke, M.D. ★★
William J. Mills III, M.D. ★

1996
David Deneka, M.D. ★
Peter Mitchell, M.D. ★★
Peter T. Simonian, M.D. ★★★
Vernon Cooley, M.D. ★
William Wagner, M.D. ★★★

1997
Daniel Stechschulte, Jr., M.D.
David Levinsohn, M.D. ★
L. Anthony Agtarap, M.D. ★
Mohammad Diab, M.D.
Randall W. Viola, M.D.

1998
Colin Poole, M.D. ★
David Belfie, M.D. ★
Don Ericksen, M.D. ★★★
Jay Crary, M.D. ★★
Oriente DiTano, M.D. ★

1999
Craig Boatright, M.D.
Jeffrey Garr, M.D.
John Michelotti, M.D. ★
Julie A. Switzer, M.D.
Thomas D. Chi, M.D. ★

2000
Brett Quigley, M.D. ★
Cara Beth Lee, M.D.
Daniel Jones, M.D. ★
Joel Hoekema, M.D. ★
Patrick McNair, M.D.

2001
Eric Novack, M.D.
Frederick Huang, M.D. ★
Matthew Camuso, M.D.
Michael Metcalf, M.D. ★
Richard Bransford, M.D.

2002
Timothy DuMontier, M.D.
Scott Hacker, M.D. ★
Timothy Rapp, M.D. ★
William Sims, M.D. ★
Carla Smith, M.D. ★

2003
Ben DuBois, M.D. ★
Andy Howlett, M.D.
Guy Schmidt, M.D. ★
Brian Shafer, M.D. ★
Emma Woodhouse, M.D. ★

2004
Jon Braman, M.D. ★
Alexis Falicov, M.D. ★
Mike McAdam, M.D. ★
Jason Thompson, M.D.
Thea Khan-Farooqi, M.D.

2005
Tony Buoncristiani, M.D.
Waqqar Khan-Farooqi, M.D.
Wren McCallister, M.D.
Tim O'Mara, M.D.
David Stevens, M.D.

2006
Heidi Ambrose, M.D.
Stacey Donion, M.D.
Eric Klineberg, M.D.
Bill Montgomery, M.D.
Mel Wahl, M.D.
Burt Yaszay, M.D.

STARS INDICATE TOTAL DONATIONS IN SUPPORT OF THE RESIDENCY

★★★★★ = $10,000 and over
★★★★ = $7,500 - $9,999
★★★ = $5,000 - $7,499
★★ = $2,500 - $4,999
★ = $1 - $2,499

Endowments

We express our appreciation to all who have contributed to the endowments of the Department of Orthopaedics and Sports Medicine. Your assistance makes possible special research activities, educational programs, and other projects that we could not offer without this extra support from our alumni, faculty, and friends in the community. Additional Contributions to these and new endowments are most welcome! If you have any questions, please contact our Chair, Rick Matsen, or our Administrator, Ken Karbowski.

Hansjoerg Wyss Endowed Chair

Ernest M. Burgess Endowed Chair for Orthopaedics Investigation

Sigvard T. Hansen Jr. Endowed Chair in Orthopaedic Traumatology

Jerome H. Debs Endowed Chair in Orthopaedic Traumatology

Endowed Chair for Women's Sports Medicine and Lifetime Fitness

Surgical Dynamics Endowed Chair for Spine Research

Douglas T. Harryman II/DePuy Endowed Chair for Shoulder Research

Synthes Spinal Surgery Outcomes Research Endowment

Zimmer Fracture Fixation Biology Endowed Professorship

Ostex Bone and Joint Research Endowment

Orthopaedic Traumatology Endowed Lectureship

John F. LeCocq Lectureship in Orthopaedic Surgery

Don and Carol James Research Fund in Sports Medicine and Fitness

Victor H. Frankel Award

Esther Whiting Award

Ed Laurnen Award

Spine Research Endowment

James G. Garrick Lectureship in Sports Medicine

Regenerative Spine Surgery Endowed Professorship

Endowed Chair for the Health of the Student Athlete